University of Stavanger

Faculty of Science and Technology

MASTER'S THESIS

Study program/Specialization: Petroleum Geosciences Engineering	Spring semester, 2017 Open
Writer: Kristina Waagbø Tegle	(Writer's signature)
Faculty supervisor: Carita Augustsson External supervisor(s): Rodmar Ravnås	
Title of thesis: Provenance of the Upper Cretaceous Lange-Lysing deep-marine sandstone in the Norwegian Sea: with implication for reservoir quality.	
Credits (ECTS): 30	
Keywords: Provenance LA-ICP-MS U-Pb zircon dating Whole-rock geochemical data Sedimentary cores Petrography Reservoir quality Norwegian Sea	Pages: 110 +enclosure: 7 Stavanger, 15.06. 2017

Provenance of the Late Cretaceous Lange-Lysing Megasequence, with implication for reservoir architecture and quality

by

Kristina Waagbø Tegle

MSc. Thesis

Presented to the Faculty of Science and Technology
The University of Stavanger

The University of Stavanger

June 2017

Acknowledgements

I am grateful to Norske Shell, who founded this thesis. I would like to express my great appreciation to my supervisors Rodmar Ravnås and Carita Augustsson for valuable support and constructive comments. I would like to thank Tom Andersen and Siri Simonsen for technical assistance on detrital zircon ICP-MS dating. I would also like to thank Berit Løken Berg and Mona Wetrhus Minde for valuable guidance in the SEM laboratory. My grateful thanks are also extended to Thomas Meldahl Olsen, Sofie Knutdatter Arntzen and Caroline Ruud for providing thin sections and milling assistance. I owe thanks to my fellow students at the University of Stavanger – it would not be the same without you. Finally, I would like to thank my family and friends for the support throughout my study.

Abstract

The provenance and reservoir properties of Upper Cretaceous Lange-Lysing sandstone in the Norwegian Sea have been determined by using integrated whole-rock geochemical, petrographic and detrital zircon U-Pb age dating by LA- ICP-MS. Three different provenance signatures are revealed within three geographical areas containing the Lange-Lysing succession. They have contributed to significant response on diagenesis, which gives implication for reservoir properties, whereby the petrographic data expose several controls on porosity development, including textural and mineralogical factors. (1) Quartzofeldspathic petrofacies in the Møre Margin are interpreted to have the highest potential as hydrocarbon reservoir due to better sorting and larger grain size, combined with preservation of intergranular and intragranular porosity, not occluded by cement. The zircon grains were derived from felsic sources in the Western Gneiss Region of Baltica, due to a prominent age peak that closely corresponds with the Sveoconorwegian (1000-950 Ma) and the Gothian orogenies (1700-1500 Ma). (2) Sandstone of the quartzolithic petrofacies from the Halten-Dønna Terrace has smaller grain size and is less sorted than the quartzofeldspathic petrofacies, yielding a lower reservoir quality. The detritus is suggested to have been sourced from more mixed ?andesitic-felsic rocks. The zircon grains derived from the Paleozoic Caledonian Nappe Domain of western Baltica and from the Lofoten Islands or Western Tromsø Basement Complex in northern Norway because of a dominance of Early Proterozoic crust-forming zircon grains (1800-1750 Ma) and an Archean component. (3) The main diagenetic features of the quartzarenitic petrofacies in the deeper Vøring Basin includes mechanical and chemical compaction, precipitation and replacement of quartz overgrowth, kaolinite, clay minerals, iron oxide and formation of secondary porosity due to dissolution of labile minerals. Grain coating of authigenic clay minerals exerts a critical control on the reservoir quality as it inhibits quartz cement. The deposits are inferred to have mixed sand distribution from the eastern Greenland and the Norwegian margins based on wide zircon-age spectra with predominance of Early Proterozoic (1900-2100 Ma) and Archean contribution (>2600 Ma). Contradictory to previous studies, the U-Pb analysis of the Lange-Lysing sandstone has proved that Late Archean zircon is present within deposits derived from the Norwegian landmass. Furthermore, the study stresses a strong correlation between provenance, diagenetic products and reservoir quality.

Table of Contents

Introduction

Deep-marine sedimentary reservoirs in the Norwegian Sea have received much attention because they are important hydrocarbon exploration targets. Earlier exploration has focused chiefly on the Jurassic pre- and syn-rift plays in the frontier basins of the Norwegian Sea and several large hydrocarbon fields were discovered (Smørbukk, Norne and Heidrun). Secondary targets were also extended in the 1980s-1990s and included Cretaceous-Paleocene post-rift strata. Ormen Lange and several smaller commercial reservoir discoveries located in the Møre and Vøring basins were made (Martinsen et al., 2005). A successful gas condensate discovery, targeting the Snadd prospect of Late Cretaceous Lysing Formation was made by BP and operating partners ExxonMobil, Shell and Statoil Norge on Dønna Terrace in 2000. These hydrocarbon discoveries initiated an interest for further exploration and improvement of reservoir distribution and quality of Late Cretaceous units.

The Cenomanian and Turonian to Coniacian Lange-Lysing sandstone encompasses the reservoirs of the underexplored mid-Cretaceous play in the Norwegian Sea, offshore Mid -Norway continental shelf. The deep-marine sandstone reservoirs comprise both commercial and uncommercial discoveries, i.e. the Snadd and Smørbukk fields, on the Halten-Dønna Terraces of the Mid Norway margin, Møre margin and on the Måløy Terrace in the northern parts of the North Sea (Fig.1; Fjellanger et al., 2005; Fugelli and Olsen, 2005). However, the reservoir quality and exploration assessments for the deep-marine Upper Cretaceous sandstone units are variable and difficult to predict due to variation in facies, burial setting and thermal history (Lien et al., 2006). Sediment distribution and drainage pattern from the source area to depositional basin are controlled by the structural and stratigraphic framework of the Norwegian Sea and conjugate margins. East Greenland and the Norwegian landmass are the potential source areas suggested for the Upper Lange-Lysing deep-marine units. Both regions have been thoroughly studied in regard of sedimentological and geochronological terms (e.g. Fonneland et al., 2004; Morton et al.,2005). Provenance gives constraints for understanding the sandstone dispersal systems. Identification of location of source region places controls on the sediment transportation pattern and intrabasinal sand distribution, which strongly affect the reservoir properties, porosity and permeability. Therefore, provenance prediction of reservoir distribution and quality has proven to be a valuable tool in exploration for the immature Cretaceous plays in the Norwegian Sea.

To date, few provenance studies with integrated detailed geochemical and petrographic analysis have been carried out in the frontiers of the Norwegian Sea. However, new geochronological work has trigged new interest, such that the origin of the Upper Cretaceous turbiditic sandstone is a matter of debate. Detrital zircon dating on sandstone from the Halten- Dønna Terrace and the Vøring basin suggests two distinct sediment transport paths: Cenomanian–Campanian deposits with zircon ages characteristic for Scandinavian landmasses, and Turonian-Maastrichtian deposits with zircon ages linked to Eastern Greenland (Fonneland et al., 2004; Morton et al., 2005). Seismic characterization by Fugelli and Olsen (2007) instead proposed a northern source parallel to the Nordland Ridge.

Due to these inconsistencies, the present study aims to compare and contrast provenance signature of Upper Lange and Lysing between the southwestern Møre Margin Måløy Slope and the northeastern Halten-Dønna Terrace along the margin of the Trøndelag Platform, in order to unravel the provenance history and examine source area(s). New wells are considered in this study and improving the provenance in this area. A secondary objective is to determine the Lysing-Lange turbidite systems' viable potential targets for further hydrocarbon exploration in the Norwegian Sea, by assessing controlling parameters on reservoir quality and diagenetic processes during burial. The prediction of spatial variance and reservoir distribution will enhance the understanding of the sedimentary responses of the Late Cretaceous Lange-Lysing sandstone. This study is expected to have implication for hydrocarbon exploration of the Late Cretaceous deep marine sandstone and for pre-drilling assessment of spatial reservoir distribution and quality.

Geological Framework

The Norwegian Sea

The Mid-Norway Margin of the Norwegian Sea is a northeast-southwest trending passive margin located between 62˚and 69˚N. The fundamental structural elements are presented in Fig. 1. The mid-Norwegian margin is bounded by a volcanic escarpment to the west and the Norwegian mainland to the east, and comprises three main segments along strike: Møre, Vøring and Lofoten-Vesterålen. The segments are 400-500 km long and separated by the East Jan Mayen

Fracture zone and the Bivrost Lineament (Transfer zone; Fig. 1.; Blystad et al., 1995; Brekke, 2000).

The Mid-Norway continental shelf has undergone several rifting episodes ranging from the Caledonian orogeny in the Early Devonian to the breakup of the North Atlantic Ocean and passive margin development in earliest Eocene time. The three main rifting episodes identified are 1) Permian–Triassic; 2) Middle Jurassic -Early Cretaceous and; 3) Late Cretaceous - Early Paleocene (Brekke, 2000; Færseth and Lien, 2002; Ziegler, 1988).

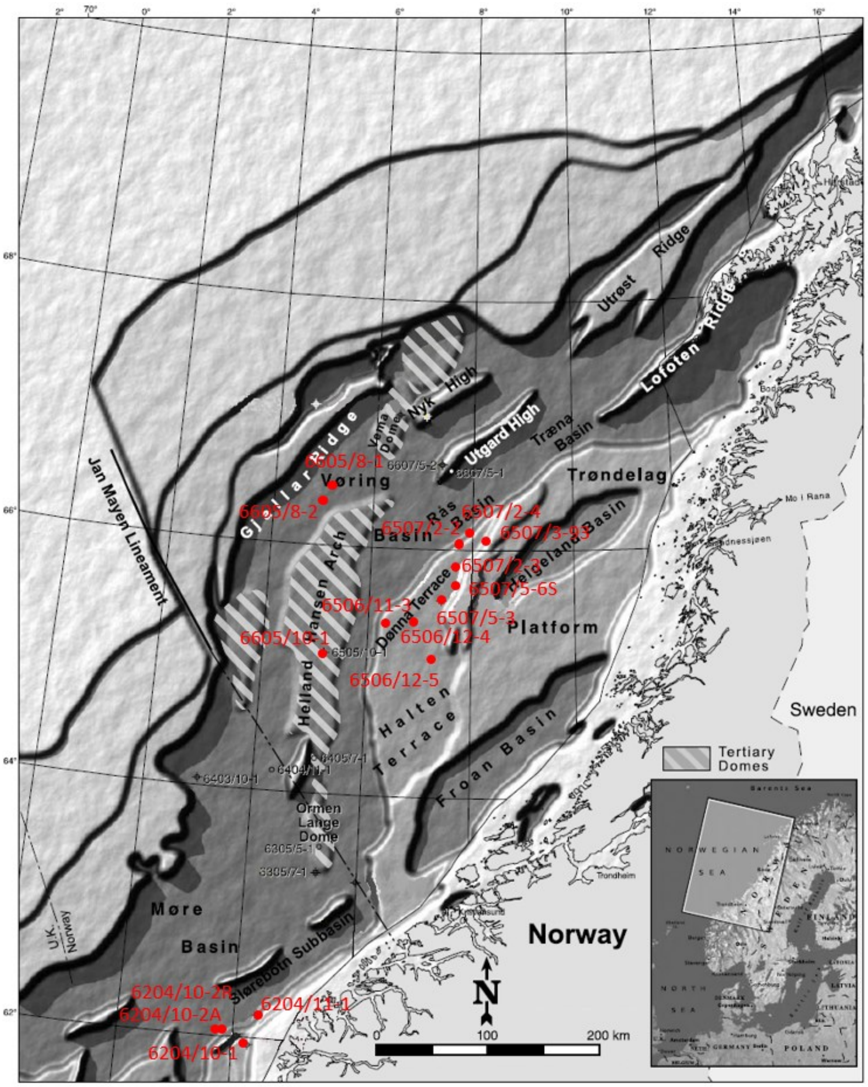

The initial development of the mid-Norwegian margin started with the collapse of the Caledonian orogen in earliest Devonian time, resulting in a west-northwest extension in the southern part of Norway (Andersen, 1998; Fossen and Dunlap, 1998). The Møre-Trøndelag fault complex is an example of a major fault complex associated with this phase of extension. Rift-flank uplift and basin subsidence along the Møre-Trøndelag fault complex was initiated by a new period of rifting during Late Permian-Early Triassic time (Steel, 1993; Mørk and Johansen, 2005). The N-S and NE-SW trending rotating faulting block system was mainly formed by rifting in Permian –Triassic time. Consequently, a thick Triassic continental succession was deposited in the basin (Brekke, 2000; Halland et al., 2013).

Fig.1. Structural elements in the Norwegian Sea displaying the Halten-Dønna Terrace, Vøring and Møre basins. Modified from Fugelli and Olsen, 2005. Wells discussed are highlighted in red.

The subsequent extensional episode in Middle Jurassic –Early Cretaceous time led to significant thinning of the crust and renewed faulting along the basin-bounding fault complexes, e.g. Møre-Trøndelag fault complex (Eide et al., 1997; Osmundsen and Ebbing, 2008). Considerable alteration of the basin topography and thinning of crust led to the development of the Møre and Vøring basins (Morton et al., 2005). They experienced rapid differential subsidence and division into sub-basins and highs (Brekke et al., 1999; Halland et al., 2013). The structural highs, Nordland Rigde and Frøya High, were uplifted during Middle Jurassic time (Halland et al., 2013). The thickness of the Jurassic deposits increases over the Helgeland Basin and Vega High, and decreasse toward the Nordland Ridge (Halland et al., 2013).

A significant transition from overfilled marginal marine (fluvial to deltaic) to under-filled, deep marine basins during Late Jurassic- Lower Cretaceous times occurred along the margin, controlled by the main basin-boundary faults (Sømme et al., 2013). Rapid subsidence west of Nordland Rigde was initiated by westward shifting of rift axis (Færseth and Lien, 2002). Simultaneously, the Lofoten – Vesterålen region and the structural highs were uplifted (Færseth and Lien, 2002; Halland et al.,2013). Several authors suggest a marked increase in tectonic activity from the earliest Cenomanian, compared to the Early Cretaceous (Brekke, 2000; Brekke et al., 2001; Doré et al.,1999; Lundin and Doré, 1997). However, Henstra et al., (2015) in their study of the Lofoten-Vesterålen margin argued for a minor rift in Aptian-Albian. An onset of the Late Cretaceous rifting occurred first in the Cenomanian. Whitham et al. (1999) have proposed similar rifting for the East Greenland margin.

Post-rifting thermal subsidence during middle- Early Cretaceous time, was accompanied by increased sedimentary deposition and leveling of the inherited rift-topography (Færseth and Lien, 2002). Thus, the Jurassic rifting faults remained the important morphological escarpments on the slope and basin floor with renewed faulting rejuvenating basin topography from the Coniacian and on-wards (Færseth and Lien, 2002). A thick Late Cretaceous succession filled most of the differential bathymetry within the Møre and Vøring basins by mid-Cretaceous.

In the central part of the Norwegian Sea, the base Cretaceous range from 9000-13.000 m in depth (Færseth and Lien; 2002). Large feeder fan systems developed due to erosion of the new hinterland areas during Late Cretaceous time (Brekke et al., 1999; Lien, 2006). Late Cretaceous sand-prone intervals are present on the Halten-Dønna to the East, whereas thick Late Cretaceous to Paleocene deep marine units were deposited in the Møre and Vøring basins to the West (Fig. 2; Fonneland et al., 2004). The lithostratigraphy of the mid-Norwegian margin sandstone is presented in Fig.2.

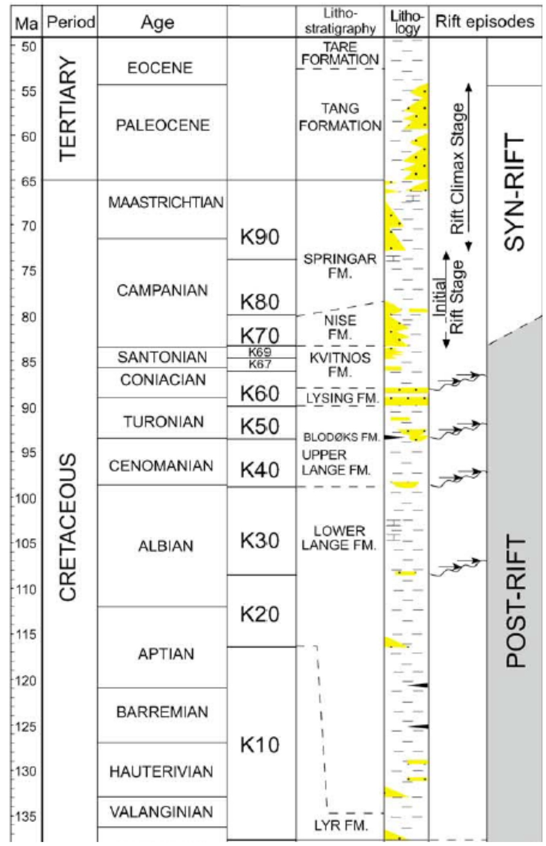

Fig. 2. Tectono-stratigraphic framework of the Norwegian Sea (from Færseth and Lien, 2002)

After an episode of tectonic quiescence, a new rift phase initiated in the Coniacian to the Early Campanian and culminated in the breakup of the North Atlantic Ocean at ~55 Ma (Brekke, 2000; Dore et al., 1999). The extensional regime in Late Cretaceous- Paleocene time gave rise to reactivation of Jurassic faults (Brekke et al., 1999), resulting in the separation of the Dønna Terrace from the Nordland Ridge, and uplift of its southern part (Fugelli and Olsen, 2005). Strike- slip compressional tectonic movements controlled the Vøring basin during Paleocene time. In contrast, the Møre basin was only subjected to continuous subsidence and was tectonically relatively quiet throughout the Cretaceous and Paleocene (Brekke, 2000).

The Lange-Lysing sandstone has commonly have been interpret as deep marine turbidite fan reservoirs (Dalland et al., 1988; Fjellanger et al.2005; Fugelli and Olsen 2005). However, also sandy slump or mass-flow deposits (Hastings, 1987; Shanmugam et al., 1994; Vergara et al., 2001), with depositional environments ranging from deltaic to slope channel and lobe complexes to basin-floor fans (e.g. Fjellanger et al. 2005; Martinsen et al., 2005; Fugelli and Olsen, 2007; Sømme et al., 2013) have been proposed. Recent publications have argued for a series of point sources along the Halten-Dønna Terrace, and the Møre Margin, delivering sediment to a series of laterally separate, seismically mappable shelf-edge deltas with fronting slope to basin-floor channel-lobe complexes (Sømme et al., 2013a, 2013b).

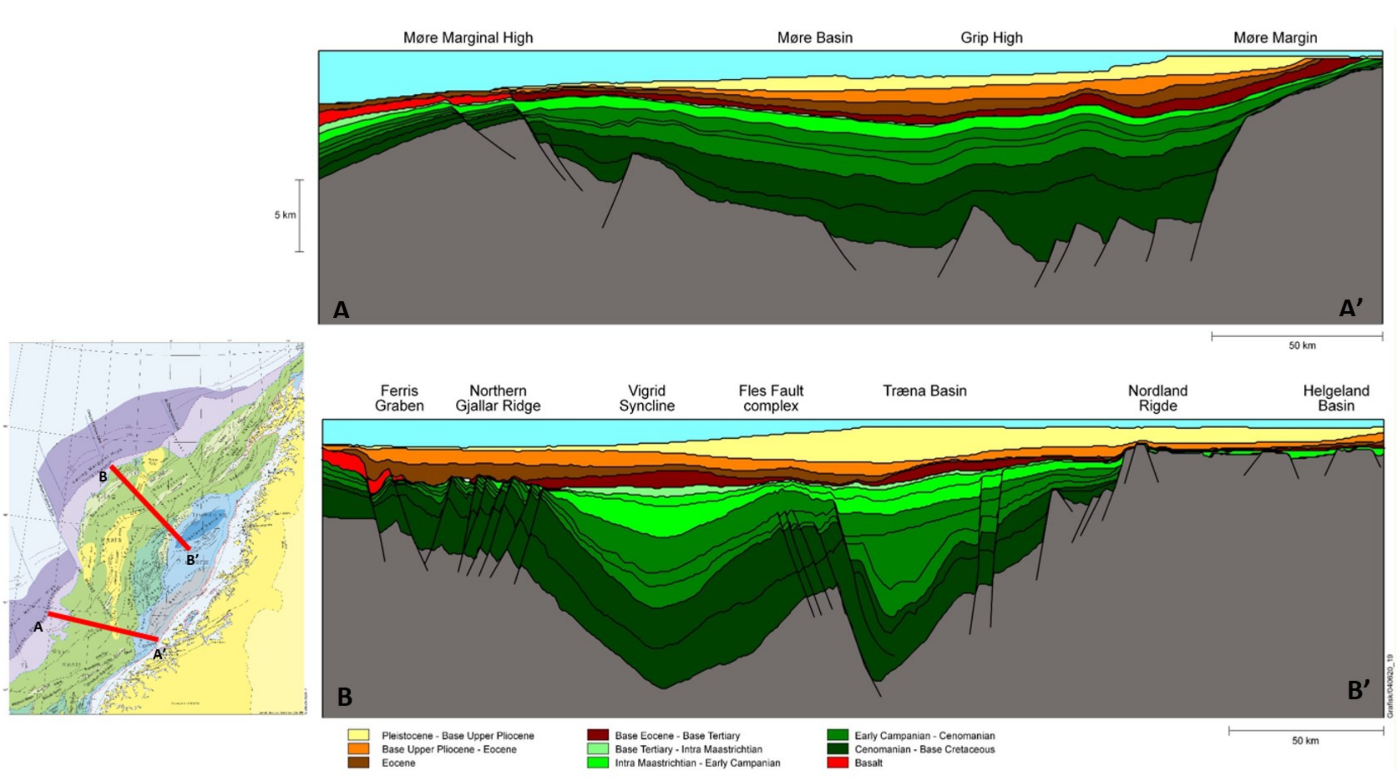

Fig.3. Basin-scale structural cross section of A) Møre basin and B) Vøring basin (Shell in house)

The Scandinavian landmass

The Scandinavian basement is chiefly of Precambrian age. The Fennoscandian Shield represents the northwestern part of the Baltica craton and formed though progressive southwestward expansion by accretion of juvenile crust to the pre-existing Archean during Paleoproterozoic time (Gaál and Gorbatschev, 1987; Bingen et al., 2008; Lahtinen et al., 2008). Late Archean rocks (3100-2600 Ma) and early Sveofennian supercrustal cover (2600-2100 Ma) are chiefly concentrated in the northeastern part of the shield (Skår, 2002). The southwestern part of the Shield and east of the Caledonian thrust belt, the basement is composed of the Palaeoproterozoic Svecofennian region(2000-1800 Ma; Korja et al., 2006), the Transscandinavian Igneous Belt (TIB; 1800-1650 Ma) and the Sveconorwegian Domain (1200-900 Ma; Daly et al., 2006). Kola Penninsula is a Paleoproterozoic collisional belt located in the northeastern part of the Shield (e.g. Daly et al., 2001).

The rocks exposed along the Norwegian margin were formed by three dominant orogenies: 1) the Caledonian (350-450 Ma); 2) the Sveconorwegian (1250-900 Ma); and 3) the Gothian (1750-1500 Ma; Skår, 1998). The Scandinavian Caledonian nappes were formed during late Silurian time as a result of the Cambro-Silurian closure of the Iapetus Ocean and collision of Laurentia and Baltica (Gee, 1975). This continental collision caused emplacement of a series of nappes to the E-SE (the Lower, Middle, Upper and Uppermost Allochthons; Roberts and Gee, 1985). These thrust sheets comprise sedimentary and crystalline rocks with a range of ages, and cover the Norwegian basement rocks. The Caledonian thrust sheets in the mid-Norwegian region consist mostly of meta-sedimentary rocks of the Upper and Uppermost Allochthon (Stephens et al., 1985). The meta-sedimentary rocks are mainly of Cambro-Silurian age and associated with the Norwegian Caledonian rocks (Roberts and Gee, 1985; Thon, 1985). Abundant basement windows are exposed throughout the Scandinavian Caledonides (Roberts and Gee, 1985; Roberts, 2003), resulting in juxtaposition, interfolding and thrust imbrication, in several areas (e.g. Tucker, 1986).

The Lofoten Islands form part of the northern segment of the mid-Norwegian margin and comprise mostly basement windows underneath the Caledonian sheet (Skår, 2002). Skår (2002) proposed Lofoten Islands to be a part of the extension of the Fennoscandian Shield west of the Caledonian thrust sheets. High-grade orthognessic rocks of mainly intermediate- acidic composition represent these basement windows. The gneiss was formed in two episodes; mostly during Early Proterozoic time (c. 1800-1770 Ma) together with meta-volcanic and meta-sedimentary rocks and also Archean ages occur (2600- 2700 Ma, Griffin et al., 1978; Jacobsen and Wasserburg, 1978; Skår, 2002). The Caledonian thrust sheets in this area chiefly belong to the Upper and Uppermost Allochthon (Stephens et al., 1985). Metasedimentary rocks (pelitic, psammitic and calcareous schist and gneiss) from the Upper Allochthon are accompanied by a range of lithologies including metasedimentary, metavolcanic and ultramafic rocks from the Uppermost Allochthon (Stephens et al., 1985). Further North, the West Troms Basement Complex (WTBC) crops out to the west of the Caledonides. The basement rocks are suggested to be an autochthonous part of the Fennoscandian Shield (Gaál and Gorbatschev, 1987; Corfu et al., 2003; Bergh et al., 2014). However, these basement suites could be in an allochthonous position as a Caledonian thrust sheet and associated with Laurentia (e.g. Bergh et al., 2012). The WTBC comprise of various Middle and Early Archean Tonalite-Trondhjemite gneiss (TTG) separated by two sets of shear zones (Corfu et al., 2003; Bergh et al., 2010; Myhre et al., 2011). The major plutonic event took place at 1800-1790 Ma (Bergh et al., 2010).

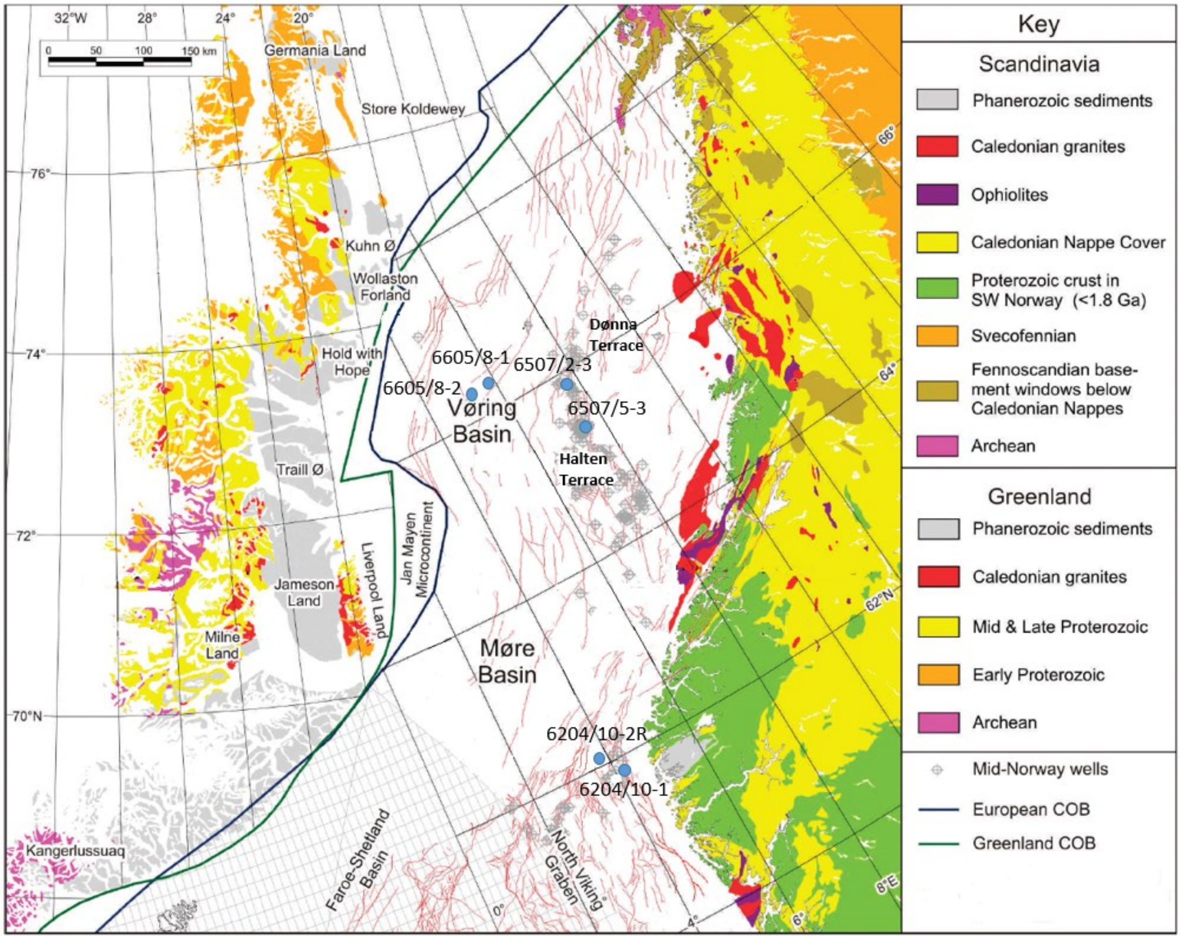

Fig.4. Reconstruction of the Norwegian Sea prior final opening of the Atlantic from Morton et al., 2009. Data sourced from the geology of the two landmasses are Gaál and Gorbatshev (1987), Sigmond (1992), Escher and Pulvertaft (1995) and Koistinen et al (2001). COB = continent-oceanic boundary.

The southern part of Møre is dominated by crystalline basement, known as the Western Gneiss Region, forming a part of the Southwest Scandinavian Domain (Gaál and Gorbatschev, 1987). This region consists mainly of Early Proterozoic autochthonous gneiss and granitoids formed predominately during the Gothian orogeny (ca. 80%) and subsequently exposed to further deformation and metamorphism during Middle Proterozoic time (Sveronorwegian, ca. 20%; Gaál and Grobetschev, 1987; Skår, 1998). The northern part of the Møre region primarily consists of Early Proterozoic intrusions (Fig.3; Morton et al., 2005). Mafic magma intruded this region at c-1470-1450 and 1260-1250 Ma (Austrheim et al., 2003; Corfu et al., 2014). The Caledonian nappes in this area mostly belong to the Middle Allochthon. The Middle Allochthon comprises mainly Precambrian gneiss (Bryhnu and Sturt, 1985). The Jotun Nappe and Dalsfjord Suite are examples of the Caledonian nappe stack, assumed to be remnants of the pre-Caledonian western margin of Baltica (Milnes and Koestler, 1985; Fossen and Dallmeter, 1998). The Middle Allochthon and Western Gneisses Region share similar lithology, comprising predominantly high-grade basic gneiss, and locally pyroxenite and peridotite (Qvale and Stigh, 1985).

East Greenland

The East Greenland margin consists predominantly of basement rocks of Archean (3800-2500 Ma), Early Proterozoic (2000-1750 Ma) and Paleozoic (450-350 Ma) ages (e.g. Kalsbeek et al., 2001; Watt and Thrane, 2001). Crystalline rocks of the Precambrian shield occupy most of the ice-free area of Greenland. Metasedimentary rocks of the Caledonian thrust belt and younger sedimentary rocks are predominantly exposed to the east of the Precambrian basement (Trane, 2002). The Archean gneiss domain is exposed in southern Greenland and extends from the west coast to the east coast, as well as the northwestern part of Scotland. The Archean and Proterozoic rocks are exposed as isolated remnants related to the Caledonian fold belt of East Greenland. Metamorphism and crustal reworking of the Achaean rocks, resulted party in the formation of the Early Paleozoic basement rocks (Nutman and Kalsbeek, 1994). The western partly of East Greenland comprises Archean and Proterozoic granitoid as part of the Caledonian Foreland. (Leslie and Higgins, 1999; Smith and Robertson, 1999). North of 72°N, basement rocks are predominantly of Early Proterozoic age (2200-1800 Ma), whereas the granitoid in South-Eastern Greenland is mainly of Achaean age (3800-2500 Ma; Watt and Trane, 2001).

Eastern Greenland has granitic rocks exposed within thick thrust related units along with meta-sedimentary cover units (e.g. high- grade metasedimentary rocks from Krummedal supracrustal sequence) and Late Proterozoic to Ordovician sedimentary rocks (Kalsbeek et al., 2001). Intrusions within the basement of Eastern Greenland are dated c. 930 Ma and c. 435 Ma (Kalsbeek et al., 2001). U-Pb geochronology by Cawood and Nemchin (2001) revealed that the zircon population of c. 760-570 Ma in East Greenland is related to the rifting of the Laurentian margin, whereas the convergent margin magmatism is associated with the zircon ages in the range of 1360-1230 Ma. In addition, Devonian- Cretaceous sedimentary rocks as well as Paleogene and Neogene volcanic and intrusive rocks are exposed on the Eastern Greenland margin (Cawood and Nemchin, 2001).

Significant fault block creation and re- organization during Late Jurassic to Early Cretaceous time impacted the East Greenland margin. During Cretaceous time, the East Greenland margin was affected by smaller rift events that resulted in a topography dominated by tilted fault blocks (Witham et al., 1999). Detrital zircon studies of the Eleanor Bay supergroup metasedimentary rocks propose evidence for Neoproterozoic ages, associated with the Grenvillian orogeny (Escher and Pulvertaft, 1995).

North-East Greenland is suggested to comprise exposed Cretaceous sedimentary rocks, as it includes parts of the Vøring Basin before the Paleogene continental separation (Skogseid et al., 2000). Early Proterozoic basement dated between c. 1900 Ma and c. 2000 Ma is prevalent (Kalsbeek et al., 1993; Thrane, 2002). The inherently onshore Jurassic rift topography was filled during Albian-Turonian time. Consequently, the landmass of East Greenland began to supply sediments across the Greenland shelf (Whitham et al. 1999). The North-East Greenland Cretaceous units deposited an over 2000 m thick unit of predominantly marine siliciclastic sediment after the major rifting event in Late Jurassic to Early Cretaceous (Surlyk, 1978).

Material and Methods

The database provided for this thesis includes 18 thin sections and 314 m core intervals from sixteen wells that encountered Coniacian-Turonian Lange and Lysing megasequences located in the Møre Margin, Måløy slope, Halten Terrace, and Dønna Terrace, offshore mid-Norway. Halten and Dønna Terraces are often considered grouped. For this report, three main categories are defined by zircon geochronology, geochemical and petrographic analysis: Møre Margin, Halten-Dønna Terrace and the Vøring Basin also referred to as the distal part of Halten Terrace (Distal Halten; wells 6605/8-1 and 6605/8-2). An overview of the sample material and location is given in Tab.1. and Appendix 1, respectively. All thin sections and geochemical and core data are provided by Norske Shell.

Tab.1. Overview of Upper Lange-Lysing sample set

Location	Well	Well name (this thesis)	Core	Thickness cored interval, m	Dig. Log, m	Fm.	Age	Facies analysis	Geochemical data	Point counted thin section	U-Pb Zircon dating
Halten Terrace	6605/8-1	HD 8-1	C1	9	9	Lysing	con	x	x	3	x
Halten Terrace	6605/8-2	HD 8-2	C1-C3	49	24	Lysing	con	x	x	1	
SW Møre Margin	6204/10-1	M10-1	C2	9	9	Lysing	mtur	x	x	3	x
			C3	7					x		
			C4	20	20				x		
SW Møre Margin	6204/10-2 A	M10-2A	C1	16		Lysing	mutur	x	x	1	
SW Møre Margin	6204/10-2 R	M10-2R	C1	18	18	Lysing	mutur	x	x	1	x
SW Møre Margin	6204/11-1	M11-1	C1-C2	18	6	Lysing	Con	x	x	1	
			C3	25			Tur	x	x		
Halten Terrace	6506/12-5	H12-5	C1-C2	41		Lysing	mutur-con	x	x		
Halten Terrace	6506/12-4	H12-4	C1	22		Lysing	mutur-con		x		
Halten Terrace	6505/10-1	H10-1	C1-C3	49		Lysing	con		x		
Halten Terrace	6506/11-3	H11-3	C1	28		Lysing	mutur-con		x		
Dønna Terrace	6507/3-9 S	D3-9S	C1	44		Lysing	utur-?con		x		
Dønna Terrace	6507/5-6 S	D5-6S	C1	19		Lysing	utur-?con		x		
Dønna Terrace	6507/5-3	D5-3	C1-C4	15		Lysing	utur-?con	x	x	2	x
Dønna Terrace	6507/2-2	D2-2	C1	28	18	Lysing	utur-?con	x	x		x
Dønna Terrace	6507/2-3	D2-3	C1-C2	42	40	Lysing	utur-?con	x	x	3	
Dønna Terrace	6507/2-4	D2-4	C1	17		Lysing	utur-?con	x	x	1	
Total	**16**			**314**	**157**			**12**	**56**	**18**	**10**

C1, Core 1; C2, Core 2; C3, Core3; C4, Core 4; con, Coniacian; utur, Upper Turonian; mutur, middle-Upper Turonian; Tur, Turonian; Dig. Log, Digitalized logs; Fm., Formation.

Sampling and logging

Fourteen days of core logging was used to manually describe 314 meters of core material from 16 wells. Textural and compositional features, sedimentary structure and bioturbation were investigated in order to predict the depositional environment and distinction of the various of sedimentary facies and facies associations. Eight core logs were digitalized and presented in figures 7, 8 and 9. The depositional character, flow units, texture and composition from the core dataset obtained for this study have permitted identification of lithofacies presented in Tab. 3. As provenance and prediction of reservoir quality are the aim of this thesis, the target was to sample sandstone packages, and clay-rich packages were discharged. Fifty-two samples were collected from the Lange-Lysing formations (core logs) for geochemical analysis. A selection of the sampled material (10) was used for zircon analysis (Tab.1.). The sandstone samples were sampled at Weatherford Core shed in Sandnes, Norway.

Petrography

Eighteen thin section from different wells, ordinarily from the lower, middle and upper sequence within the core interval, were point counted (Tab.7.). Thin sections were examined under Zeiss Optical Microscope (petrographic microscope) and point counted with an average of 300-350 framework grains per thin section. Intergranular volume (IGV) and detrital grains (except quartz, feldspar, lithic fragments), are not represented in the framework composition. Sorting, roundness and sphericity were determined by using the comparisons chart from Compton (1962) and Powers (1982), respectively. Grain contacts were evaluated using the comparison chart from Tucker (1988). Porosity was estimated based on point counting and some thin sections were filled with blue epoxy. Grid spacing was set to 1x1 mm.

Framework mode and mineralogical composition were determined by using the standard method of Ingersoll et al. (1984). This method provides a detailed interpretation of the sedimentary environment and extracts more information about the lithic fragments, in contrast to the Gazzi-Dickinson method, where minerals of sand-fraction within lithic fragments are counted as separate grains, regardless of what they are associated with (Dickinson, 1970; Ingersoll et al., 1984). The detrital framework modes, which is the result of point counting, are plotted in QFL ternary diagrams in order to obtain information about the tectonic setting of depositional basins and its provenance, and for classification purposes (Dickinson et al.,1983; Folk, 1980, Suttner et al., 1981). Point count results are presented in Tab.7.

Original Porosity Loss

The porosity loss due to compaction (COPL) is expressed by the following equation (Ehrenberg, 1989):

$$COPL = OP - \frac{(100 \times IGV) - (OP \times IGV)}{100 - IGV}$$

Assuming original porosity, OP= 40%, and IGV= the intergranular volume (intergranular porosity + intergranular cement).

The porosity loss due to cementation (CEPL) in a sandstone is calculated by following equation (Ehrenberg, 1989):

$$CEPL = (OP - COPL) \times \frac{CEM}{IGV}$$

Where CEM is the cement volume in percentage. The total of the CEPL and COPL gives the porosity loss compared to the initial rock volume. However, not all preconditions are met for the various sandstone, and they must be interpreted with caution (Ehrenberg, 1989).

Geochemistry

Fifty-two samples were analyzed for their whole-rock element and trace element composition. The samples were powered in an agate mill. An ICP-AES (oxides Ba, Ni and Sc) and ICP-MS (trace elements) were the element composition instruments analyzed by ACME laboratories in Vancouver, Canada. Geochemical major and trace element composition of the different samples are represented in Appendix 1. Calculation of Eu/Eu* is defined by the following equation

$$2 * \frac{EU}{(Sm+Gb)}.$$

The chemical index of alteration (CIA) is expressed as the molar volumes of $|Al_2O_3/(Al_2O_3+ CaO^*+ K_2O)|$ x 100, where the CaO* represents the silicate fraction solitary (Nesbitt and Young, 1982, 1989). Because some of the sandstone samples contain large quantities of marine carbonate ($CaCO_3$), it is assumed that CaO* is equivalent to Na_2O for CaO* >2wt. % as an approximation (McLennan et al., 1993).

Detrital Zircon Geochronology

The sandstone samples (15-40 g sample material) were crushed in a steel crusher and the lighter fraction <250 µm was separated from the coarser fraction (>250µm) by sieving. Heavy liquid Na-Poly wolframat with density of > 2.91g/cm^3 was used to concentrate heavy minerals. The extraction of zircon crystals was performed by handpicking under a binocular microscope. The zircon grains were mounted in epoxy and polished until the grain surface center was exposed. The mounts were carbon coated. Morphology and internal structure of the studied zircons by cathodoluminescene (CL) and backscattered electrons (BSE) was conducted prior to U-Pb analyses in order to find suitable spots for the analysis (Fig.21.). Zircon of magmatic origin tend to have oscillatory zoning or sector zoning, and metamorphic zoning is usually characterized by rounded concentric zoning and irregular or unzoned (Corfu et al.,2003). CL and BSE images were taken using a Hitachi SU5000 FE-SEM scanning electron microscope equipped with EDS detector and low-vacuum mode at the at Department of Geoscience, University of Oslo, and a Zeiss Supra 35VP FEG scanning electron microscope coupled with an EDS detector at the Department of Mechanical and

Tab. 2. Whole-rock geochemical sample set

Location	Well	Name	Depth (m)
Halten Terrace	6605/8-1	HD8-1-1	4190.88
		HD8-1-2	4194.2
		HD8-1-3	4198.65
Halten Terrace	6605/8-2	HD8-2.1	3897.1
		HD8-2.2	3909.69
		HD8-2.3	3921.42
		HD8-2.4	3923.8
SW Møre Margin	6204/10-1	M10-1.1	1894.8
		M10-1.2	1949.66
		M10-1.3	1976.55
		M10-1.4	1993.82
SW Møre Margin	6204/10-2 A	M10-2A. 1	2105.25
		M10-2A. 2	2112.35
		M10-2A. 3	2119.69
SW Møre Margin	6204/10-2 R	M10-2R.1	1887.5
		M10-2R.2	1882.45
		M10-2R.3	1872.2
		M10-2R.4	1957.62
SW Møre Margin	6204/11-1	M11-1.1	2011.1
		M11-1.2	2008.65
Halten Terrace	6506/12-5	H 12-5. 11	3176.48
		H 12-5. 12	3179.44
		H 12-5. 13	3185.73
		H 12-5. 21	3149.7
		H 12-5. 22	3157.72
		H 12-5. 23	3163.57
Halten Terrace	6506/12-4	H12-4. 1	3129.57
		H12-4. 2	3138.56
		H12-4. 3	3142.8
Halten Terrace	6505/10-1	H10-1. 1	3694.75
		H10-1. 2	3711.5
		H10-1. 3	3717.28
Halten Terrace	6506/11-3	H11-3. 1	3148.69
		H11-3. 2	3159.6
Dønna Terrace	6507/3-9 S	D3-9S. 11	2851.6
		D3-9S. 12	2856.57
		D3-9S. 13	2865.78
		D3-9S. 14	2869
		D3-9S. 15	2879
		D3-9S. 16	2884.7
		D3-9S. 17	2881.9
Dønna Terrace	6507/5-6 S	D5-6S. 1	4438.8
		D5-6S. 2	4445.68
		D5-6S. 3	4452.85
Dønna Terrace	6507/5-3	D5.3-1	2838.33
		D5.3-2	2846.18
		D5.3-3	2854.33
Dønna Terrace	6507/2-2	D2-2.1	2830.95
		D2-2.2	2827.15
		D2-2.3	2832.45
Dønna Terrace	6507/2-3	D2-3.1	2852.18
		D2-3.2	2869.69
		D2-3.3	2887.53
Dønna Terrace	6507/2-4	D2-4.1	2835.05
		D2-4.2	2843.67
		D2-4.3	2851.9

Structural Engineering and Material Science, University of Stavanger. For CL imaging, the operating condition were at 15kV and 20nA.

U-Pb analyses on detrital zircons of nine sandstone samples were preformed using a Nu Plasma HR multicollector ICP-MS, equipped with a U-Pb collector block and NewWave LUV213 laser microprobe at the Department of Geoscience, University of Oslo. From each sample, 9-115 detrital zircons were analyzed, using the procedures for data acquisition and standardization detailed by Rosa et al. (2009, and references therein). Analyzes were conducted using a 40 μm spot laser beam operating at 10 Hz. The zircon rims with last growth stage were favored. Standard zircon GJ-01 (609±1 Ma; Widebeck et al., 1995) and 91500 (1065± 1Ma; Jackson et al., 2004), were used for calibrate isotope fractionation. ISOPLOT v. 4.15 by Ludwig (2003) was used for calculating ages and visualize concordia and relative probability density diagrams for U-Pb zircon ages. Zircon grains with discordance ≤10% were excluded, because they were considered statistical invalid (considering 1σ uncertainty). The detrital zircon ages in this study are represented as Pb-Pb ages. The zircon spectra presented in the result chapter, with the exception of sandstone samples in Vøring Basin, have a lower and upper interval from the same well. The two intervals within each well are merged because of the low concentration of detrital zircons in these samples.

Results

Lithofacies and sedimentary stacking patterns

Two main sandstone lithofacies are observed (with their subfacies) and include massive sandstone (LB) and graded and laminated sandstone (LC). Three non-reservoir facies are identified: clay clast conglomerates (LA); heterolithic sediments, (LD) including deformed sediment, slumps, debrites, and pelagic and hemiplegic mudstone and marls (LE; Tab. 3). Representative lithofacies are demonstrated in core intervals for the Møre Margin (6204/10-1) and the Halten-Dønna Terrace 6507/2-3) in Fig.5.

Tab. 3.		FACIES ANALYSIS	
Lithofacies	**Subfacies**	**Description**	**Process/ Interpretation**
LA Conglo -merates	LA1 Mud clast conglomerates	Centimeter to decimeter thick sandy- matrix to gravel supported conglomerate. The base is usually erosive with fining upward trend. Commonly located at the base of massive sandstone beds. Clasts mainly comprise of sand- to pebble-size mud clasts or siderite mud clasts and abundant granules of quartz and glauconite.	High energy, rapid dumping from erosive high-density turbidity flows. Bypass lag, or mark the initiation of the channelized turbidite systems.
LB Massive sandstone	LB1 Massive sandstone with sedimentary structures LB2 Massive sandstone without sedimentary structures	Medium to thick bedded, coarse- to fine-grained massive sandstone, typically Ta Bouma (1962) turbidite facies with structure-less and massive appearance. The massive sandstone units have different degree of amalgamation. Faint horizontal lamination or ripple lamination are observed in some of the sandstone. Beds often have sharp to erosive bases. Commonly non-graded and are often overlain by mud-clast breccia or conglomerate. Subangular green mud clasts or granule occur often at base. Some of the massive sandstones are dominated by fluid escape structures, such as dish structures and vertical pillars (few millimeters to few centimeters). Individual beds are usually 1 m thick, but the amalgamated massive sandstone can be few meters thick.	B1: The nonappearance of stratification evidence rapid deposition, either from a hyper-concentrated flows (turbulence suppressed by a high rate if sediment settling close to bedding, (Sensu Lowe, 1982; Mulder and Alexander, 2001; Kneller and Branney, 1995) or rapid fall-out from suspension from high-density turbidite currents. B2: High-density turbidite current post-deformed by dewatering and remobilization.
	LB3 Disorganized mud clast sandstones	Thin to medium bedded, fine- to medium-grained massive sandstone with abundant floating mud chips and granules. The bases are sharp to erosive and bed tops are amalgamated or abrupt.	The abundant floating mud clasts in a massive sandstone may reflect rapid dumping from highly erosive high-density turbidity currents.
LC Graded and Laminated sandstone	LC1: cross stratified sandstone	Fine- to coarse-grained cross-stratified sandstone of medium to thick beds (0.1 -0.8 m). Erosional bases and sharp to gradual tops. Typical capped by massive sandstone intervals. Abundant angular mud clast (flakes) have a tendency to cluster on the forests, especially near the base of the unit. Both, clean to heterolithic textures (contains glauconite, intercalated mudstone and lithic fragments) occurs.	LC1 is interpreted to record deposition by traction currents. The occurrence of glauconite indicate that the sediments mainly are sourced from shelfal systems.
	LC2 ripple cross-laminated sandstone and stratified sandstone	Thin-bedded, fine to very fine grained, poorly to moderately sorted, non-graded to graded sandstone. The sandstone show a parallel stratification and/ or ripple cross-lamination (Tbc, Tb, Tc). The ripple cross-laminated sandstone are typical mud draped. The sandstone beds range from 5 centimeter to about one meter thick. The sandstone usually have a fining upward trend. Climbing ripples are observed. Ductile grains and glauconitic in	Deposition from low-density turbidite flows with gradual waning flow, together with repeated pulses of traction current modification and fallout of suspension (Bouma, 1962; Mulder and Alexander, 2001). Dense bioturbation may be caused by enhanced oxidation rates combined with lower sedimentation rates.

		sand fraction size occur. Bioturbation is common, but to a varying degree.	
	LC3 Graded sandstone	Centimeter to decimeter thick beds (commonly 30-80 cm) of fine to medium grained sandstone, normally graded. Occasional interbedded with mudstones. Partly to fully developed Bouma sequence. Parallel lamination, infrequent followed by ripples is usually present on the upper part of the bed. Commonly bioturbation in uppermost. Coarse glauconite grains occur scattered in the lower part of the beds. Ta/Tb Tabcde divisions of Bouma (1962).	Grain size and grading suggest these sandstones to originate from classical turbidity currents. Mud interbedding reflects a period of low sedimentation and fallout of fine sediments.
LD Heterolithic sediments	LD1: Debrite, Clay clast breccia	Poorly sported, matrix rich sandstone with disorganized scatted sub-angular mud-clasts (up to 8 cm). Centimeter to meter-scale thick beds, and variable range in grain size. The sandstone are generally massive and structure-less with sharp to gradual base. Inverse grading occur. Banded, matrix- rich sandstone also fall under this facies category.	LD1 represent deposition by cohesive mud-rich matrix "plastic" flows (e.g. Shanmugam, 1996). The disrupted mudstone could be transported from an adjacent collapsing channel margin or submarine slope and incorporated into the sandstone. The banded matrix- rich sandstone is inferred to reflect transformation of flow events, known as linked debrites or hybrid beds (e.g Haughton et al., 2003).
	LD2: Slide, slump/ deformed sediment	Slide and slumps are general decimeter-thick-units. The sandstone and associated mudstone are contorted and or mildly deformed and folded.	Post depositional deformation by slumping and sliding. Comprises in low-density turbidite sands, and mild deformation and folding.
	LD3: Injected sandstone	Sand sills and dikes, and deformed sandstones are representative for this facies. Sills make layer parallel to the stratification, whereas dykes are frequently injected from the base upwards. Sand injection are common in Variable thickness of beds (mean=30cm)	Post depositional deformation by loading and injection.
LE Pelagic and hemiplegic mudstone and marls	Turbiditic, Contouritic, Hemipelagic, Pelagic	Millimeter to tens of meter-scale laminated mudstone, occasionally interbedded with sand lenses and mm-cm silt stripes. Commonly occurring between beds of different lithostratigraphy. Bioturbation is common.	LE represents one of the following two possible products, or a combination these: 1) low-density turbidity current in a general low-energy setting; 2) hemipelagic background fallout of suspended fine material.

Facies associations

Lithofacies were grouped into eight major facies associations that represent their sub-environments (Tab.4.). These facies associations include channel-fill sandstone, channel -to lobe transition zone sandstone, central lobe sandstone, marginal to peripheral lobe successions, lobe fringe heterolithics and background strata. The distribution of facies associations are noted as following: FA1= 28%, FA2=6%, FA3=0%, FA4=35%, FA5=4%, FA6=13%, FA7=6% and FA8= 9%. The cores intervals from the Dønna Terrace (6705/2-2, 6705/2-3 and 6507/2-4 are dominated by channel fills and peripheral to marginal lobe (35%) in an upper fan slope setting. Mass tranport complex (13%) is common on the Halten-Dønna Terrace and the Møre Margin and verify slope settings. Distal to marginal lobes in an outer-fan setting (FA4) are the dominated facies assoiations in wells in the Vøring Basin (Distal Halten).

Apparent tidal facies association are identified in 6506/12-5, but not listed in the table because of its limited occurrence. This facies comprising tough-cross bedding, rip-up mud casts, rhythmic bedding and double mud draping at current ripples. However, the lower core interval consists of contorted sand and mudstone and ripple-cross laminated sandstone, indicating a deep marine environment. Representative detailed core logs with interpreted facies associations for the wells in the Vøring Basin, Halten-Dønna Terrace and Møre Margin are presented in figures 7,8 and 9.

Tab. 4. Facies association

Facies associations	Facies Description	Subenvironment
FA1: Channel fills, Channel margin, channel belts	Bed sets commonly amalgamated, meters thick and erosive based. Fining upward trends are prominent. Dominant facies are stratified sandstone, ripple cross-laminated sandstone, mud-chip sandstone and conglomerate (LC1, LC2, LB3, LA1). Subordinate, interbedded mudstone intervals and slump strata and slides (LD2).	Upper fan channels, proximal channel belt 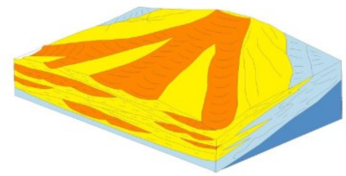
FA2: Channel to lobe transition, proximal lobe	Meter thick bed-sets. Amalgamated to channelized bed-sets, which are erosive and scoured. Fining upward trend or complex thickening and thinning upwards trend. Constituent facies include stratified and cross- stratified sandstone (LC) and shale clast conglomerate. Thin mudstone commonly separating the sandstone.	Channelized lobes in proximal fan setting, channel to lobe transition. 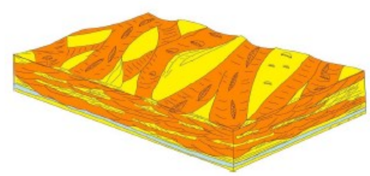
FA3: Central lobe	Thick-bedded, layered to amalgamated bedsets. Thinning and thickening motifs are close to symmetrical. Dominantly comprised of massive sandstone (LB) as well as Tabc turbidite facies. Hemipelagic facies (LE) separates the Tabc and stratified sandstones.	Channelized/scoured to non-channelized lobes in mid-fan and outer fan location. 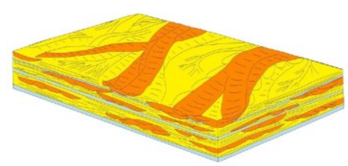
FA4: Intermediate-distal lobe (Peripheral to marginal lobe)	Thin to thick sheet-like layered bedsets. Main components are massive (LB), stratified and ripple laminated sandstones (LC2), and thin to intermediate bedded Tbcd and Tcd beds. Additionally, facies such as, slump and slides (LD2) and debrites (LD1) occur. Sandstone bed sets are commonly separated by thin mudstone packages.	Distal to marginal lobes in midfan and outer-fan settings. 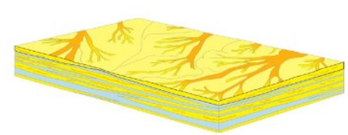 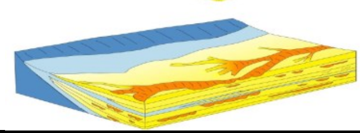

FA5: Fan-fringe, interlobe, distal lobe	Thin- bedded, layered sandstone sheets, frequently coarsening to fining upward trends. Tbcd and Tc turbidite beds dominating (LC), and separated by thin- to thick-bedded mudstone intervals.	The distal margin of individual lobes in outer-fan setting. 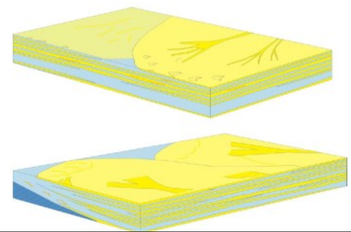
FA6: Mass-Transport complex: Slump and debrites	Layered, sandstone packages of variable thickness. Thick-bedded intervals of slumped typical turbidites (Tabcde) and deformed sandstone and injectites are common. Sandstone alternates with mudstone intervals. Debrites and hybrid beds (banded colors, common dewatering structures also induced)	Channel-mouth lobes, slump-folded. Debris flow tongues or diverse mass transport deposits in mid to inner-fan settings. Hybrid bed: Deposit from a flow fluctuated between cohesive and turbulent state (eg. Baas et al., 2009).
FA7: Overbank	Intercalated mudstone and thin-bedded silt and fine sandstone.	Fine-grained facies outside the main (slope) channel(s).
FA8: Background	Millimeter to centimeter thick silt and fine sand laminae interbedded with centimeter to decimeter hemipelagic to turbiditic mudstone.	Slope-to basin floor mudstone sheets. 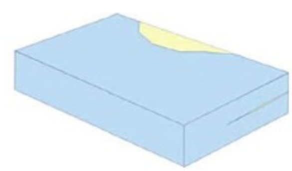

Representative figures are from Shell in house.

Halten-Dønna Terrace

The well 6507/2-3 is located within the elongated north-south trending slope on the Dønna Terrace, and consists of 43 m thick Lysing sand succession. The base of the formation is characterized by a relatively thin conglomeratic lag (LA1). Several thick sandstone intervals, constitute of a numerous intervals with 1-3 m thick fining upward trends of massive and dewatered sandstone (DB), rippled and laminated sandstone (LC2), laminated mudstone (LE) and deformed mud- prone heteroclites and debrites (LD1, LD2). The deformed area observed below the conglomerate is assumed to be produced by an overriding gravity flow due to shearing effect onto previously deposited clay and silt (Fig.5B). In addition, the coarse sand-filled burrows within the mudrocks indicated that the sediments bypass this. The common slumped events and presence of tree debris and coal fragments suggest a proximal setting. An overall thickening upward is marked, together with a gradual cleaning of sandstone from mud clast-rich at the lower interval to relatively clean sandstone at top of the Lysing unit in well 6507/2-3. This implies that the base are characterized with lower energy compared to the top Lysing, which has higher energy for deposition. Granule lag lithofacies and scoured and rippled bed tops can be indicators of bypass (Kneller and McCaffrey, 2003).The planar and erosional bases of dewatered and massive sandstone, with locally angular mudstone clasts, is consistent with a channeling setting (FA1-FA2) and bypass (Fig.6.).

Well-established contorted mudstone, with slump folds are present in 6507/2-2. The well is located west of the well 6507/2-3, on the Dønna Terrace and comprise 18 m of lysing core interval. The dominant lithofacies contain sandy-debrites with abundant floating mud chips (LD1 and LB3) and larger mudstone clasts (Fig.8.). The random to planar orientation of these elongated to rounded mud chips and mud clasts located at top of the bed, may indicating a laminar flow (plastic rheology) that are common in debris flows (Fisher, 1971).

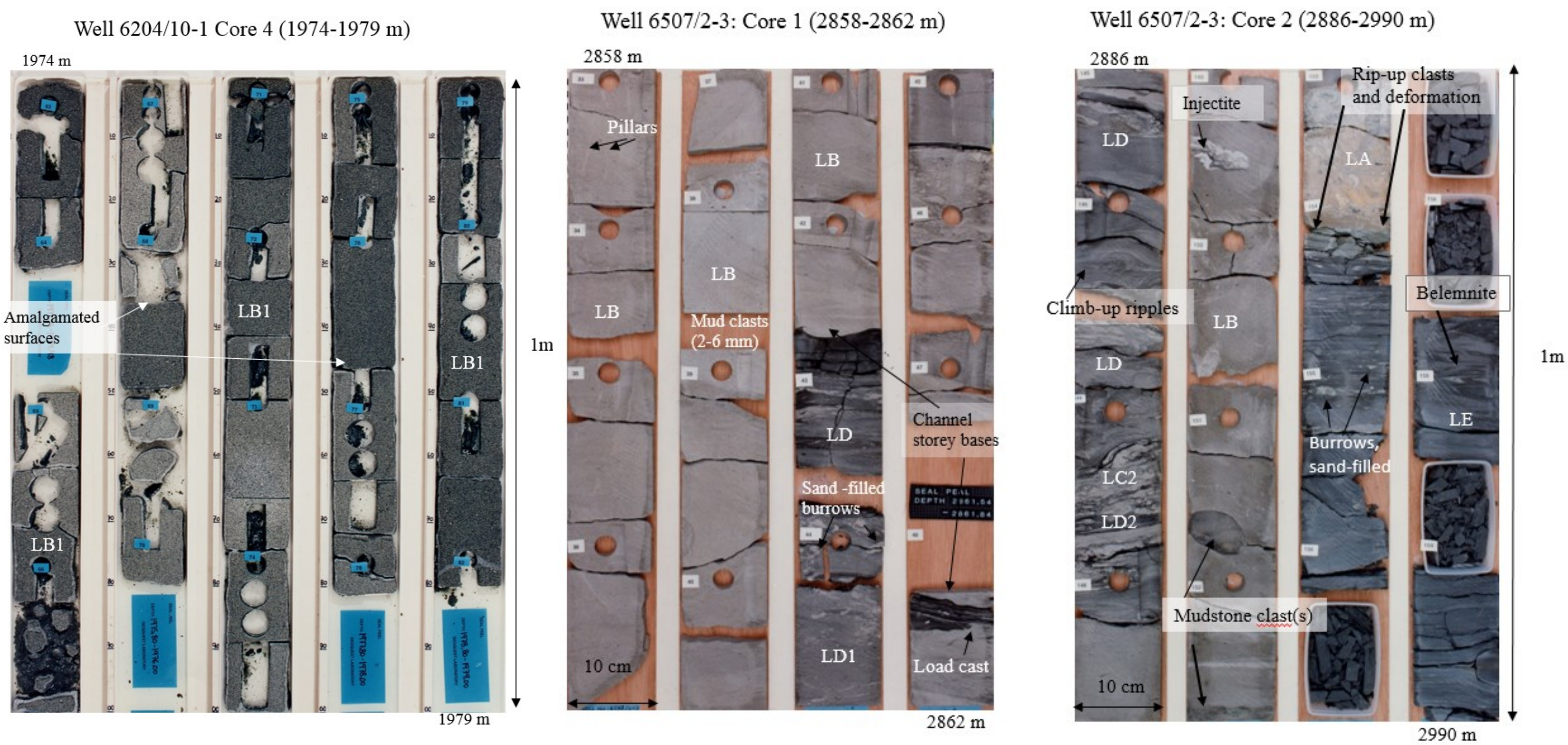

Fig. 5. Well core photographs with lithofacies interpretation. from A) Møre Margin and B) Halten-Dønna Terrace. The core is 10 cm wide.

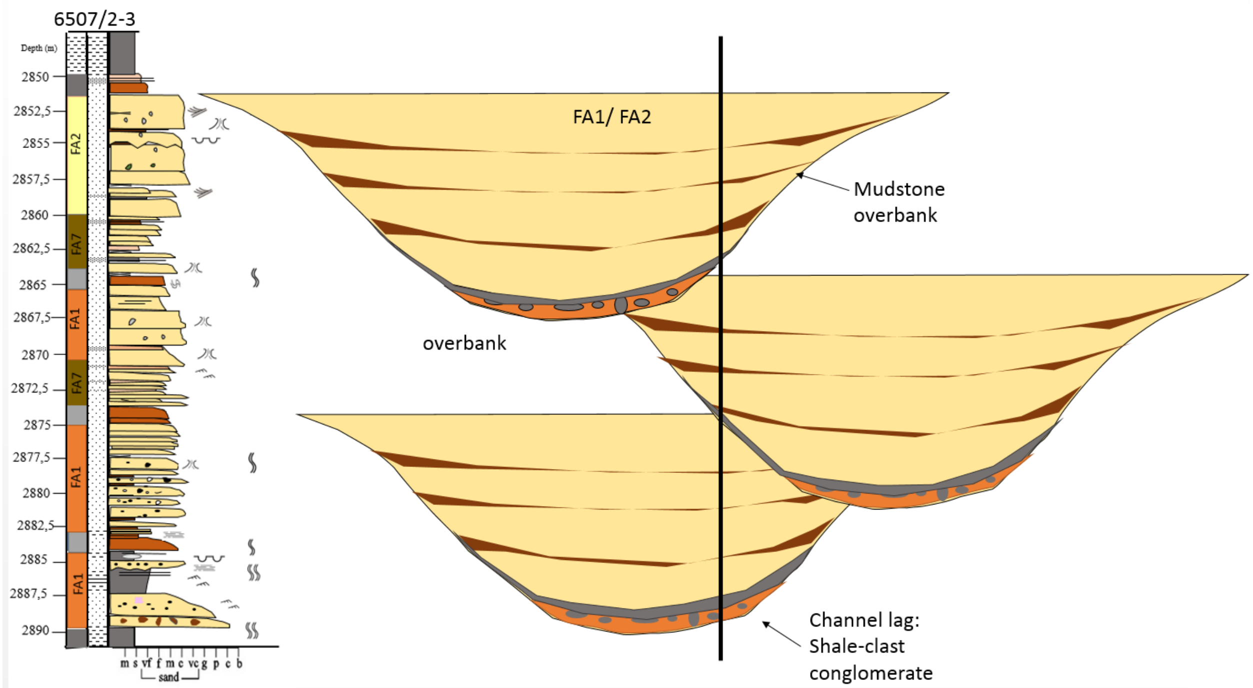

Fig.6. Schematic representation of possible channel elements in core interval for well 6507/2-3.

Dilution and deceleration of the flow may transform a turbulent flow to a debrite flow. Pulses of these may result in the colored banding as seen in well 6507/2-2. The sandstone bodies of Lysing in well 6507/2-2 are characterized by an overall fining upward trend. The combination of facies favors an intermediate to distal lobe setting. Fan fringe to marginal lobe setting, are also indicated by the dominance of massive sandstone (LB), stratified and ripple laminated sandstones (LC2), subordinately with slump and debrite facies (LD).

Well 6507/5-3 is located at the slope of Dønna. The upper core interval comprise 55 m thick sandstone, with series of 1-1,5 m thick fining upward sequences of cross stratified sandstones (L1), massive and dewatered sandstone(LB1, LB2) and overlain by banded sandstone, associated with linked debrites (LD1). A 5 cm layer of siderite is observed, indicating prodelta material, reducing part (2838m). The banded sandstone, large ripples, and deformed strata suggest rapid dumping of sediments and alteration between turbulence, debris and more cohesive and cogenic flows (linked debrites). The sandstone in this core defines a general coarsening upward trend.

The distal part of Halten Terrace (Vøring Basin) is characterized by marginal lobe association and background hemipelagics. It is dominated by the fine –medium grained, thin to medium interbedded graded sandstone or laminated sandstone, typical Bouma divisions of Tabdf and Tbcd. Cross-laminated matrix-rich sandstone are also well developed. Abundant pin-striped bioturbated laminated mudstone intervals separating the sandstone are common in well 6605/8-2 (Fig.7.). The sediment dispersal is controlled by topography basin bounding faults.

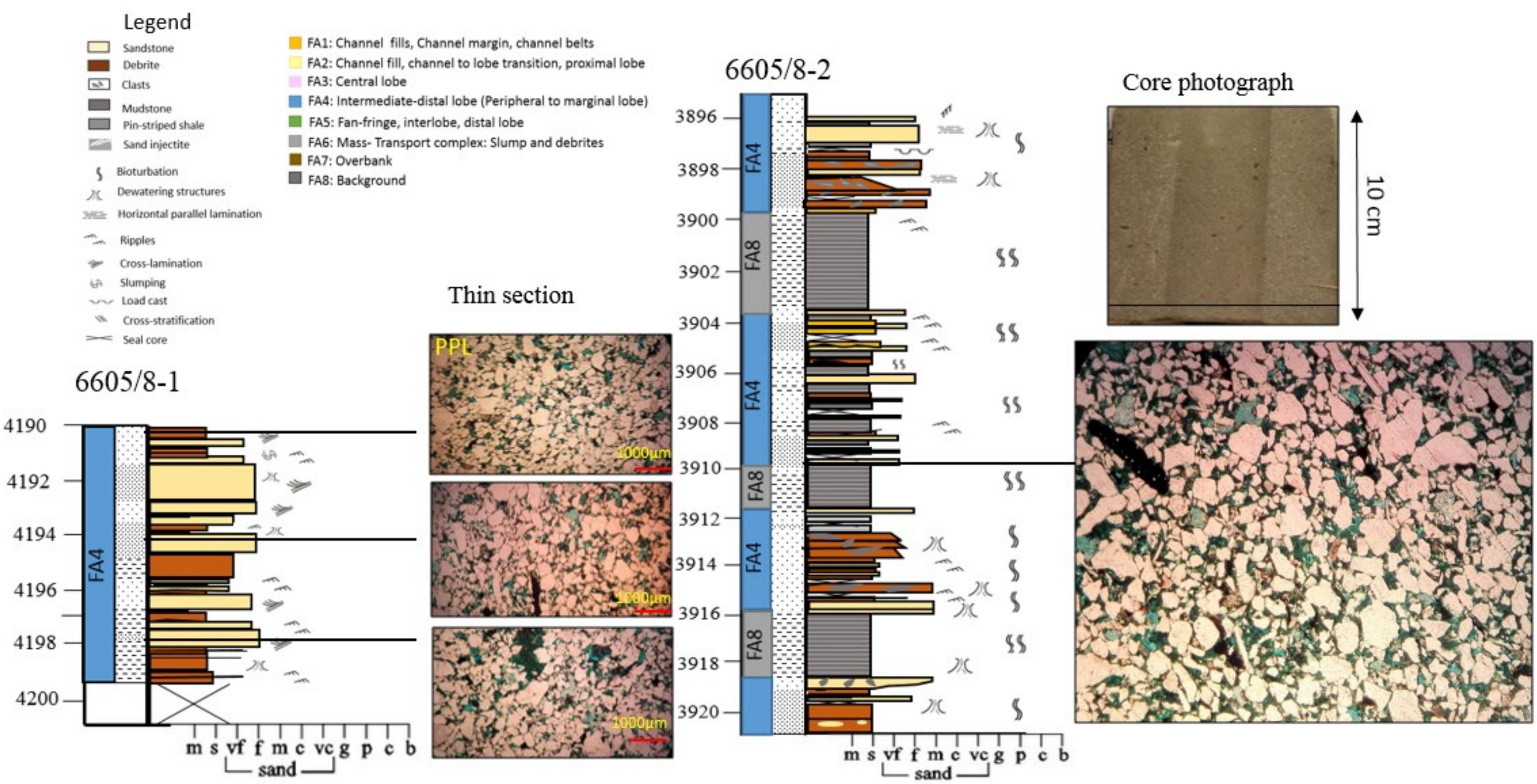

Fig.7. Detailed sedimentary logs with interpreted facies associations for wells in Vøring Basin with associated core photograph and marked sample position of the thin sections

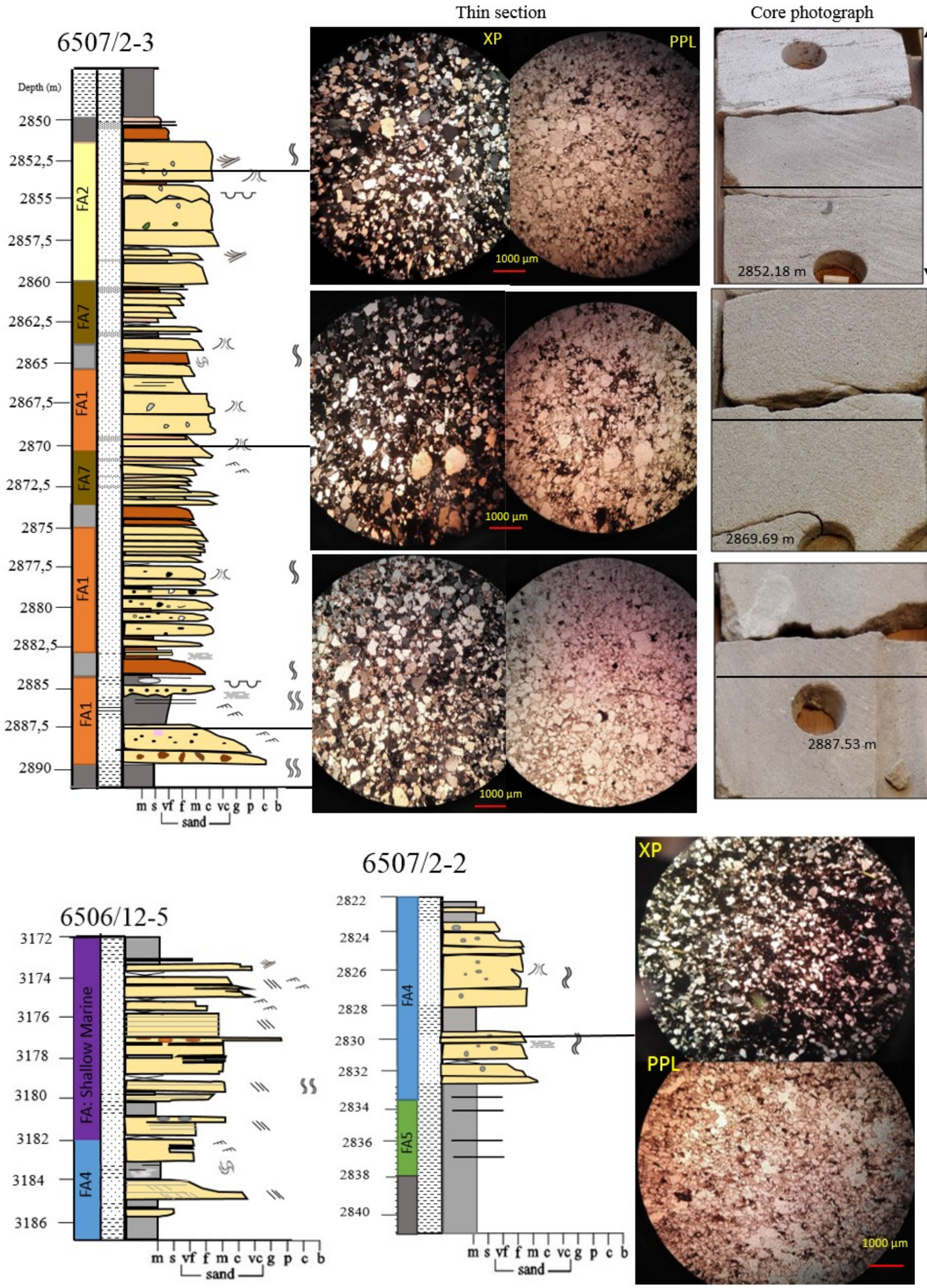

Fig. 8. Sedimentary logs with facies associations for wells on Halten-Dønna Terrace combined with core photographs and sample position of the thin sections

Møre Margin

The bulk of the sand-rich facies in 6204/10-1, located to the SW of the Møre Margin (Slørebotn) have a massive appearance, denoting Ta division from Bouma (1962) .Vague stratification, with faintly parallel mineral alignment are also observed in this massive sandstone (LB). Amalgamated surfaces are abundant, as well as erosive and sharp bases separating these sandstones. Subordinate facies include silty sandstone with claystone clasts. This facies favor deposition at the base of the channel, whereas the amalgamated sandstone represents channel fill in an overall channelized setting. The high abundance of glauconite in the sandstone suggest redepositing from a paleo-shelf.

Well 6204/11-1 encountered a 6 m-thick Lysing sandstone interval on the Møre margin. The basal part consists of matrix -rich sandstone and slumped facies, overlain by beds with common coarse grained- sand injectites (LD3). Folded and deformed silty sandstone beds are also present (LD1). Thin-bedded parallel laminated fine-grained sandstone (LC2) dominates the mid-section of the core interval and represent variable and waning flow conditions with variation from low to high turbidite currents. In addition, common banded facies suggest transitional flow regimes dominated.

The lower part of 6204/10-2R (Møre Margin) show distinct low-density turbidite to medium-density turbidite currents. Well-developed Tabcde is observed in this interval (LC). The upper part is characterized by debrites, banded facies, deformed and sand injectites (LD). These units are capped by heterolithic interval. In addition, muddy to silty sandstone with abundant limestone-clast are present within core interval of 1954-1960m in 6204/10-2R. Channel-to-lobe or slump-folded and diverse mass transport deposits in an inner-fan settings are suggested subenvironment for the middle interval, whereas the lower and uppermost interval is inferred to have distal lobe setting.

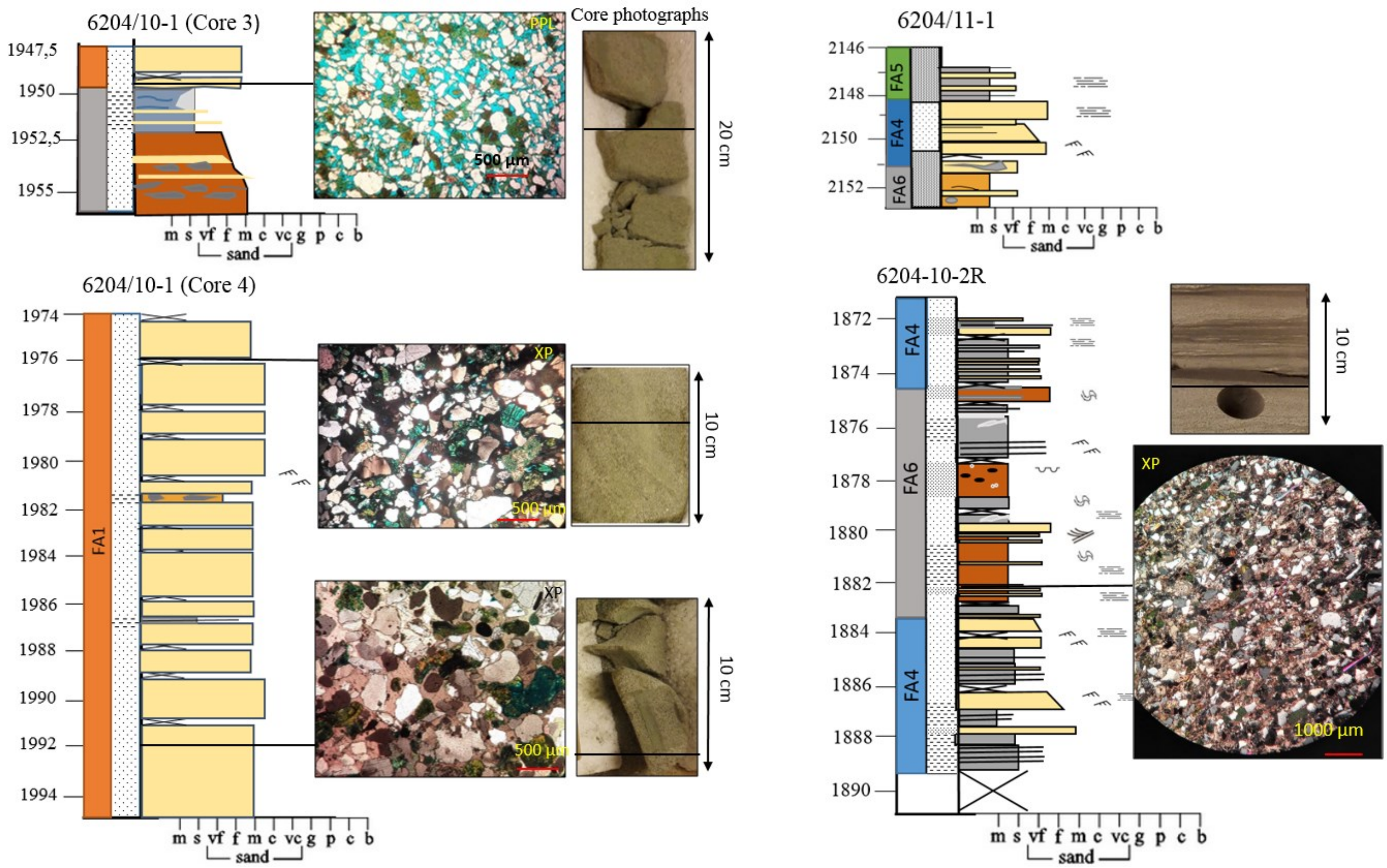

Fig.9. Sedimentary logs and facies associations from cores in the Møre Margin combined with core photographs and thin section photographs. The black line marks the sample position of the thin sections.

Petrography

The analyzed sandstone of the Lysing turbidities are mostly fine to coarse grained, sub-angular to well-rounded and moderately to well sorted (Tab.7.). The sandstone samples from Møre Margin tend to have a coarser sand fraction and better sorting than samples from the Halten-Dønna Terrace. However, the grain size is bimodal in samples from Vøring Basin with large quantity of larger sand fraction 500-700µm. The major grain-to grain contacts observed include floating grains, plane contact, suture and point contact (Tab.5). The granulometric characteristics of the different sandstone petrotypes are presented in Tab.5.

The sandstones of Upper Lange-Lysing comprise of framework grains (avg., 61.7%), porosity (avg., 8%) and diagenetic cements (avg., 15%) together with near absent amounts of matrix. The framework grains consist predominantly of quartz and minor amounts of lithic fragments and feldspars. The majority of the sandstone samples are classified subarkose and sublithic arenite and subordinate quartzarenite using the classification diagram after Folk (1974; Fig.10B). The average sum of the total detrital framework mode is $Qt_{94}F_4L_2$ (%, Q=total quartz, including chert and polycrystalline quartz; F= feldspar; L= lithic fragments). Including the total lithic fragments, gives a different composition, with average framework $Qm_{82}F_4Lt_{14}$ (%, Qm=monocrystalline quartz, F=Feldspar, Lt = Total lithic fragment). The sandstone in the Møre Margin has an average framework composition of $Qt_{90}F_8L_2$, whereas the sandstone on the Halten- Dønna Terrace has average framework of $Qt_{95}F_3L_2$ (Fig. 10A). Most of the sandstone samples are textural and compositional mature, particular the samples from the Vøring Basin, with average framework composition of $Qt_{97}F_2L_1$. Their framework composition is in accordance with craton interior and subordinate recycled orogeny, according to the provenance fields of Dickinson (1983). For comparison, the QmFLt ternary plot after Dickinson 1983 display a cluster that is equally divided between craton interior and recycled orogen.

Three petrofacies are identified by looking at framework composition: 1) quartzarenitic; 2) quartzolithic; and 3) quartzofeldspathic petrofacies. The quartzofeldspathic facies comprise over 10% feldspar of the total detrital grains, with irregular but usually amounts of lithic fragments, whereas the quartzolithic petrofacies, encompass (meta-)sedimentary lithic arentites, and mainly included pelites, psammites and metapelites lithoclasts. The quartzofeldspathic facies is typical medium-coarse sand. Samples from Møre Margin is in accordance with quartzofeldspathic facies, and the Halten-Dønna Terrace have patterns of quartzolithic petrofacies. The samples from the Vøring Basin have particular high quartz amount and low abundance of other detrital framework grains.

Tab.5. Granulometric scheme of the sandstone samples from Lysing Formation

Sample	Depth	Mean grain size (µm)*	Max grain size (µm)*	Sorting	Roundness	Sphericity	Main grain contact	Sand fraction size
HD 8-1,1	4190.78	250	1100	M	SA-SR	L -M	Pl+ CC	f-m
HD 8-1,2	4194.16	275	1250	MW	SA-SR	M	Pl+ CC	f-m
HD 8-1,3	4198.03	250	1300	M	SA-SR	H-M	PL+S	f-m
HD 8-2,2	3909	275	1700	MW	SA-R	M-H	Fl	m-c
M10-1,1	1949.66	325	1150	M-W	SA-R	M	Fl + Po	m-c
M10-1,2	1976	425	1500	M-W	SA-R	M	Fl + Po	m-c
M10-1,3	1992	300	1100	M-W	SA-R	M	Fl + Po	m-c
M-10-2A	2112.2	125	1500	P-VP	SA- AR	L-M	Fl	vf-f
M-11-1	2017.5	175	1100	M	SR-SA	M-H	Pl + Po	f-m
M-10-2R	1882.27	150	650	W	A-SA	L-H	Pl + Po	vf-f
D2-3, 1	2852.18	225	800	W	SA-SR	M-H	Pl +CC	f-m
D2-3, 2	2869.69	175	1150	M	SA-SR	L-H	Pl + Po	f-m
D2-3, 3	2887.53	175	100	M-W	SA-SR	M	Pl + Po	f-m
D2-2, 2	2827.15	150	550	W	SA-SR	L-M	Pl + Po	f
D5-6S,2	4445.68	200	1000	M	SA-SR	L-M	Fl+ Po + Pl	f-m
D5-3, 2	2846.18	175	1200	M-P	SA-SR	M	Pl + Po	f-m
D5-3, 3	2854.33	190	1150	M-P	SA-SR	L-H	Fl+ Po + Pl	f-m
D-2-4, 2	2843.67	180	1000	MW	SA-SR	M-L	Pl+Po	f-m

P, Poor; M, Moderate; A, Angular, SA; Subangular; SR, Subrounded; L, Low; M, Medium; H, High; CC, Concave-convex; Pl, Plane; Fl, Floating; Po, Point; S, Suture; vf-f, very fine-fine sand; f-m, fine-medium sand; m-c, medium-coarse sand. *Longest axis of grain is measured.

Tab.6. Point counted cement, matrix, porosity in percentage of total rock volume and calculated IGV

Sample	Clays	Qz	Ka	Illite	Siderite	CC	Glau.	Fe	Micritic matrix	Mix cl/cc	Sum cement	MP/PS-G	Sum porosity	Inter. Poro.	Intra. Poro.	Oversized Pores	Fracture porosity	IGV
HD 8-1,1	-	1.5	3.4	1.5	-	3	-	-	-	-	9.4	-	17.3	11.3	4.7	1.3	-	20.7
HD 8-1,2	0.4	1.6	7.8	1.2	1.4	2.2	-	1.8	-	0.6	17	-	14.3	10.4	3.5	0.4	-	26.1
HD 8-1,3	-	-	5.9	0.5	-	0.3	-	-	-	-	7.3	4.4	5.7	2.4	1.6	1.4	-	9.2
HD 8-2-	-	0.3	3.2	1.6	0.7	2.0	-	1.4	-	-	9.2	13.2	5.8	3.2	0.9	1.6	-	12.4
M10-1,1	-	0.3	-	6.1	-	-	1.6	1.3	-	-	9.3	-	22.8	14.1	8	0.8	-	23.4
M10-1,2	-	0.4	0.5	5.4	-	0.2	-	0.5	-	-	7	8.6	19.7	14.3	2.7	2.7	-	21.3
M10-1,3	-	0.3	-	6	-	0.3	-	-	-	-	6.6	-	17.1	5.7	5.7	1.2	-	12.3
M-10-2A	-	-	-	-	-	-	-	-	63.8	-	0	-	-	-	-	-	2.5	
M-11-1	-	-	0.3	-	-	1.9	-	0.8	-	10	13	-	10.6	6.9	3.2	0.3	-	19.9
M-10-2R	-	-	0.5	-	1.5	21.5	-	1.4	-	-	24.9	-	0.7	0.7	-	-	-	25.6
D2-3-1	-	1.3	3.3	6.1	1	0.3	-	3.5	-	-	15.5	-	7.3	3.8	3.3	0.5	-	19.3
D2-3-2	-	1.4	0.2	3.1	-	0.2	0.8	24	-	-	29.7	-	3.3	2.6	0.2	0.4	-	32.3
D2-3-3	3.5	3.8	3.3	0.9	-	14.8	-	2.1	-	-	28.4	-	4	3.5	-	0.2	-	31.9
D2-2,2	-	1.3	0.9	8.1	0.2	4	-	7.7	-	-	22.2	-	9.1	8.4	-	0.7	-	30.6
D5-6S,2	-	-	0.9	1.9	-	1.4	0.9	4.7	-	-	9.8	-	-	-	-	-	-	9.8
D5-3-2	-	2.3	0.3	4.5	0.6	-	-	6.2	-	-	13.9	-	3.7	3.1	-	0.6	-	17
D5-3-3	-	3.6	1.2	10.9	-	-	-		-	-	15.7	-	-	-	-	-	-	15.7
D2-4-2	-	1.70	0.8	5.8	-	2.5	-	5	-	-	15.80	-	8.3	5.8	1.7	0.8	-	21.60

MP/PS-G, Microporosity/ Pseudomatrix of glauconite; Inter.Poro, Intergranular porosity; Intra.Poro, Intragranular porosity; Fe, Iron oxide cement; CC, Carbonate cement; Ka, Kaolinite; Qz, Quartz; Mix cl/cc, Mix of clay cement, chlorite, and calcite; IGV, Intergranular volume

Tab. 7. Total framework composition in percentage of total counted grains

Sample	Depth (m)	Qm, nu	Qm, u	Qp, 2-3 xx	Qp, >3 xx	Cht	K	P	Lv	Ls-pel	Ls-psa	Lm-pel	Lm, psa/ silt	M	Bt	Op	Gla	Bio clast	cl. clast	Psed.	QFL % Qt	F	L	QmFLt % Qm	F	Lt
HD 8-1,1	4190.78	1.7	80.2	5.5	6.7	-	1.5	0.3	-	-	-	1.7	-	1.2	0.3	0.3	0.6	-	-	-	96.4	1.8	1.8	83.9	1.8	14.3
HD 8-1,2	4194.16	3.8	81.8	2.6	5.8	-	0.9	-	-	-	-	-	-	2	-	2.9	-	-	-	-	99.1	0.9		90.2	0.9	8.8
HD 8-1,3	4198.03	9.5	71.8	4.7	4.7	-	1.3	0.3	-	-	-	-	-	5.0	0.3	-	0.6	-	-	0.6	98.3	1.7		88	1.7	10.3
HD 8-2,2	3909.00	8.4	69.9	4.2	5.2	-	1.9	1.3	-	1.9	-	0.6	-	1.6		3.2		0.3	1.6	-	93.8	3.5	2.8	83.7	3.5	12.8
M10-1,1	1949.08	2.3	47.7	4.3	14.5	0.4	9.4	0.4	-	0.4	-	-	-		0.4	0.8	19.5	-	-	-	87.2	12.3	0.5	63.1	12.3	24.6
M10-1,2	1976.55	2.7	52.6	5.2	18.6	-	8.9	1.0	-	0.3	0.3	-	2.4	0.6	1.4	1.7	3.8	0.3	-	-	85.8	10.8	3.4	60.1	10.8	29.1
M10-1,3	1992.00	3.2	63.1	7.4	13.8	-	9.7	2.3	-	-	-	0.5	-	0.9	1.8		32.7	0.9	-	0.5	87.6	12.0	0.5	66.4	12.0	21.6
M-10-2A	2112.2	0.7	38.8	2.2	3.7	-	0.7	-	-	-	-	-	0.7	3.7	5.2	1.5	13.4	29.1	-	-	96.8	1.6	1.6	84.1	1.6	14.3
M-11-1	2017.50	2.4	53.1	4.1	4.8	-	3.8	1.0	-	-	-	0.3	-	2.1	2.4	2.1	17.6	2	-	4.1	92.6	4.8	0.5	79.7	0.5	19.8
M-10-2R	1882.27	1.1	35.2	1.4	3.0	-	3.2	-	0.2	1.6	-	-	0.7	2.3	1.1	1.1	6.6	7.1	-	9.8	87.7	6.9	5.4	78.3	5.4	14.8
D2-3,1	2852.18	8.8	66.7	4.1	3.5	0.9	1.3	0.6	-	1.3	-	0.3	0.6	2.8	-	-	1.2	0.3	5.3	1.9	95.4	2.1	2.3	85.7	2.1	12.2
D2-3,2	2869.69	6.1	73.9	2.4	3.0	0.6	1.2	0.6	-	1.50	1.9	0.6	-	3	0.9	-	2.1	-	0.6	1.2	94.6	2.0	3.4	88.0	2.0	10.0
D2-3,3	2887.53	4.9	81.3	5.3	3.6	0.3	2.0	-	-	-	-	0.3	-	0.3	-	-	0.3	-	-	-	95.0	3.6	0.4	86.8	6.6	13.2
D2-2,2	2827.15	7.1	83.8	2.9	2.5	0.4	1.4	1.1	-	-	-	0.4	-	5.4	-	2.2	2.2	-	4.3	-	96.7	2.9	0.4	90.8	2.9	6.3
D5-6S,2	4445.68		0.65	0.03	0.05	0.01	0.02	0.01	-	0.5	0.5	0.5	1.5	1.5	-	3.6	1.5	-	-	16.0	95.3	2.7	2.0	88.0	2.7	13.3
D5-3,2	2846.18	7.9	59.1	3.1	2.7	1.4	0.7	1.0	-	1.7	-	1.7	-	3.4	6.9	1.7	2.7	1.4	0.3	7.6	93.5	2.2	4.3	84.5	2.2	11.3
D5-3,3	2854.33	1.1	50.8	0.5	2.6	0.5	1.1	1.1	-	-	0.5	0.5	-	1.1	-	-	-	-	-	25.7	94.6	3.6	1.8	88.3	3.6	8.1
D2-4,2	2843.67	8.8	67.0	3.3	2.2	3.3	2.2	-	-	1.1	-	-	-	4.4	-	4.4	1.1	-	-	2.2	93.3	2.5	1.2	86.3	2.5	11.25

Q, quartz; Qm, monocrystalline quartz; Qt, quartz total (=Qm+ Qp+ Cht); Qmu, undulatory monocrystalline Q; Qnm, non-undulatory monocrystalline Q; Qxx, crystals; F, feldspar; L, lithic fragments, Lt, total lithic fragments (= L+Qp); Cht, chert; K, K-feldspar; P, Plagioclase; Lv, volcanic L; Ls, sedimentary L; Lm, metamorphic L; pel, pelite; psa, psammite; M, Muscovite; Bt, Biotite; Op, Opaque minerals; Gla, Glauconite; Bio, biological; cl, clay; Pseu, Pseudomatrix

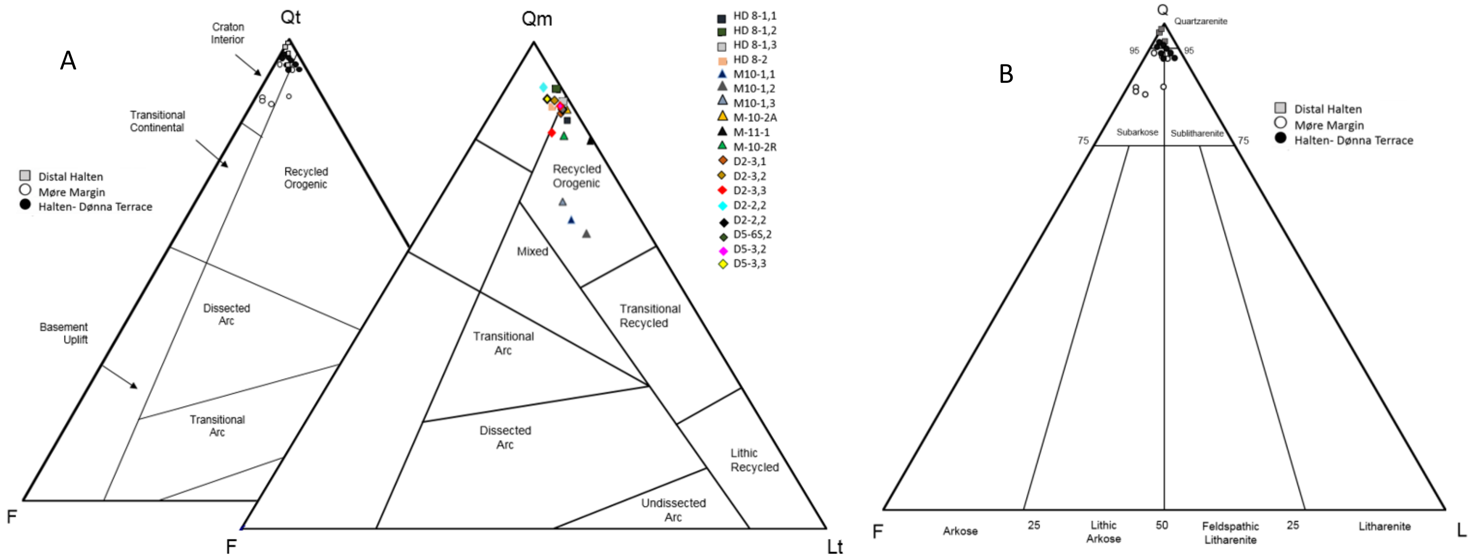

Fig. 10A) QtFL and QmFLt provenance diagram after Dickinson (1983); 9B) Classification scheme with discrimination fields after Folk (1980).

Quartz (Qt) is the major framework component and ranges from 85.8 to 99.1% of the total grain composition, with an average value of about 93.5%. Monocrystalline grains usually show undulose extinction and irregularly comprise inclusion (such as zircons, tourmaline). Polycrystalline quartz are most abundant in medium-coarse sand fraction. The intercystalline boundaries of the sub- crystals in the polycrystalline quartz range from straight to suture. The chert content is overall low. The quartz composition plots in discrimination field of low-grade metamorphic granite source area (Fig. 11.).

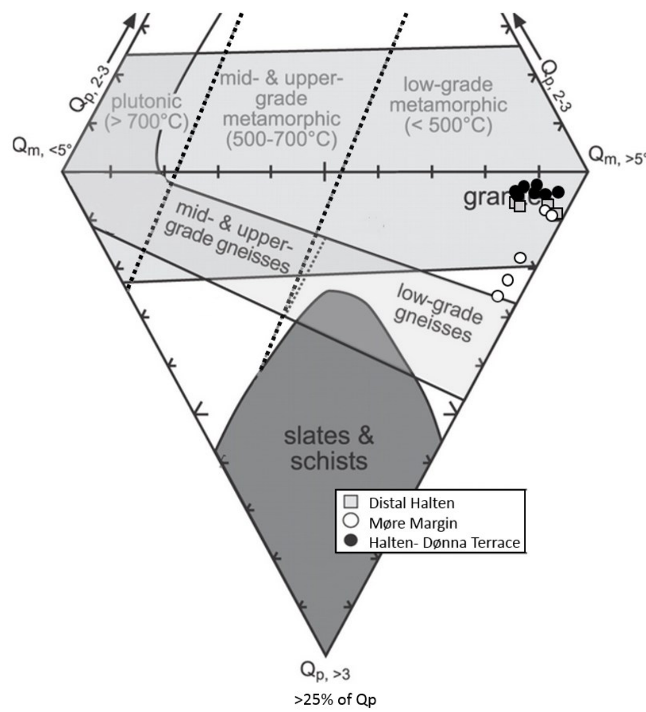

Fig.11. Quartz diamond diagram with discrimination fields from Tortosa et al. (1991) and the black dotted lines indicate provenance fields by Basu et al. (1975). Qm<5°= non-undulatory monocrystalline quartz; Qm<5°= undulatory monocrystalline quartz; Qp.>3= Polycrystalline quartz, > 3 crystals per grain; Qp,2-3= Polycrystalline quartz, 2-3 crystal per grain.

Feldspar is the second abundant framework grain in the sandstone samples, (0.9 to 12.3 % of total counted grains) with an average of 4.3%. They occur in higher quantities in sandstone from the Møre Margin than on the Halten-Dønna Terrace. K-feldspar (avg.

2.3%) tend to be more abundant than plagioclase (avg. 0.6%). Microcline, perthite and sericitised K-feldpsar are the dominant K-feldspar types in the samples. Plagioclase with albite twins could often be identified. The feldspars are fresh to intensively altered to clay minerals, or replaced by cement (calcite or iron oxide). Albitization of K-feldspar is common.

The Lithic fragments (L) are recorded in the majority of the sandstone, with trace amounts to 5.4% of counted grains. They include sedimentary (siltstone, sandstone, pelite, avg.=3.8%) and metamorphic (slate, metapsammite phyllite, schist, quartzite, avg.= 2.7%) detritus, as well as carbonate rock fragments. High abundance of the pelite lithoclasts, (consist of clay minerals, chlorite, microquartz and mica) form ghost-structures, and some are partly deformed (e.g. 6507/5-3). Many of the bioclasts (i.e. foraminifera) are leached and is associated with moldic intragranular porosity. Volcanic fragments are exceptionally rare in the studied samples. Overall, samples located in Møre are richer in polycrystalline quartzose, and consequently have a higher total lithic fragment content (Lt). Mud clasts are commonly observed.

Other detrital minerals include mica (avg., 3.5%), glauconite (avg., 6.6%), opaque mineral/ iron oxide clasts (avg., 1.4%) and bioclasts (carbonate clasts/fossils, avg.,2.3%) are of variable abundance in the sandstone (Tab.7.). Glauconite grains are especially abundant in samples from Møre Margin (6204/10-1: up to 30%) and decreasing trend seaward, thus Vøring Basin samples have lowest content. The glauconite grains are commonly deformed and squeezed between adjacent detrital grains. Bioclasts are mostly found in wells from Møre Margin, however, low quantities are detected in the Vøring Basin and on Dønna Terrace. The mica grains are often observed bendend or derformed. Few of the muscovite have partly altered to chlorite. The abundance of muscovite is higher in thin sections from Halten-Dønna Terrace and distal Halten, with the exception of sample D5-3.2. Frequently, iron oxide had replaced the mica along some of the cleavage planes.

The content of matrix is scares, except for the calcareous sandstone (6204/10-2A) from the Møre Margin. Pseudomatrix is more abundant and generally composed of very fine-grained quartz, mica and clay minerals). The pseudomatrix content is usually low, and range from trace amounts to 25.7%, (avg. = 3.9%) of the total rock volume, and is assumed to derive from intensively deformed fragile lithic clasts. Particular sample in the lower debrite facies of well 6507/5-3 on Dønna Terrace, have high pseudomatrix content (25.7%). However, there is some uncertainties in differentiation between primary matrix and alteration of fragile detrital minerals into pseudomatrix (criteria defined by Dickinson, 1970). Disregard of pseudomatrix can explain framework dissimilarities and lead to different framework composition.

The accessory heavy minerals include major component of zircon and minor abundance of rutile and tourmaline. The heavy mineral assemblage range from trace amount to 1% of the rock volume. The shapes of the zircon crystals vary from elongated euhedral or partly broken to rounded equant and range in size between 40-150 µm, with mean size of 110 µm (see zircon analysis). The rutile observed were euhedral and size of 80-90 µm. The heavy mineral assemblage is highest in 6204/10-1, and intermediate in Distal Halten, and Halten Dønna, and lowest in 6705/5-3 and calcareous sandstone (6204/10-2A, 6204/10-2R).

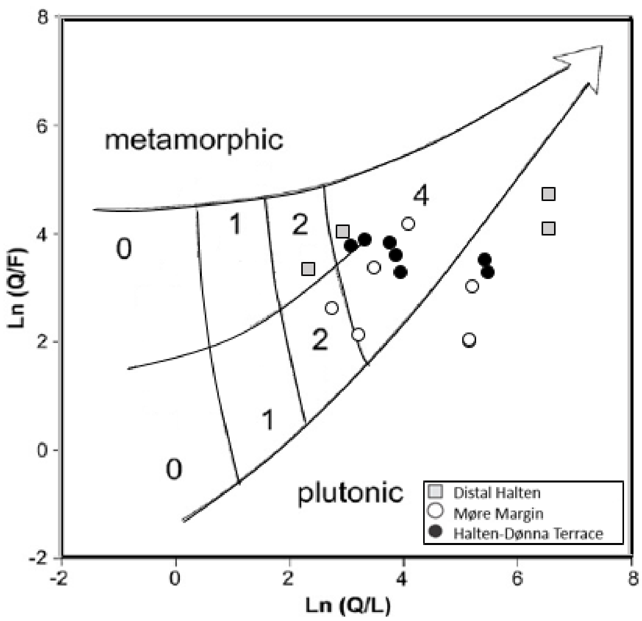

semi-quantitative Weathering Index		Relief: high (mountains) 0	moderate (hill) 1	low (plane) 2
Climate (Precipitation)	(semi-)arid, mediterranian 0	0	0	0
	temperate subhumid 1	0	1	2
	tropical, humid 2	0	2	4

Fig. 12. Log-ratio diagram after Weltje et al. (1998.) The semi-quantitative weathering indices is listed in table to the right, based on the relief and climate.

Diagenesis

The samples have irregular contributions of cement and range between trace amounts to 29.7%, with an average cement of 13.8 %. Matrix content near absent, except sample M-10-2A, where the micritic carbonate matrix constitute over 63% of total rock volume.

Authigenic quartz syntaxial overgrowths are of low to intermediate abundance, in most of the thin sections from Halten-Dønna Terrace (avg., 1.5%) but such feature is less represented in samples from Møre Margin (avg., 0.17%). The quartz cement is regarded as secondary cement, after iron oxide in most of the samples. Intergranular porosity is formed in fractured quartz and grain-edge dissolution of the quartz grains. The quartz cementation is usually inhibited by clay coating but to varying degree. Samples from distal Halten (6605/8-1) have excessively clay and iron coating and consequently quartz overgrowths are limited. Replacement of feldspar and detrital grains by calcite is observed. The secondary porosity build up is often replaced by precipitated cement. K-feldspar overgrowth cement is not obvious.

Carbonate cement occur as recrystallized, sparitic, patchy and pore-filling poikilotopic. Iron-rich calcite cement is percent prominent in Halten- Dønna Terrace samples. Some of the calcite crystals show impurities or murky appearance from incomplete replacement of detrital grains. In addition, Siderite cement occur as brown, rhombic clasts in minor amounts in some wells (up to 2%, Tab. X). It is present as pore-filling or replacement of detrital grains. Bioclasts, such as foraminifera, are abundant in some samples from the Møre margin and provide shelter porosity if they are complete. Sample D2-3.2, is completely calcite poikilotopic cemented.

Fe-oxide cement occur in most of the samples, particular in sandstone on the Halten-Dønna Terrace, and is most prominent in sample D2-2.2. The iron oxide is recorded as opaque to dark red coating around detrital grains and less frequently overlap them. The coatings are locally thick and occlude the original pore space.

Clay minerals are common in the sandstone as, pore lining or pore-filling cements, alteration products and argillaceous rock fragments. The clay minerals observed in sandstone are illite, kaolinite and siderite. The amount of clay minerals are of variable content (Tab.6.). Pore-filling kaolinite is well developed in oversized pore, dissolved minerals or intergranular pore spaces, and account for a considerable part of the total porosity. The kaolinite cement dominates in distal Halten Terrace sandstone, whereas sandstone in proximal part, Halten-Dønna Terrace, have both kaolinite and illite/smectite. The kaolinite content increases with burial depth. Overall, there is high abundance of illite pore lining the detrital grains.

The point counted porosity ranging from trace amounts to 22.8% for the Lysing Formation. The thin sections from Møre encountered the highest porosity (22.8%) with average of 11.8% of total rock volume. Average porosity on samples from Halten-Dønna Terrace is 4.5% and distal Halten Terrace are 10.8% The intergranular volume varies between 0% and 14.3% in Møre margin, while is slightly less in distal part of Halten Terrace (5.8%-11.3%). Clay coating is more developed in distal part of Halten, and well 6204/10-1, preventing quartz overgrowth. The average porosity loss by compaction is 25.1 % and average porosity loss due to cementation is 10.2%. Intragranular porosity and oversized pores are the most dominant pore system in distal Halten Terrace. Some thin section at Dønna Terrace have higher uncertainties regarding their intergranular and oversized porosity because of high abundant fall out of material during thin-section preparation.

The original porosity loss

The potential of the reservoir rock characteristics and modification of initial porosity can be determined by investigating the significance of compaction versus cementation for the initial loss of porosity (Ehrenberg, 1989). The diagram of Ehrenberg (1989) shows that most of the sandstones of quartzofeldspathic petrofacies, particular from the Møre Margin and distal Halten Terrace, were subjected to intense compaction that lead to significant porosity loss. Thus, mechanical compaction is the dominant process for porosity loss, except for samples D2-3.2, D2-3.3 and D2-2.2. A gradual change in grain contact with increase of burial depth is marked, from predominance of floating, point -and plane contacts to concave-convex contacts. The increasing compaction will, in turn, decrease the intergranular porosity and pore space. Mechanical compaction is limited in carbonate cemented sandstone (e.g. 6507/2-3, 2887.53 m), but largely occlude the initial porosity. Fe-oxide cement and illite cement is also preventing compaction and porosity loss is dominantly due to precipitation of clay cement (illite) and Fe-oxide cement

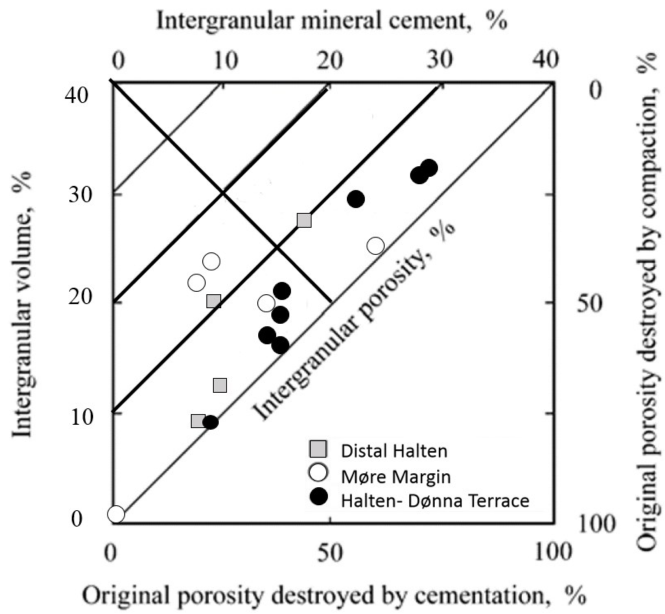

Fig. 13. Diagram displaying the relative significance of compaction versus cementation to porosity development (Ehrenberg, 1989)

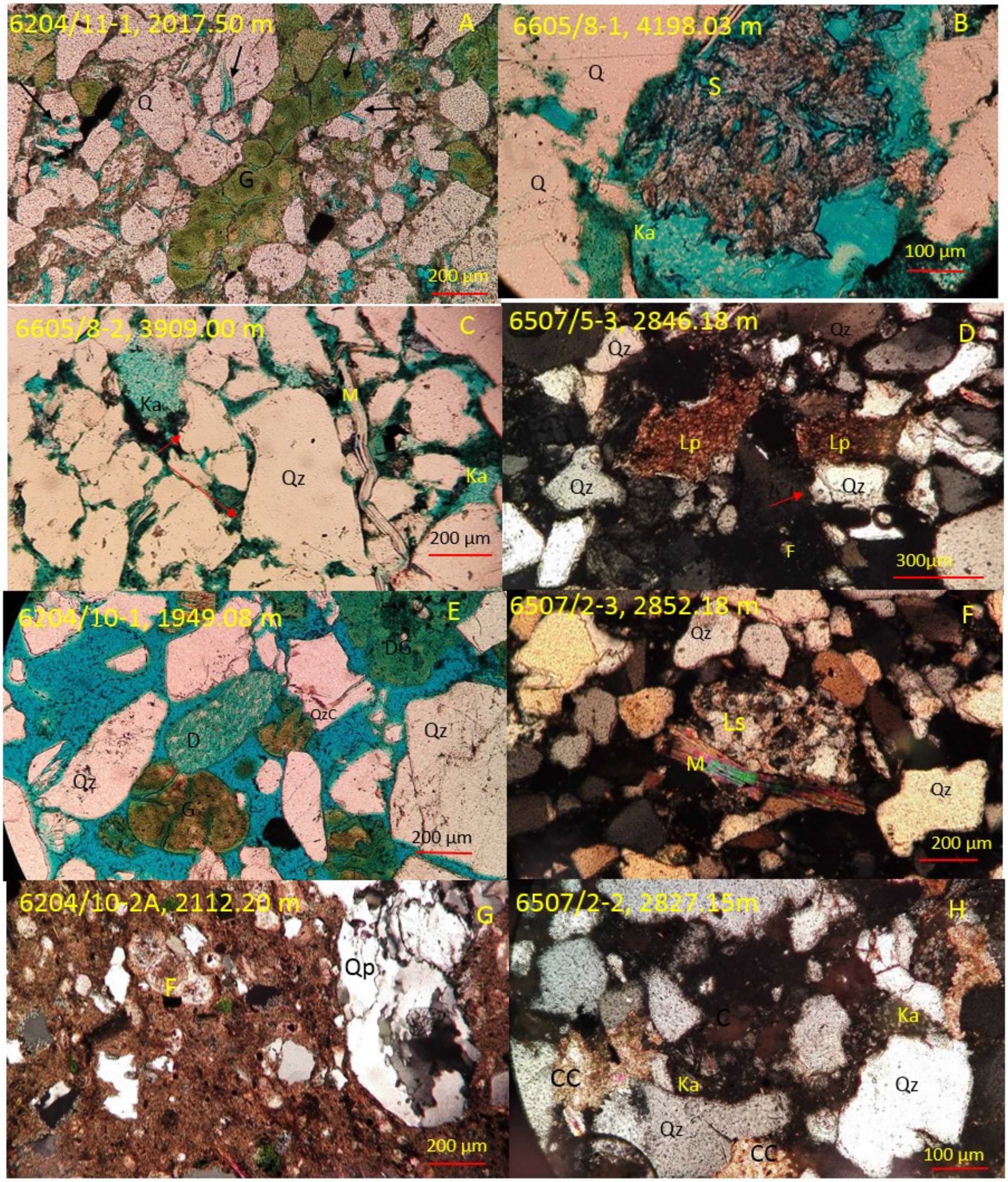

Fig. 14 Photomicrographs displaying textural composition, authigenic phases and relations in plane polarized light (PPL) and cross-polarized (XP) of the various sandstone: A) PPL. Abundant glauconite pellets clustered and developed secondary porosity (arrows). The sample contain patchy carbonate cement and opaque minerals; B) PPL. Siderite cement and kaolinite replacing detrital framework grain. C) PPL. Pore-filling kaolinite of completely dissolved grain and intergranular clay microporosity between the detrital grains. Bended muscovite grain and syntaxial quartz overgrowth (red arrows) with dust rim of approximate position of the quartz-cement boundary are marked; D) XP. Ductile pelite fragments (Lp) are indicated and quartz overgrowth (red arrow); E) PPL. Extensively dissolution have created moldic porosity with remnants of clay coating, marked by dotted line. Glauconite has replaced biotite (G) and feldspar (D) is partly dissolved. The rock was quartz cementing prior dissolution, which stabilized framework and preserved the newly created secondary porosity. F) XP. Lithic sedimentary fragment of psammite, carbonate cemented. G) XP. Calcareous sandstone, comprising micritic matrix. Poorly sorted, floating quartz grains, glauconite pellets and bioclasts. Note the Qp>3 with metamorphic origin;. H) XP. Another example of authigenic kaolinite cement that grew as booklets (Ka). Abundant calcite cement and authigenic clay cement, such as pore- lining illite, are present.

Geochemical results

Major elements

Major and trace elements analysis for the 56 sandstones from Lange-Lysing succession are listed in Appendix.1. The sandstone samples have SiO_2 content of great variations ranging from 48.0 - 94.8%, with average of 80.0 wt. %. The Al_2O_3 content is the most abundant major oxide, but show relatively low to moderate values for the sandstone analyzed on average (2.0-17.0 wt. %; mean= 5.5 wt. %). The K_2O/Na_2O ratio Upper Lange-Lysing samples are irregular and range from 0.7 to 12.7 with mean value about 4. Several samples in the Møre Margin, show enrichment of CaO, but are overall low on average (0.07-24.06 wt.%; mean=3.60 wt.%). Low concentration (less than 1 % average) of MgO, P_2O_5, TiO_2 and Na_2O are observed. Compared to the Upper Continental Crust (UCC), the samples have a considerable higher SiO_2 values and lower concentrations of Al2O3, TiO_2, MgO, K_2O, P_2O_5 and Na_2O. The relatively high SiO_2 content combined with K_2O/Na_2O are typical for sandstone from a passive margin (Roser and Korsh, 1985). The log plot of SiO_2/AL_2O_3 vs Na_2O/K_2O, with geochemical classification fields after Herron (1988) displays a general cluster around sublithic arenite (Fig.19B).

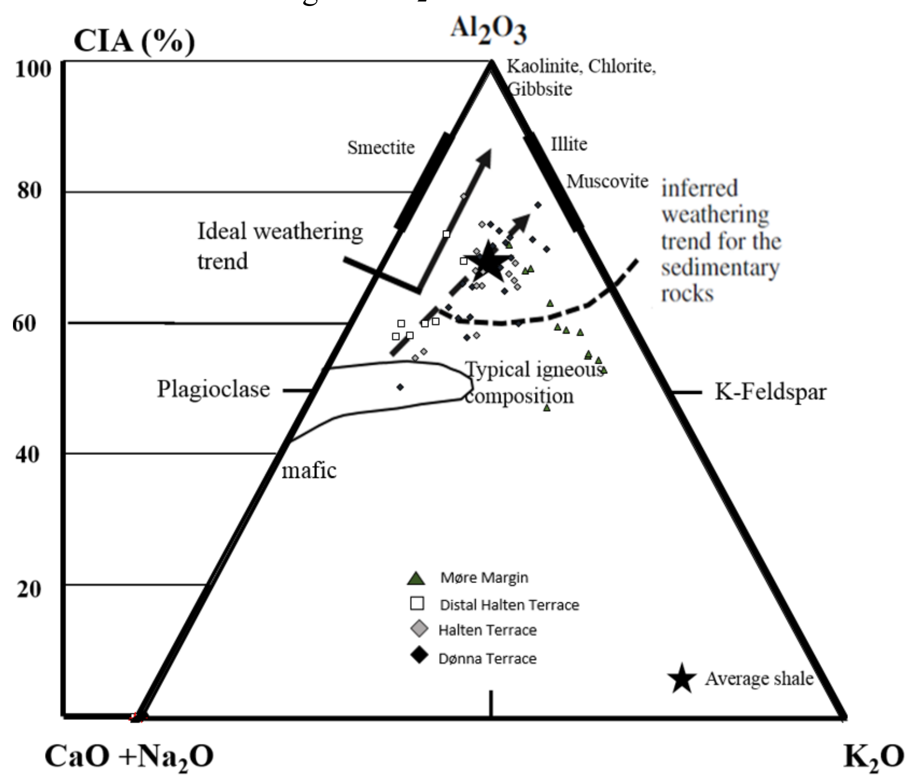

Fig.15. Chemical index of alteration (CIA) diagram after Nesbitt and Young (1984). Molecular calculations from Fedo (1995). Black dotted line show the predicted weathering for the sedimentary rocks (Achaean crust) and the solid black line represent the ideal weathering trend.

Alteration and Weathering trends

The chemical index of alteration (CIA) value of the sandstone samples show significant variations and range between 48.1% and 79.9%, with average value of 65.5% (Fig. 15). Samples from the Halten-Dønna Terrace tend to have CIA values corresponding to the arrow of predicted weathering for sandstone (Archean crust). Sandstone from the Møre Margin plots close to the illite/muscovite composition area, slightly to the right.

REE patterns

The Rare Earth element (REE) chondrite normalized diagram is presented in Fig.16. The sandstone samples show REE pattern comparable to the Post-Archaean Average Australian Shale (PAAS) and upper continental crust (UCC), with nearly flat HREEs (Eu-Lu) and enrichment of LREEs (La-Sm; Taylor and McLennan, 1993). However, there is a low Nd concentrations for most of the samples (2.4-24.8 ppm; mean= 9.7 ppm) that gives a negative anomaly. The concentration of ΣREE range from 46.9-356.4 ppm (ΣREE mean= 125.6 ppm). Average Eu/Eu* anomaly is largely negative (mean=0.67; 0.5-0.83), which is typical for the UCC (0.63, Taylor and McLennan, 1985). All samples exhibit intermediate-high La_N/Yb_N, ranging from 4.26 -16.4, with average 10.6.

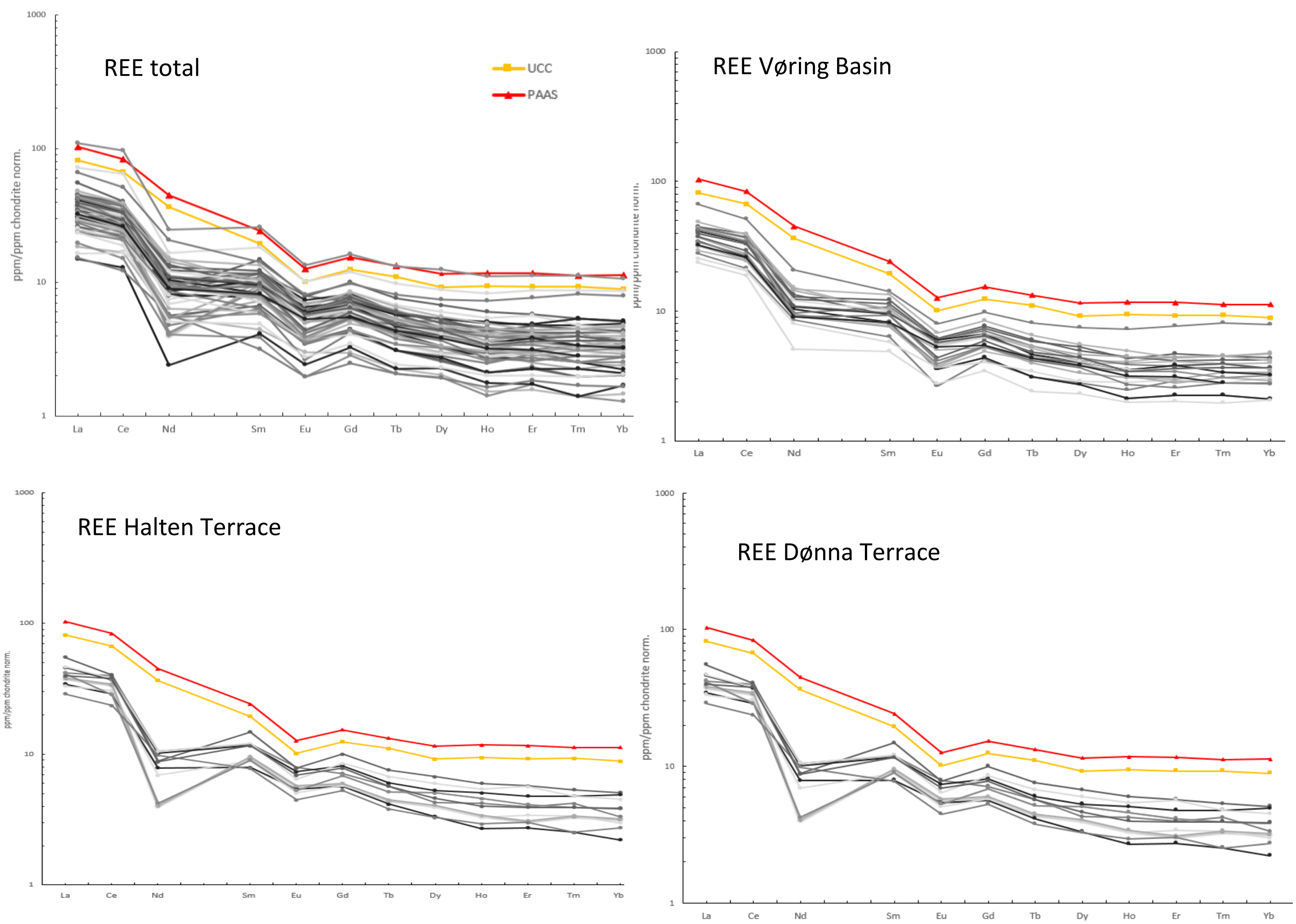

Fig.16. Chondrite-normalized REE diagrams displaying pattern for the total samples (REE total), and the three main areas (Halten Terrace, Dønna Terrace and Vøring Basin). UCC, Upper continental crust; PAAS, Post-Archaean Average Shale (Taylor and McLennan, 1985).

Trace elements

Trace element concentrations of the sandstone samples are reported in Appendix.1. The trace element ratios listed in Tab.8 including reference average data of the upper continental crust (UCC; Taylor and McLennan, 1985). Th/Sc ratios from the samples are of vareity (0.4-2.8), with average of 0.90. La/Sc versus Ti/Zr ratios are presented in Fig.18B (McLennan et al., 1993) and plots in the discrimination fields of passive continental margin and continental island. The intermediate to high values ratios of Nb/Y and Zr/Ti plots in the transition between tracyandecite to rhyolite compositional discrimination fields, with exception of two sandstone samples from the Møre Margin, which plots in rhyodacite field (Fig.17A).

Tab.8. Elementary ratios of the sandstone compared with similar fractions derived from upper continental crust (Taylor and McLennan, 1985) and felsic and mafic rocks (Cullers and Podkovyrov, 2000).

Elemental ratio	Upper continental crust	Range of sediment from mafic sources	Range of sediment from felsic sources	This study: Sandstone samples (Average)	Møre Margin (Avg.)	Halten-Dønna Terrace (Avg.)	Distal Halten (Avg.)
La/Sc	2.21	0.43–0.76	2.50–16.3	3.94	3.54	4.21	3.31
Th/Sc	0.79	0.05–0.22	0.84–20.5	0.90	0.69	0.98	0.84
La/Co	1.76	0.14–0.38	1.80–13.8	4.2	4.91	4.00	3.1
Th/Co	0.63	0.04–1.140	0.67–19.4	0.91	0.90	0.93	0.78
Eu/Eu*	0.63	0.71-0.95	0.40-0.95	0.67	0.71	0.66	0.63

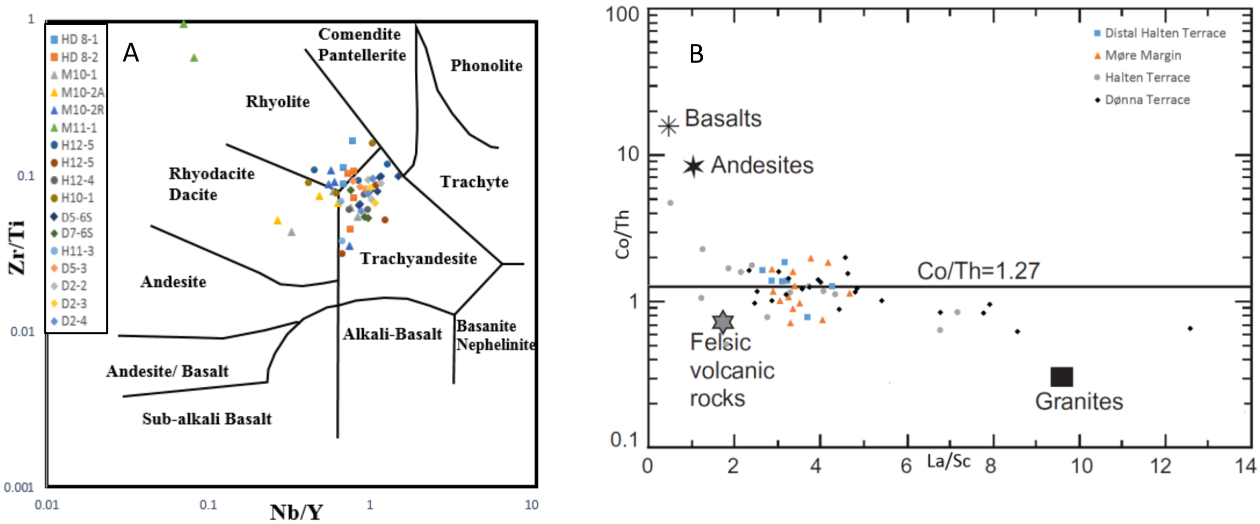

Fig.17. Source rock composition discrimination diagram with trace element ratio A) Nb/Y versus Zr/Ti after Winchester and Floyd (1977); B) Log plot Co/Th versus La/Sc after Gu et al. (2002) with average composition of volcanic rocks after Condie (1993).

Discrimination plot of La/Th vs Hf (Floyd and Leverigde, 1987) show a wide scatter, and plots mainly in the felsic arc source field and minor amounts plots in mixed felsic/mafic and andesitic arc field (Fig.18A). The analyzed sandstone show trend in the upper continental crust field in the plotted sedimentary recycling diagram (Th/Sc vs. Zr/Sc; Fig. 20A). From this plot, an apparent trend with enrichment in incompatible elements (Zr, Th) is marked (Vøring and Dønna Terrace),

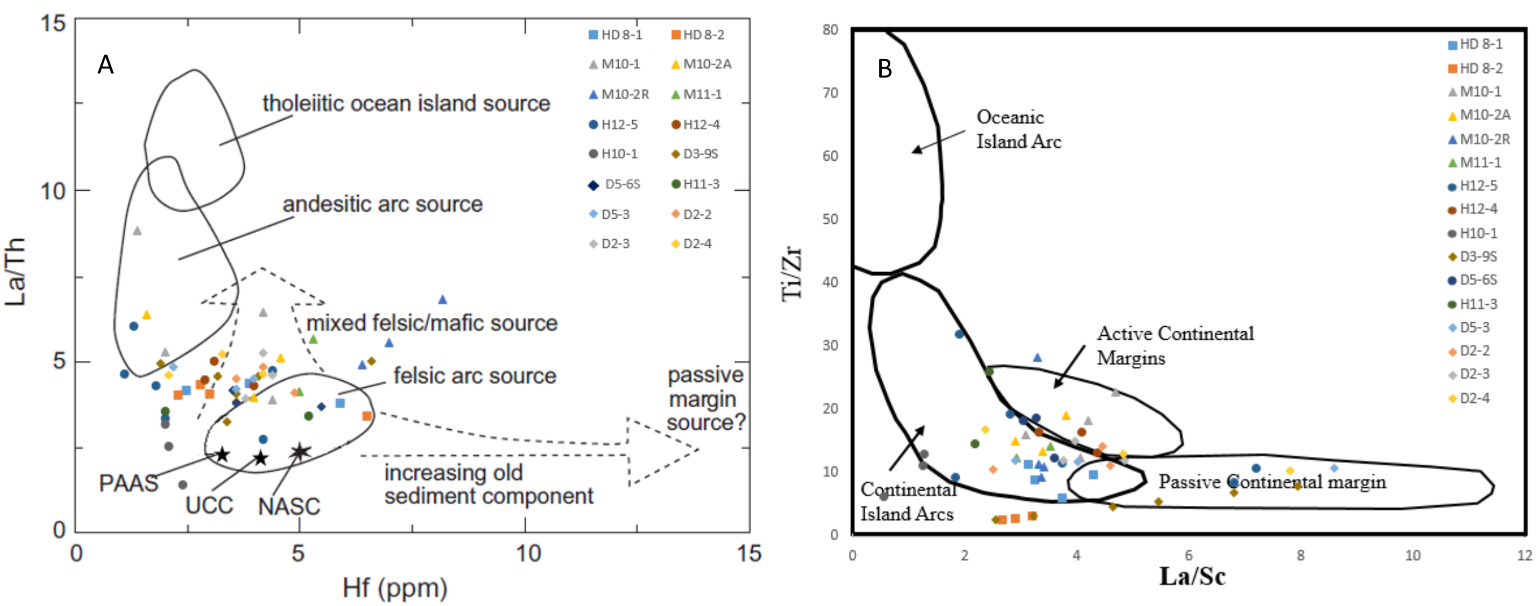

Fig. 18. Discrimination plot of source composition A) La/Th vs Hf plot after Floyd and Leverigde (1987) and B) tectonic setting La/Sc versus Ti/ Zr after Bhatia and Crook (1986)

whereas the samples from the Møre Margin and Halten Terrace obtain lower values and plot within the compositional differentiation field.

In the source area discrimination plot with Co/Th versus La/Sc (Gu et al., 2002) most of the samples cluster around the felsic volcanic rocks region and some towards granites (Fig.17B). It appears that samples from Distal Halten (Vøring Basin) and Møre Margin have resembling cluster, Halten Terrace have more rhyodacitic towards andesitic, and Dønna show rhylotic to granitic composition signature. No ophilitic input is observed based on the discrimination limits (>100 ppm Ni and >150 ppm Cr) after Garver (1996: Fig.20B). Some of the trace element concentration are of great variations i.e.; Ba (56-8688 ppm), Sr (21-589 ppm) and Rb (5-107 ppm). Rb and Cs are clearly depleted, whereas Ba and Sr are enriched compared to the UCC.

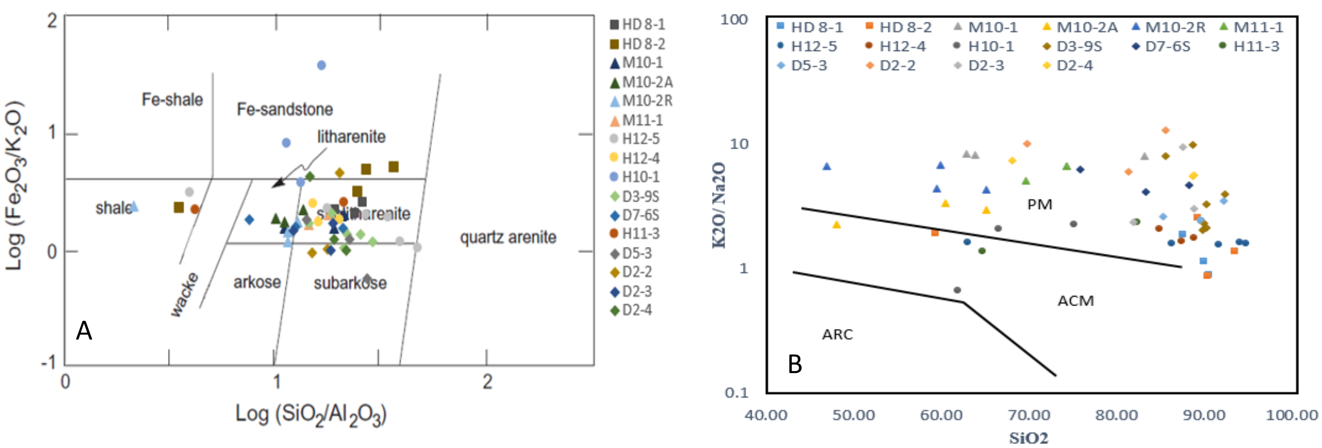

Fig.19. Chemical classification diagrams according of the logarithmic ratios A) SiO2/AL2O3 vs Na2O/K2O after Herron (1988) B) SiO2 vs K2O/Na2O after Roser and Korsh (1985).

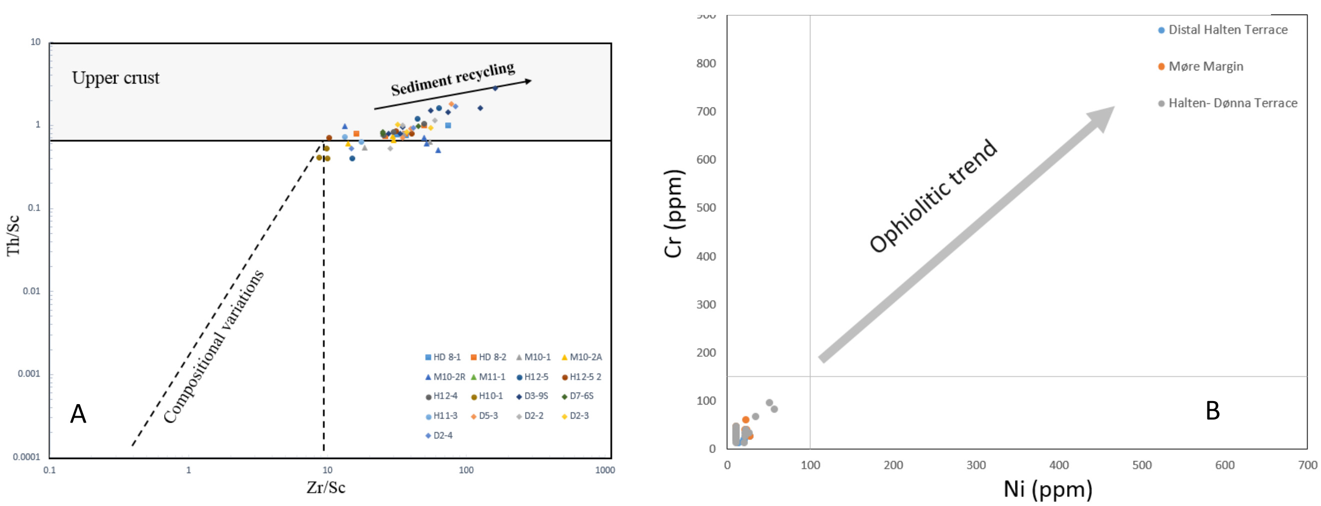

Fig.20. A) Recycling plot of Zr/Sc versus The/Sc (McLennan et al., 1993); B) Discrimination diagram between Cr and Ni (ppm) after Garver et al., 1996.

U-Pb Geochronology La-ICP-MS U-Pb dating of detrital zircon

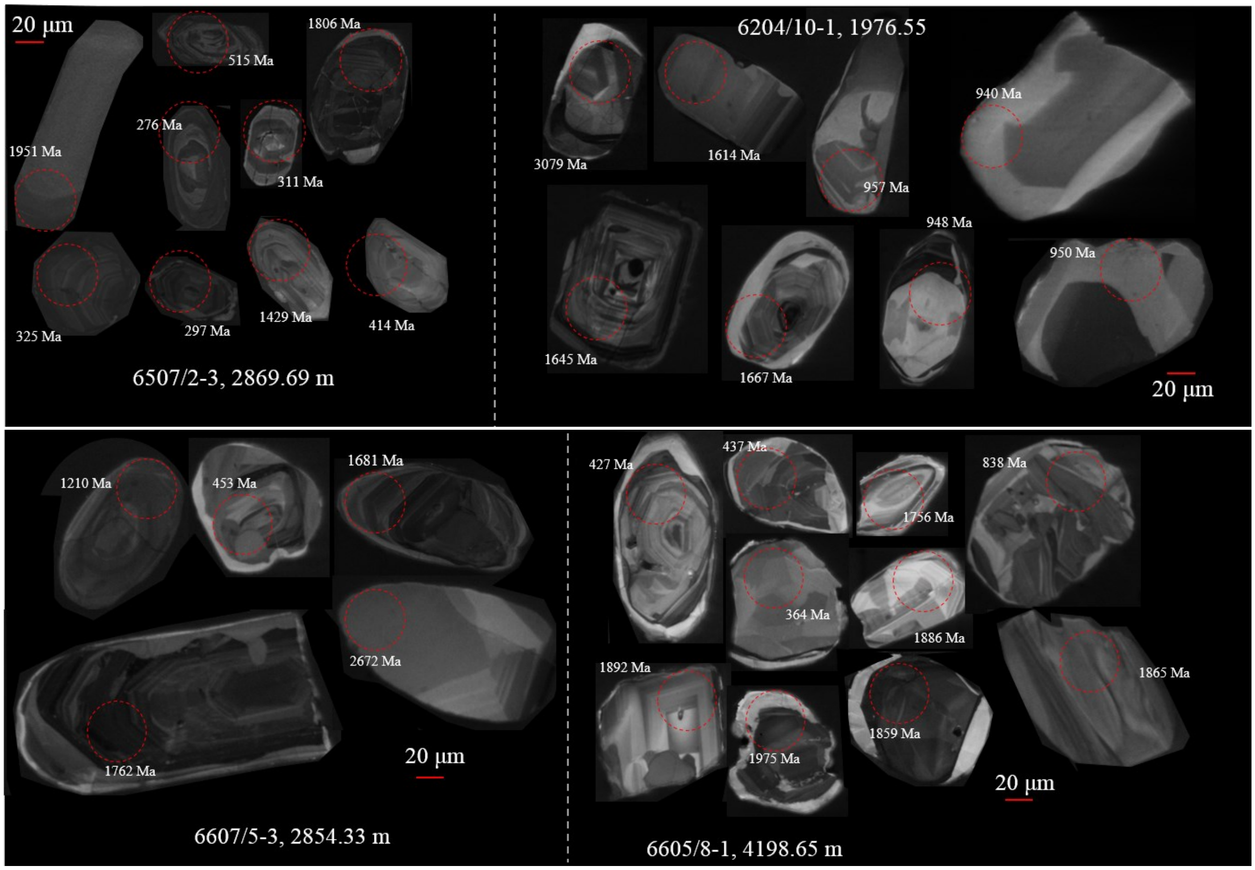

Fig. 21. Representative Cathodoluminescene (CL) images for four different samples. Note the variability in zircon morphology and internal zoning. A bright rim is observed in many of the samples.

U-Pb ages were established for a total of 274 zircons and presented in relative probability plots (figures 21,22,23). Cathodoluminescence (CL) images of representative zircons from samples 6507/5-3 (2854.33 m), 6605/8-1(4198.65 m), 6204/10-1 (1976.55 m) and 6507/2-3 (2869 m) are displayed with their Pb-Pb ages in Fig.21.

The zircons analyzed from sandstone samples from Halten-Dønna Terrace (including distal Halten) and Møre Margin are commonly 50-150 um in length, typically subrounded to rounded and range from oval to elongated in shape. The dominating shape are divided equally, in both of the study areas. Quite abundant part of the elongated zircon grains are (partly) broken and abraded. The rounded zircons tend to be smaller and the elongated zircons are usually larger. Some samples are zircon infertile (6507/5-3), while others are quite zircon rich (6204/10-1).

The euhedral zircons are frequently of a magmatic origin, whereas rounded zircons often have metamorphic characteristics. Elongated zircons tend to contain simple banding or oscillatory. Sector zoning are also abundant zoning types present. In addition, a large quantity of the zircon grains consists of a textural irregular core with oscillatory zoning remnants. Note the bright concentric bright luminescent and irregular overgrowth rim for most of the zircons (Fig 21). The maximum age of deposition is estimated to c.100 Ma given by the youngest concordant zircon grain dated (in sample 6507/2-3).

In Møre (6204/10-1, 1993.82m), the cathodoluminescence (CL) zoning of the zircons show that 31% are of typical magmatic origin and 69% of metamorphic character. Comparatively, Halten-Dønna terrace (6507/2-3, 2887.53) shared similar trend with slightly higher magmatic appearances (38%), and lower metamorphic features (62%). However, in distal part of the Halten Terrace (6605/8-1), zircons are less euhedral with oscillatory zoning (magmatic origin), and exhibit about 20% magmatic and 80% metamorphic zoning.

The analyzed sandstones in Møre Margin area (6204/10-1, 1976.55 m + 1993.82 m) show a relatively narrow zircon age distribution pattern (Fig.21). The dominant age signatures range from 900 Ma to 1700 Ma. Within this age interval, a prominent cluster between 1500 Ma and 1700 Ma is marked, and a distinct peak around 970-950 Ma. There is also a minor age peak populations in the range from 1000 Ma to 1200 Ma, and a Paleozoic constituent (500 Ma). Both of the assessed samples have zircon age pattern that are equivalent, except from the presence of an Archean component in the sample from the upper interval (1976.55m).

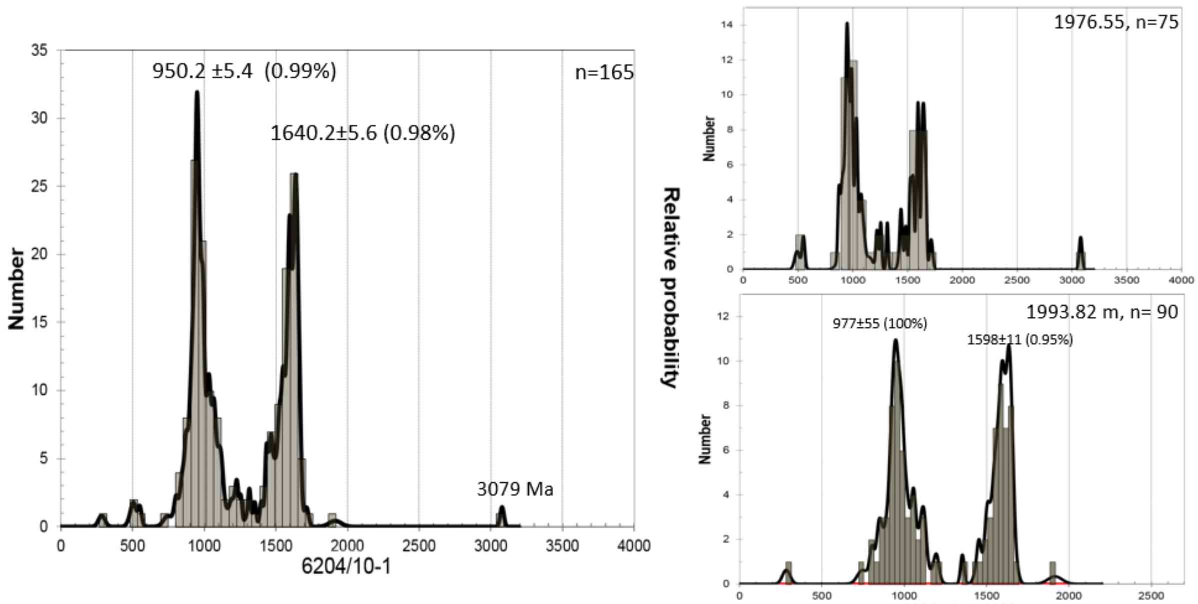

Fig.21. Relative probability diagrams combined with zircon age histogram for samples from well 6404/10-1 (total: 1976 + 1993 m; and separated).

The age pattern of the calcareous sandstone in Møre Margin region (6204/10-2R) vary with stratigraphy and is possibly related to grain-size effect. The two samples show significant different age signatures: at 1882 m, the age spectra concentrate between 1650 Ma and 1500 Ma, with a prominent peak at 1650 Ma, whereas sample at 1887 m show zircon population with a broader age interval with contribution of older zircon grains that range from 2845-1850 Ma, together with a principal Phanerozoic component. Both samples have contributions at c.1270 Ma and c.1000 Ma. The combined spectrum show a similar pattern to sandstone sample 6204/10-1 located in Møre Margin, with main zircon concentration of Late Proterozoic (c. 1000-900 Ma) and Early Proterozoic (c. 1650 Ma; blue color in Fig. 25).

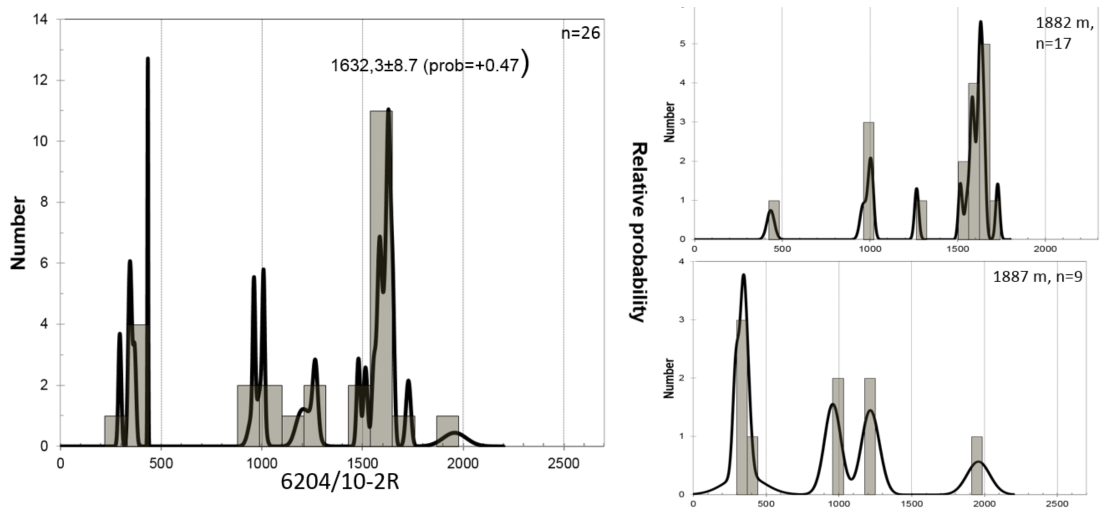

Fig.22. Relative probability diagrams combined with zircon age histogram for samples from well 6204/10-2R (total: 1882 + 1887 m; and separated).

The detrital zircon grains from sample 6507/2-3 located on Halten- Dønna Terrace display a narrow range between 450-300 Ma and 1950-1650 Ma, with a minor component with Archean ages. Stratigraphically, the two samples give two unique age distribution. The lower part of the formation (2869 m) have a major cluster around 550-300 Ma, and several minor peaks at c.1080 Ma, c. 1450 Ma, c.1600 Ma, c.1800 Ma and c. 1950 Ma. Contrariwise, the upper part of the formation (2887 m) have dominant zircon ages that range from 2000 Ma to 1650 Ma with two major peaks at c.1890 Ma, c. 1750 and a smaller Phanerozoic component (550-450 Ma). Furthermore, one Achaean grain is identified at c. 2845 Ma. The U-Pb data from well 6507/5-3 (Halten-Dønna Terrace) show detrital zircon signature with four major peaks at c. 450 Ma, c. 1200 Ma, 1800-1700 Ma and 2800-2550 Ma.

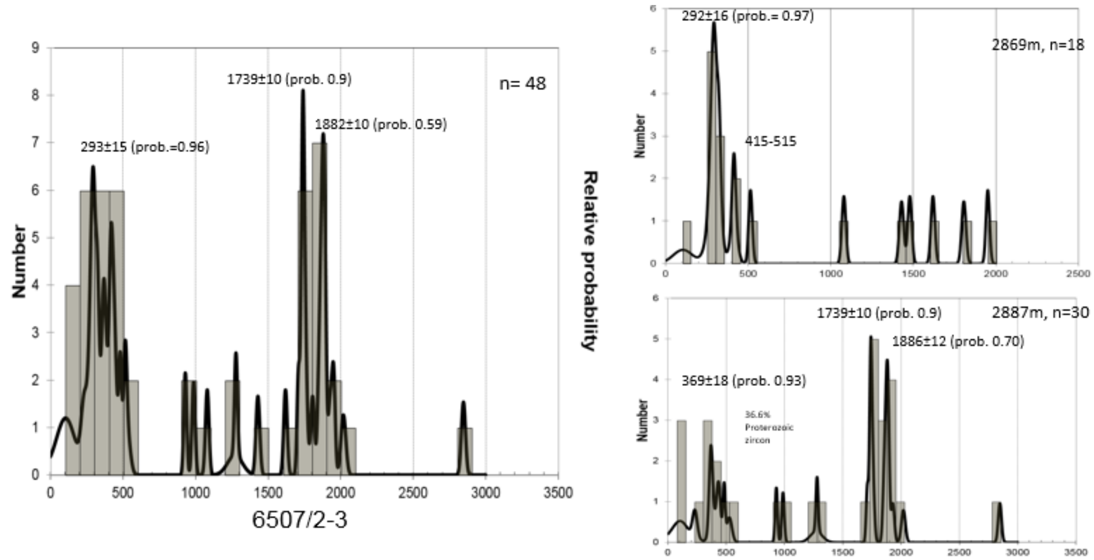

Fig.23. Relative probability diagrams combined with zircon age histogram for samples from well 6507/2-3 (total: 2869m + 2887 m; and separated

Sample 6605/8-2 located on the distal part of Halten Terrace contain a broader and more complex age pattern. The dominant concentration of zircon ages are between 600 Ma and 2800 Ma, with several major clusters that range from 1450-1500 Ma, c. 1890-1870 Ma, and c. 2100-2000 Ma. Additionally, two minor component occur, with Early to Middle Proterozoic ages and one with Archean ages about 2800-2500 Ma. 54% of zircons in 6605/8-2 were discordant. If >80% of concordant zircons were accepted, it would give higher contribution of Proterozoic and Archaean zircon (Tab. X). The adjacent well , 6605/8-1, have a different age spectrum, and including a higher zircon population of Caledonian grains around 500 Ma, and have two distinct peaks at c. 1750 Ma and 1860-1890 Ma. An Archean contribution is recognized with age at c.3022 Ma.

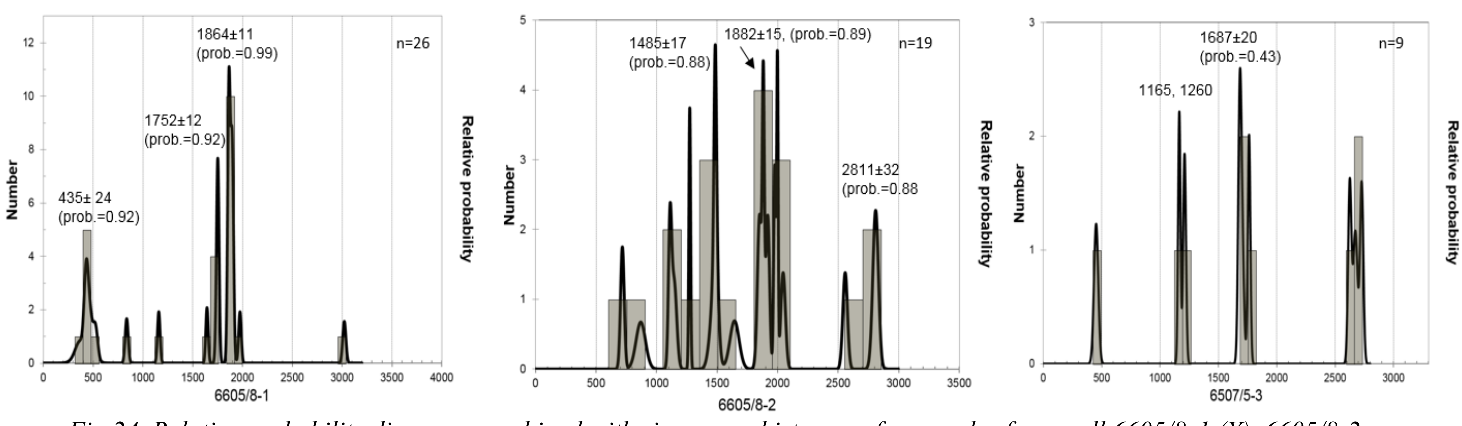

Fig.24. Relative probability diagrams combined with zircon age histogram for samples from well 6605/8-1 (X), 6605/8-2 (X) and 6507/5-3(X type).

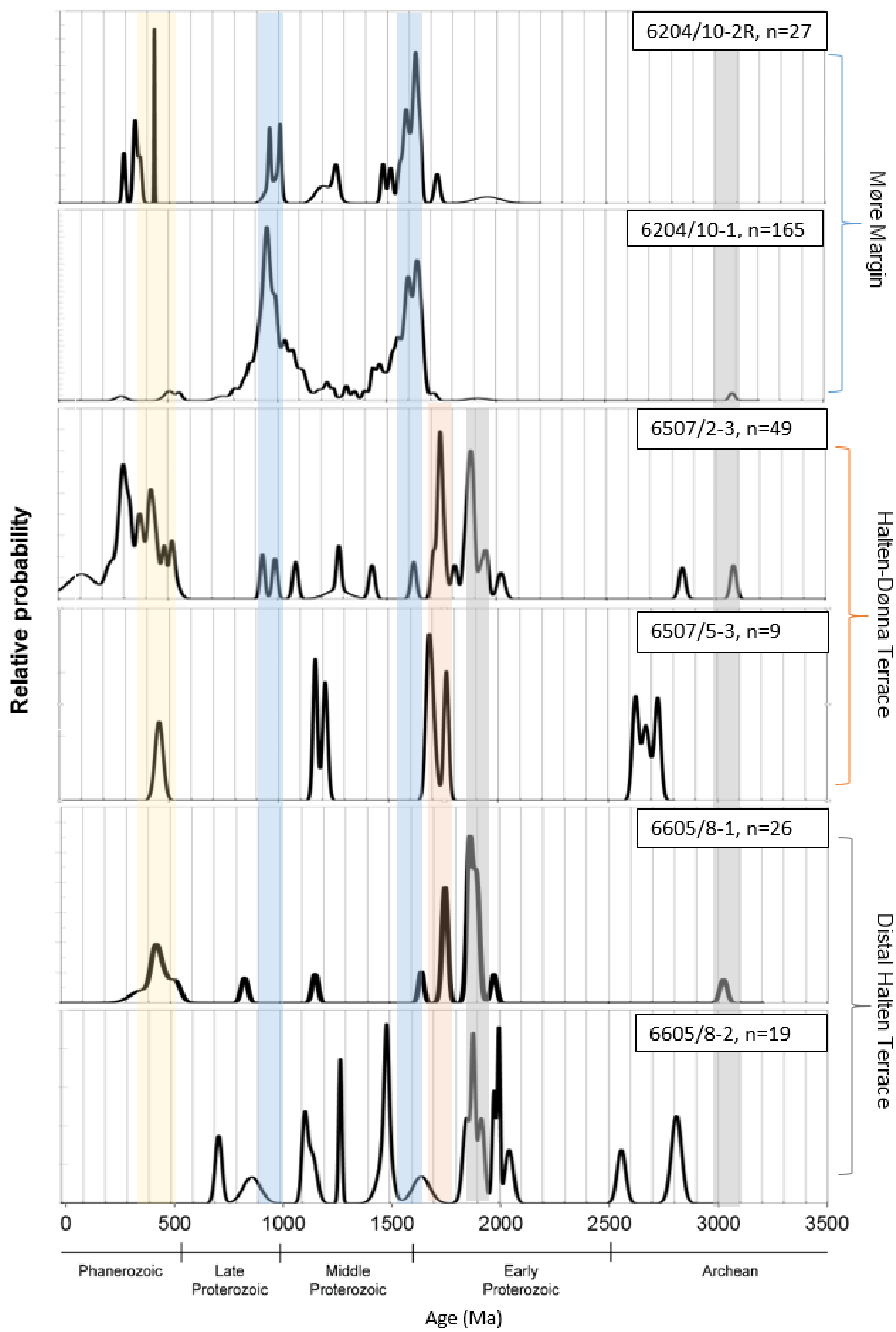

Fig.25. Relative age probability diagrams for the Lower Cretaceous sandstones from Møre Margin, Halten-Dønna Terrace and Distal Halten Terrace. The colour coded shades areas correspond to ages characteristic for each location. The yellow shading match up to the Caledonian orogeny. Only concordant ages ≥90 % are represented in this plot.

Discussion

Weathering of source area(s)

The paleo-weathering condition of sedimentary rocks can be assessed by the Chemical Index of Alteration (CIA; Fedo, Nesbitt and Young, 1995). The chemical index of alteration (CIA), as indicated by the ternary plot of molar units Al_2O_3-(CaO+Na_2O)-K_2O displays the progressive weathering trend of sandstone (Nesbitt and Young, 1984; Fedo et al., 1995). Calculated CIA, values of about 50 represent un-weathered upper continental crust material, whereas values around 100 are indicative of highly weathered residual soils, (alkali and alkaline-earth elements completely removed; McLennan et al., 1983; McLennan 1993). The average of the sandstone samples have CIA value about 65, implying low degree if weathering. However, the high SiO_2 content in some of the quartz arenites may disguise the amount of weathering related the alteration, resulting in lower CIA values (Nesbitt and Young, 1982).

Samples from Halten-Dønna Terrace cluster around intermediate CIA values (65-75%) and tend to lie close to the line almost parallel to Al_2O_3- (CaO+ Na_2O) axis, which is the predicted weathering profile of granite (Nesbitt and Young, 1984). The quartzofeldspathic petrofacies (Møre Margin) have relatively high K-concentration in the samples compared to the scarce abundance of feldspar, which could be related to the transformation of clay minerals to illite (Fedo et al., 1995). Furthermore, the abundance of coarse-grained feldspar in Møre Margin implies a relatively low degree of chemical weathering within the sandstone provenance region. The low to moderate CIA values indicate a relatively stable tectonic setting for deposition of the sandstone from the Møre Margin, than what is inferred for the Halten-Dønna samples. The low degree of weathering could inferring higher erosion rate and shorter exposure time during transport of the sediment (Møre Margin), than for material with a moderate degree of weathering, experience longer exposure time and more vigorous transport (Halten-Dønna Terrace). The dominance of monocrystalline quartz, subangular to subrounded grains, moderately well-sorted sediment and low abundance of fragile grains (<10%) in samples mainly from the Halten-Dønna Terrace favor a long transport distance from the source area (Pettijohn, 1975).

A shorter transport distance is inferred for sandstone on the Møre Margin, due to the relative high proportion of both fresh and altered feldspar (10.8-12.3%) and the coarser grain size. In addition, low relief and tropical climate during deposition is suggested by the major framework detrital grains as observed in the log-plot of Weltje et al. (1998; Fig 12; cf. Suttner et al.(1981). Low proportions of unstable detrital feldspar and lithic fragments suggest the notion of prolonged chemical weathering and warm humid conditions, and long transport path for the samples in the distal part of Halten (Vøring Basin; Amireh, 1991; Al-Habri and Khan, 2008). Hart (2007) reported a global warm, greenhouse period for the Late Cretaceous, with a distinct "hot house" interval in the latest Cenomanian and earliest Turonian, i.e. partly covering the time interval just before and into the inferred hinterland weathering period.

Recycling

It is assumed that the detritus of the investigated samples are either recycled or sourced directly from multiple geological source regions due to the relative broad detrital zircon pattern, with U-Pb ages ranging from the Archean to the Paleozoic. An alternative explanation would be unroofing of a hinterland region composed of multiple distinct terranes or thrust sheets of widely different origin.

Geochemical signatures indicated by Zr/Sc ratios suggest an increase in the amount of recycled material of the sedimentary rocks on the Dønna Terrace relative to those along the Møre Margin, (and in turn, pointing to a regional trend increasing in the degree of recycling from SW to NE). The sandstone on the Halten-Dønna Terrace is expected to have been recycled due to the variable Th/Sc ratio, close to 1, but with no systematic correlation (archiving or failing the criteria, mean =0.98; McLennan, 1993. This notion is supported by petrography.

The sandstone along the Møre Margin are assumed to be first- cycle sediment, because they are failing the criteria of dominant recycled sedimentary sources (Th/Sc > 1; Eu/Eu* ~0.6-0.7; McLennan et al., (1993). This is consistent with their petrographic characteristics, with only a minor proportion of sedimentary lithic fragments. However, the particular high content of quartz and quartzose lithic fragments, together with an overall dominance of K-feldspar over plagioclase suggests that at least a fraction of the sandstone grain population is multicyclic and that the source exhibited prolonged weathering (Osae et al., 2006). The low signal of reworking for the Møre Margin could be due to abundant glauconite (up to 30%; iron potassium phyllosilicate mineral). The higher content of feldspar and dissolution-products such as authigenic clay could also have produced lower Zr/Sc values for Møre Margin samples. The presence of glauconite, especially in the Møre Margin, is assumed to reflect re-deposition of shallow marine sediments from the palaeoshelf (Martinsen et al., 2005), possibly representing reworking of older (Lower?) Cretaceous sediments.

Tectonic setting and conditions in the source areas

A passive margin setting is suggested by the high silica proportion and the K_2O/Na_2O ratio (SiO_2> 70%; K_2O/Na_2O > 1; Bhatia, 1983), in combination with the low quantities of FeO + MgO (less than 5 %; Taylor and McLennan, 1985). Most of the sandstone are consistent with these characteristics. The low SiO_2 values in the classification discrimination diagram after Roser and Korsh (1985), in contrast to the mature quartz arenite as indicated by the point count, is attributed to the aluminous, iron clay minerals (glauconite) and/or calcium carbonate (e.g. 6204/10-2A) present in most of the sandstone.

The K_2O/Na_2O ratio reflects the proportion of K-feldspar to albite plagioclase, and show an overall dominance of K-feldspar in the Upper Lange-Lysing sandstone from the, which is consistent with a felsic provenance and derivation from an old interior cratons and recycled old continental tectonic settings. This notion is consistent with the petrographic data (McLennan, 1990; Taylor and McLennan, 1985). The QFL framework modes of the Lange-Lysing samples display that most samples cluster in transition between the discrimination fields of recycled orogeny and craton interior, with a subordinate sample population in craton interior (Fig.10; Dickinson et al., 1983). The mineralogy of the samples, with a dominance of monocrystalline quartz grains and presence of mica, suggest that most of the sediments are derived from felsic sources (Fig.11; Dabbagh and Rogers 1983). This is also verified by the major grouping within the discrimination field of granite and to some degree low-grade gneiss in the quartz composition diagram after Tortosa et al. (1991). A dominance of polycrystalline quartz in sandstone from the Møre Margin and the Halten-Terrace with an internal metamorphic crystal structure, verify that some of the parent rock material are of metamorphic origin (gneissic composition).

Trace elements are useful for providing provenance signals, as they often are insoluble and commonly immobile. Consequently, they preserve the chemical signatures of their parent material during weathering processes, transportation and burial, as well as under diagenesis and low-grade metamorphic events (McLennan et al., 1990;1993). The high abundance of Th, Hf, Zr in sediment is related to derivation from felsic source rocks and in their erosional products, whereas Sc, Co and Cr are more concentrated in mafic source rocks and in their weathered products. Thus, the ratios Th/Sc, La/Sc, Th/Co and La/Co are suitable indicators for providing information about the average source composition (Cullers et al., 1988; Cullers, 2000; Taylor and McLennan, 1985). The high and similar element ratios in the main three study areas for La/Sc, Th/Sc, La/Co, and Th/Co point to hinterland area(s) dominated by felsic source rocks rather than basic rocks (Cullers and Podkovyrov, 2000). In addition, the dominance of light REE over heavy favors sediment derived from an old felsic upper continental crust, deposited in passive margin setting (McLennan, 1993). The negative Eu anomaly is in the range of values from the upper continental crust and indicates a differentiated source, similar to a granitoid source terrane (Fig.16; McLennan, 1993).

The tectonic setting of a source area(s) can be identified by using several trace element ratios. Floyd and Leverigde (1987) constructed a tectonic source discrimination scheme using trace element ratio of La/Th vs concentration of Hf. The studied samples plot mainly in a mixed felsic to mafic source field with a minor proportion in the andesitic arc source field. An andesitic source terrane is not consistent with the chemical and petrographic characteristics. However, the oceanic and andesitic arc affinity in the provenance signal may be explained by erosional unroofing of the Upper and Uppermost Caledonide Allochthons. Along the stretch from southwestern to northern Norway these comprise nappes of oceanic arc to continental margin detritus, original formed along and emplaced onto the Laurentian margin before thrusted onto the Fennoscandian margin during the closure of the Iapetus ocean and the final stages of the Caledonian orogeny (Pedersen and Furnes, 1991; Ramberg et al., 2008).

Correspondingly, signals recording continental island arc and active continental margin, in the discrimination plot of Bhatia and Crook (1986; Fig.18B.) can be traced back to recycled signals from island arc and other terranes or thrust complexes within the Caledonian Nappe Domain. Trace elements from the Upper Allochthon, where ophiolite fragments dominates are related to subduction zones and volcanic arcs would be expected to plot in the continental island arc and continental active margin fields. The Uppermost Allochthon is usually located above the Upper Allochthon and assumed to consist of thrust sheet complexes derive from a continental margin related to either eastern margin of Laurentia and Baltica,, or to a microcontinent between these two (Augland, 2013; Ramberg et al., 2008).

The presence of sedimentary and metasedimentary detrital grains combined with the low-grade metamorphic quartz grains in Halten-Dønna Terrace support a recycled orogeny with a sedimentary component. The occurrence of rounded sedimentary lithic fragments and zircon crystals confirms that a constituent of the source area consisted of older sedimentary rocks (Young, 1976). The relatively high to moderate abundance of muscovite grains may reflect derivation from a source region with components of granite and pegmatite (Boggs, 2009). The petrographic character of quartzolithic and quartzarenitic petrofacies suggest recycling of eroded metasedimentary and sedimentary rocks, likely from the Caledonian Allochthons, as well as erosion of basement windows of granitic-gneissic composition. However, the bimodal grain size (fine and coarse sand fraction) in Vøring Basin suggest a mix of minimum two sources. The various shapes of the zircon grains and the U-PB data also support a bimodal source (See U-Pb section).

The high proportions of polycrystalline to monocrystalline quartz for the samples from the Møre Margin are usually related to sands derived from a recycled orogen setting (Dickinson et al., 1983). However, the relatively high proportions of K-feldspar to plagioclase and low percentage of sedimentary lithic fragments, favor a granitic- gneissic craton orogen or a mix of sources with supplement of recycled sediment. Low degree of weathering and scarce bioturbation have probably preserved the feldspar. Furthermore, high abundance of ultrastable heavy mineral assemblages, particularly zircon, (e.g. in the 6204/10-1 samples) indicates a strong influence of a cratonic source in the hinterland. The quartzofeldspatic petrofacies, present in samples from the Møre Margin, favor sediment derivation by erosion from coarse crystalline rocks of granitic-gneissic composition, with high abundance of gneiss. The abundance of bioclasts in some of the samples may be related to recycling of carbonate deposits of presumed Cretaceous (Chalk) origin (Ramberg et al., 2008).

The petrographic and geochemical composition show similar behavior regarding classification and mineralogy of the sandstone. Most of the samples in the Nb/Y versus. Zr diagram after Winchester and Floyd (1977) fall in trachyte composition field, which is in accordance with a modern rhyolitic trend. The chemical character using trace elements (Co/Th vs La/Sc) is predominantly felsic, with an insignificant influence of mafic (Gu et al., 2002). The separation of samples from the Halten and Dønna Terrace is demonstrated in this plot, by Dønna samples displaying more granitic composition, whereas Halten samples are akin towards an andesitic source.

U-Pb Geochronology

Northern Nordland and Lofoten-Vesterålen; Halten-Dønna Terrace provenance region

The zircon age signatures from the Halten-Dønna Terrace samples (6507/2-3 and 6507/5-3) provide strong support for derivation from tectonic basement windows within the Caledonian Nappe Domain (Fig.26;27). The tectonic windows are assumed to have been uplifted and locally deformed during the Caledonian orogeny (Ramberg et al., 2008). The Proterozoic population in the studied samples (1880-1600 Ma) indicate a provenance composed of rocks representing several Proterozoic crust-forming events in Baltica (Corfu, 2004; Morton et al., 2008). The prominent peaks at c. 1760 Ma, c.1740 Ma and c. 1680 Ma in the sample set is inferred to represent detritus from basement windows of the western continuation of the Fennoscandian Shield (Gaál and Gorbatschev, 1987), previously considered as a component of the Trans-Scandinavian Igneous Belt (TIB; Skår, 2002). Mineralogical data is consistent with derivation from basement windows similar to these in Nordland (mica schists and metamorphosed sandstone fragments; Ramberg et al., 2008). The main U-Pb age peak at c.1880 Ma may be sourced from Lower Svecofennian granitoid (Skår, 2002) or the granitic-gneissic terrane from tectonic basement windows. Lateral change in provenance signals within samples from the Dønna Terrace is indicated by dominant U-Pb ages of 2000-1800 Ma and 350-100 Ma in well 6705/2-3 and absence of these in well 6705/5-3. The provenance diversity within the Dønna Terrace may indicate changes in the source area(s) and extent of weathering during the sedimentary cycle.

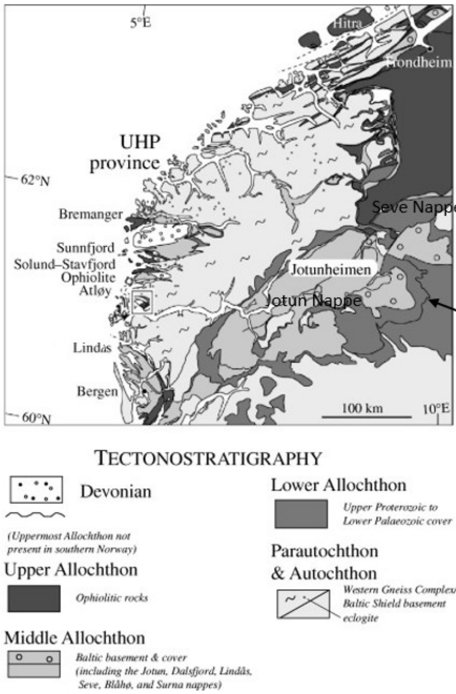

Geological map of southwestern Norway (Western Gneiss Region: after Hacker et al., 2003)

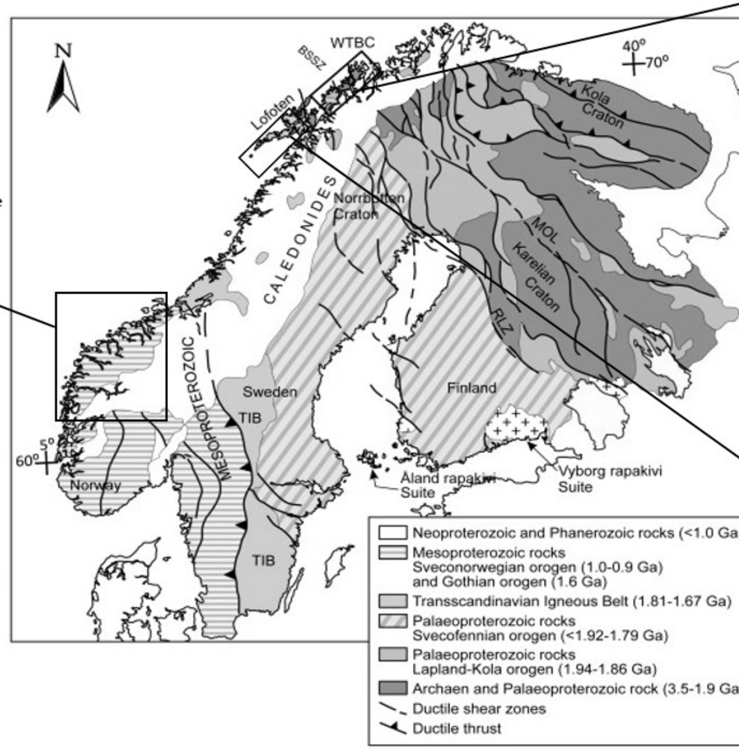

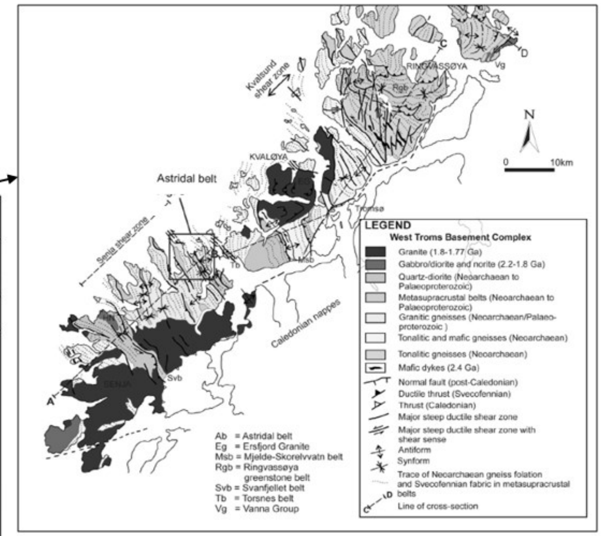

Geological map of West Tromsø Basement Complex. From Bergh et al., 2015 (Zawaan et al., 1998; Kullerud et al., 2006; Bergh et al., 2010)

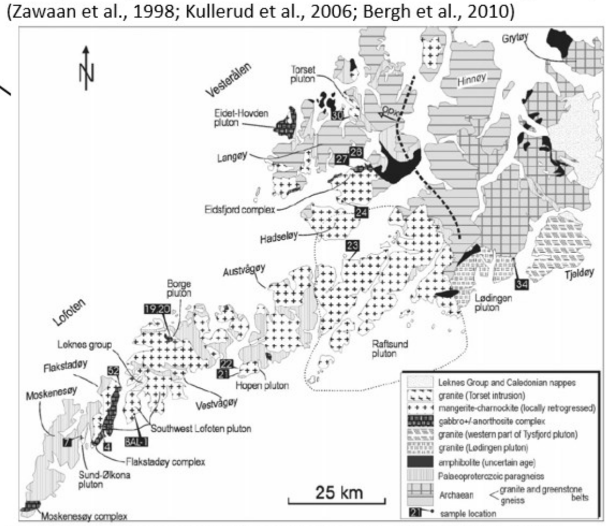

Geological map of Lofoten-Vesterålen region. After F. Corfu, 2004 (Tvedten, 1978; Andersen and Tull, 1983; Sigmond et al., 1984).

Fig. 26. Overview geological map of the Fennoscandian Shield displaying the timing of the main tectonic events (modified after Bergh et al., 2015; Ductile shear zone based on Koistinen et al., 2001). WTBC: West Troms Basement Complex; TIB, Transscandinavian Igneous Belt; MOL, Malangen-Onega lineament, RLZ, Raahe-Ladoga shear zone; BSSZ, Bothinian-Senja shear zone

Contribution from the Upper and Uppermost Allochthon are also considered as potential source area(s). Proterozoic grouping in the sample set is in close agreement with provenance similar to the Uppermost Allochthon in the Helgeland Nappe Complex (Barnes et al. 2007). The Helgeland Nappe Complex records Neoproterozoic to Ordovician zircon ages from various events, with prominent contribution of Caledonian ages (460-370 Ma; Ramberg et al., 2008). The location of the Halten-Dønna Terrace offshore mid-Norway is in close proximity to these basement windows, which makes them a viable source. Another potential provenance candidate responsible for the Proterozoic zircons is the Upper Allochthon of Sweden, known as the Seve Nappes. These nappes have varying composition and often include gabbro, mica schist and greenstone of ophiolitic affinity(Williams and Claesson, 1987). However, derivation of sediment from the Seve Nappes is not considered likely, because of the petrological and geochemical signatures (Cr vs Ni); which do not support ophiolitic derived detritus.

The derivation of sediment from the Upper or Uppermost Allochthon can, however, not be ruled out entirely because of the scarcity of published data on zircon ages on granitoid and metasedimentary rocks within the Caledonian thrust sheets. However, an input from this source terrane is strongly supported by the content of the metasedimentary and sedimentary fragments linked to the quartzolithic petrofacies, as well as the high pseudomatrix content present in sample 6507/5-3. Slump and soft-sedimentary deformed facies common in cores indicate a slope position proximal to the Norwegian landmass and supports an eastern provenance. Petrographic evidence, including heterogeneous roundness, sphericity and grain size relations (e.g. coarser grains are rounder, and have higher sphericity) provide important information regarding the mechanical effect on the grain shape configuration. The poor to moderate sorting in sample 6507/5-3 is related to rapid dumping of sediment, associated with deposition from ?matrix supported debris flow.

The scatter of Meso- and Neoproterozoic ages (1600-900 Ma) may depict first-cycle sediment derived from tectonic basement rocks formed during these repeated Proterozoic events or from the Caledonian Nappe Domain. However, it can also be assumed that the Proterozoic zircon with younger ages should be erosional products from metasedimentary rock from the Caledonides because the basement windows in Nordland have main crustal forming event at c. 1790-1780 Ma. In addition, the gneiss and granitoid of the southwest Scandinavian Domain and the Western

Gneiss Region (WGR) are feasible sources with matching U-Pb ages, (Gaal and Gorbatschev, 1987; Gower et al., 1991). However, as both samples have a significant component of Archaean in addition to Early Proterozoic ages, the derivation from a WGR source is considered unlikely.

The basement in Lofoten-Vesterålen and the West Troms Basement Complex (WTBC) also include ages of intrusive events with zircon population similar to those encountered in the Upper Lange-Lysing sandstone (e.g. Corfu, 2004). The main peak at c. 1740 Ma in sample 6507/2-3 have zircon ages corresponding closely to ages of granitoid in the Rombak-Sjageli basement windows (Rehnström and Corfu, 2004) and anorthosite and ferrodiorite in the Eidsfjord complex (Corfu, 2004). Another possible candidate is the Astridal supracrustal belt with analogous U-Pb ages, composed of post-Svecofennian (1750-1560 Ma) pegmatite dykes in the Archaean-Palaeoproterozoic basement rocks of the West Troms Basement Complex, North Norway (Bergh et al., 2015; Bingen et al., 2008). Lofoten-Vesterålen is suggested to be the main source for Upper Lange-Lysing sandstone on the Halten-Dønna Terrace, because of the main crust-forming intrusions indicated by the U-Pb zircon ages. The WTBC region is also a viable candidate as its geological history and supracrustal units, especially in terms of Achaean and Proterozoic events, resembles that of the Lofoten-Vesterålen domains (Corfu et al., 2003; Bergh et al., 2010).

The high abundance of zircon grains that have Permo-Triassic origin may derive from the high-grade metamorphic core complexes of the Lofoten Islands, with matching ^{40}Ar-^{39}Ar ages presented in Steltenpohl et al. (2004). In addition, a predominance of Caledonian and Phanerozoic zircon grains could reflect the highly diversity of Caledonian zircon grains and may indicate recycling of an exotic terrane. East Greenland is a plausible source for the Permo-Triassic zircon grains; however, this source region is considered less likely because of the inferred proximal depositional setting along the Norwegian conjugate margin and the long distance to the Greenland margin. Both potential source regions, the Lofoten-Vesterålen and the WTBC, have significant exposures of Archean Gneiss with c. 2900-2600 Ma ages, (Jacobsen and Wasserburg, 1978; Corfu et al., 2003) is closely in agreement with the zircon data in this work.

Origin of the Archean population in the sample set

The U-Pb ages of the Lange-Lysing sandstone gives new constraints for sediment drainage and provenance from the Halten –Dønna Terrace. The Archean population present in samples from the Halten-Dønna Terrace, with provenance signatures associated to the Norwegian landmass places a question mark on earlier interpretations in terms of the origin of the Archean source for the Upper Lange-Lysing sandstone, and especially whether this component is derived from the Norwegian landmass or the East Greenland Margin. Moreover, Morton et al. (2005) excluded Lofoten-Vesterålen and WTBC as source regions for Lysing sandstone because of absence of an Archean component. A conclusion appear invalid based on the zircon population from this study.

The oldest Archaean exposures in the Lofoten Islands and the Troms area are tonalitic gneiss dated c. 2880 Ma (protolith age: Kullerud et al., 2006; Ramberg et al., 2008). The presence of

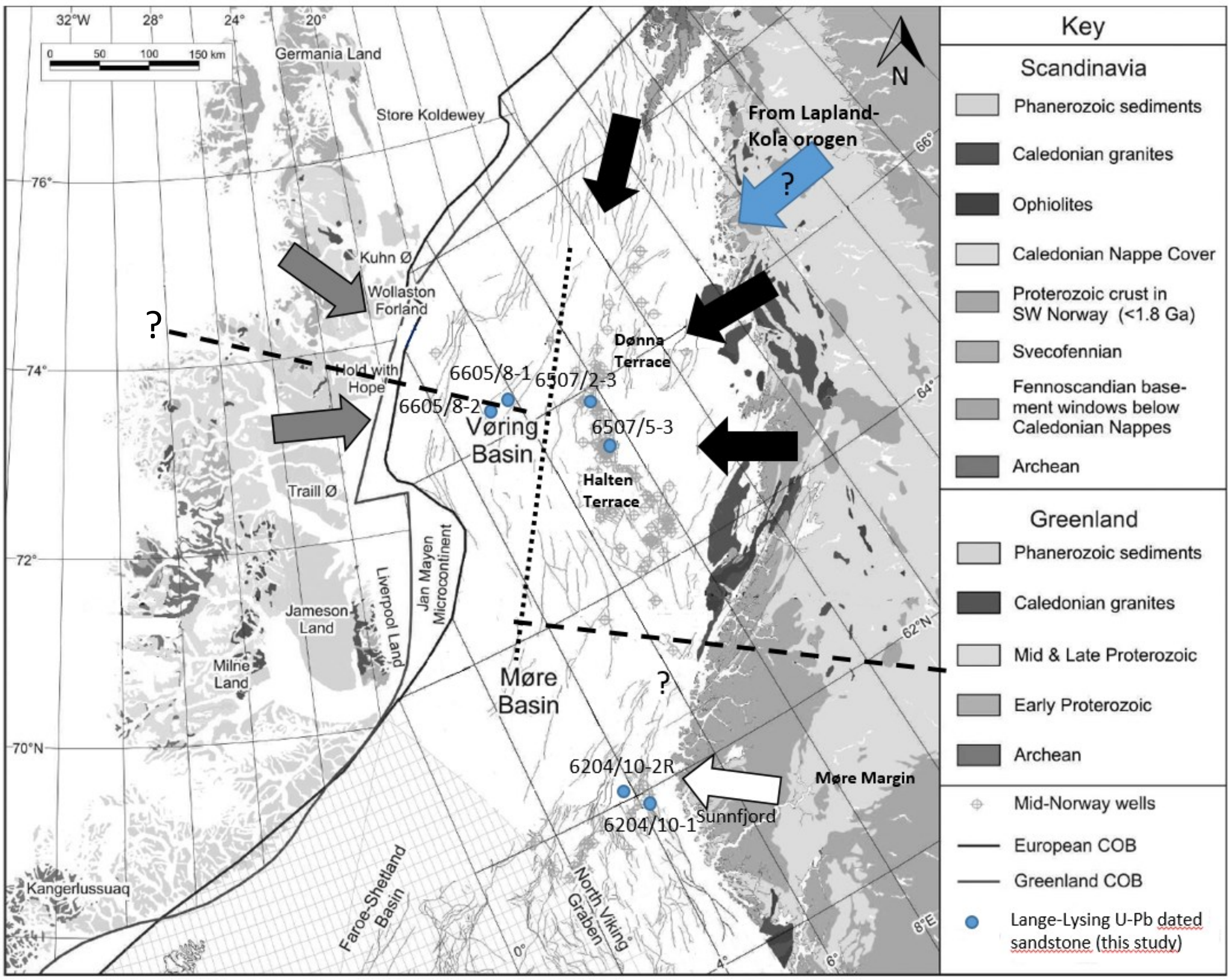

Fig. 27. The regional distribution of the suggested sediment sources for the studied sandstone samples. Stippled line is inferred approximate boundaries of source regions based on petrography,whole-rock geochemistry and U-Pb dating (Modified from Morton et al., 2009).

Late Archaean component(>2900 Ma) in samples from the Halten- Dønna Terrace could alternatively reflect long transport distance from the Kola Peninsula in Sør-Varanger, East

Finland, where Late Archaean (c.3100-2500 Ma) rocks are abundant (Slabunov et al., 2016; Ramberg et al., 2008;). The contribution of concordant ages with >80% and <120% would give higher contribution of Archean zircon (maximum age = 3144 Ma), which further support a contribution from the Kola Peninsula. Furthermore, the paleo-Norwegian geology was different during Cretaceous time and therefore derivation of Late Archean zircon from the Caledonian nappes in Nordland or Fennoscandian shield cannot be excluded entirely. Morton et al. (2008) reported U-Pb ages on modern rivers draining the Fennoscanian Sheild, which display significant similarities with respect to tectonic evolution, supracrustal units and age constraints, particular in terms of the Archaean component (2.78 Ma and 2.65 Ma; Morton et al., 2008).

East Greenland; The Vøring Basin provenance region

The contribution of sediment into mid-Norway Cretaceous basins from the East Greenland landmass across the Greenland shelf was initiated during middle Albian-Turonian time (Whitham et al., 1999). Morton and Grant (1998) proposed a North-East Greenland source for Turonian-Campanian coarse clastic sediment with wide zircon age population with a notable Achaean component. The occurrence of an Archaean component has been considered to be an indicator of East Greenland provenance (Whitehouse et al., 1997; Morton and Grant, 1998; Rainbird et al., 2001). Broad range of zircon ages combined with an Archean component has been proposed to be characteristic for a western sediment source and observed in the wells on the Gjallar Rigde, the Helland- Hansen Arch and the Nyk High Upper Cretaceous sandstone (Fonneland et al., 2004). The wide spectra reflect a more complex and higher diversity of terranes (lithologies) within this landmass.

The U-Pb age spectra patterns for the sandstone in the Norwegian Sea can be used for differentiation between the surrounding landmasses, i.e. Norway and East Greenland. The sediments derived from the Norwegian landmass are characterized by a narrow zircon distribution, whereas those derived from Eastern Greenland have a wider range of zircon ages (Fonneland et al., 2004; Morton et al.,2005). However, common U-Pb zircon ages (Early Proterozoic, Middle Proterozoic and Cambrian-Ordovician) in sandstone derived from the Norwegian landmass and East Greenland, make it challenging to distinguish a distinct western source from a mixed source, or one a dominant western source with supplements from an eastern source.

Strong evidence for derivation from East Greenland or mixed sources for the samples in wells 6605/8-1 and 6605/8-2 is indicated by the wide zircon age population and highly diversity of Proterozoic zircons between 2000 Ma and 1000 Ma, together with a small but significant Archean component. The central position of the wells in the Vøring Basin suggest that derivation of sediment is about equally likely from the Greenland Margin as the Scandinavian landmass.

The zircon spectra in well 6605/8-1 favor a North East Greenland source because of the prominent age interval of Early Proterozoic zircon ages between 1800 and 2100 Ma, with a main peak at c. 1900 Ma. (Tucker, 2000). The occurrence of a Late Archean component (>2900 Ma) supports this notion. The Greenland basement north of 76°N was developed during Early Proterozoic time (1900-2000 Ma; Kalsbeek et al., 1993; Thrane, 2002) and partly formed by metamorphic reworking of the Archaean basement (Kalsbeek et al., 2001; Nutman and Kalsbeek, 1994). In addition, abundant juvenile Early Proterozoic basement crust is present in this terrane (Thrane, 2002). Hence, this region could provide Archaean zircon and reworked Archaean zircon into Early Proterozoic rocks together with pre-1800 Ma Proterozoic zircons. The Smallefjord sequence in the northeast Greenland Caledonides consist of rock suites that record event that are in close agreement with zircon spectra from the sample in well 6605/8-1. The zircon population ages for this sample resemble the MN2a category of Morton et al. (2005, 2009).

The relatively high diversity of zircon ages (2000-1000 Ma) with high abundance of Early to Middle Proterozoic zircon ages (1500-1100 Ma) in combination with an Archaean component (>2500 Ma) in sample from 6605/8-2, 3909 m corresponds well with Krummedal supracrustal sequence and the Eleanore Bay Supergroup metasedimentary rocks within the Caledonian nappes in Central East Greenland. These successions predominantly include Early to Middle Proterozoic zircon ages (Strachan et al., 1995; Watt et al., 2000; Watt and Thrane, 2001). The main peak of Neoproterozoic zircon grains (950-920 Ma) are associated with the last stage of the Grenvillian orogeny (Watt and Thrane, 2001). The Krummedal Sequence has the closest comparable zircon spectra, with zircon ages that host both Caledonian and c. 930 Ma granites, as well as Paleoproterozoic (c. 1800-2000 Ma) and Archean components (c. 2800 Ma; Elvevold and Gilotti, 2000). Additionally, this sequence and adjacent units were subjected to granitoid plutonism and high-grade metamorphism during the Caledonian Orogeny (Henriksen, 1985;

Watt et al., 2000), which resulted locally in granulite facies (Leslie and Nutman, 2000) dated at c. 430 Ma (Leslie and Nutman, 2003). The bright zircon rim and high abundance of discordant zircon ages (54%) in well 6605/8-2 located in Vøring Basin indicate a relative high-grade metamorphic provenance.

The petrographic data for the sandstone samples in well 6605/8-1 and 6605/8-2 provide strong support for a Greenland provenance with supplement from the Norwegian landmass. The petrographic data from these wells are at variance with data from the Halten-Dønna Terrace, which are located close to the Vøring Basin wells, and hence would have expected to have similar petrographic signatures, if they share same source region. An equally mix of sediments from both landmasses and interfingering of turbidite systems from the two conjugate margins, or by additional transport by sea floor oceanic currents are also feasible option, and cannot entirely be ruled out.

Western Norway; The Møre Margin provenance region

The U-Pb results are strongly analogous to zircon age spectra from other Cenomanian – Coniacian sandstone in Slørebotn subbasins (Møre Margin) obtained by Fonneland et al. (2004) and Morton et al. (2005). Likewise, the zircon spectra from the Møre Margin (6204/11-1; 6204/10-1) indicates a likely source in southwestern Norway, inferred to be the Western Gneiss Region, due to the narrow zircon spectra with two prominent age peaks that are in agreement with the Sveoconorwegian (1000-950 Ma) and Gothian (1700-1500 Ma) orogenies. The formation of the WGR basement is accurately dated in the range between c. 1657 Ma and c. 1689 Ma (Tucker et al., 1990), which is closely comparable to the main peak of the ICP-MS spectra at c. 1640 Ma and 1632 Ma. Involvement of subordinate metamorphic rocks in the adjacent parts of the Caledonian Nappe Domain could be a feasible potential source. The dominance of metamorphic lithic fragments over sedimentary (Lm>Ls) also support this.

The minor zircon peaks in the range of 1550-1200 Ma (Middle Proterozoic) are suggested to represent derivation from several younger intrusions in the region. Examples of such intrusions are augen orthogneiss in Molde with U-Pb zircon age of c. 1508 Ma, (Tucker at al., 1990b) mafic magmas from the Dalsfjord complex Region, (1470-1460 Ma; Åhäll and Connelly, 1998) and the Jotun Nappe (1280-1224 Ma; e.g. Schärer, 1980).

By contrast, a small Archaean component is present in 6204/10-1. Since the Archean zircon has an age at c. 3079 Ma, derivation from the Norwegian landmass is not considered likely. East Greenland is a well-known source of Archean rocks (2800-3100 Ma; Ramberg et al., 2008). However, Greenland is not regarded a potential source for the Møre Marin sample set because of its proximal positon to the Norwegian landmass, the inferred short transport and the dominance of proximal facies suggest that transport over the Norwegian Sea would most likely be too far in extent. This conclusion is in line with the seismic interpretation presented by Sømme et al. (2013 a,b). Sediment derivation from Kola Penninsula (2900-3200 Ma; Ramberg et al., 2008) is suggested as a potential source, although one would assumed a general different zircon spectra and higher proportions of reworked sandstone from such a source region.

Granite and gneiss occupying most of the Western Gneiss region and are in line with source area lithology proposed by the petrographic data (high content of quartz and K-feldspar) of the Møre Margin sample set. High abundance of zircon also support a granite-gneissic terrane. Quartzose fragments or polycrystalline quartz grains are indicators of contributions from metasedimentary (gneissic composition) rock. The proximity of the Western Gneiss Region to the Slørebotn sub-basins and the combined zircon U-Pb dating, petrographic and geochemical characters of the Møre Margin sample set makes the WGR the likely provenance candidate for the Lange-Lysing sandstone of this part of the mid-Norway margin.

Discrimination between a northern and southern source within this region can be determined by the relative proportions of Early Proterozoic and Middle Proterozoic zircon ages. A southern source in the Western Gneiss region (close to Sunnfjord) is indicated by the higher abundance of Sveconorwegian zircons (Middle Proterozoic) in relation to Gothian zircons (Early Proterozoic). This implies a more granitic source area as the 1000-950 Ma are granitic intrusions. Furthermore, U-Pb zircon dating of quartz diorite in Sunnfjord (Atløy) obtained age at c. 1641 Ma (Skår, 2000), which is almost accurate with U-Pb ages in the Møre Margin samples.

The far-travelled crystalline Jotun Nappe (anorthosite-mangerite –charnockit suite) and equally units such as the Dalsfjord Nappe complex are present the southern part of the Western Gneiss Region. These suites are composed of rocks with U-Pb zircon age at c. 1634 Ma (Vander Auwera et al., 2011) and the Jotun Complex have an upper intercept ages of c. 1694 Ma and c.1666 (Corfu and Andersen, 2002); and these suites accordingly constitute potential subordinate source candidates.

Since Caledonian granite is scarce in the western gneiss region, the “Caledonian” zircon ages are more likely to derive from high-grade metamorphism (Tucker et al., 1990) or ultra-high pressure (UHP) zones in the area (e.g. Terry and Robinson, 2003). The bright rimming of the zircon grains give solid support for high-grade metamorphism. Fossen (2010) proposed a high to medium metamorphic event at c. 500-405 Ma during the Caledonian orogeny in the southern areas of the Western Gneiss Region. Furthermore, a succession of Late Silurian and Early Devonian Caledonian thrust sheets are present underneath ultrahigh pressure (UHP) metamorphic rocks (Terry and Robinson, 2003). Sample 6204/11-1 have zircon ages with Permo-Triassic origin that are in accordance with zircon data from WGR, recording Permo-Triassic felsic igneous activity. Furnes et al. (1982) recognized exposures of ultrapotassic syenite dikes (261-256 Ma) in the Sunnfjord area (western Norway) and alkaline dikes in the Sunnhordaland are dated at c. 275 Ma, c. 220 Ma and c. 160 Ma (Færseth et al. 1976).

Provenance regions and depositional systems

The grain size, sorting effect, clay content are strongly linked to lithofacies, which in turn, are controlled by the depositional environment with petrography and mineralogy ultimately reflecting provenance. Hence, reservoir properties are at least partly controlled by provenance. The abundant facies and channel- lobe stacking controls the gross continuity and flow barriers within the reservoirs. The conceptual depositional model summaries the key features during deposition of the different sedimentary systems (Fig.28). A narrow shelf and proximal location within the basin is suggested for Møre Margin in Cenomanian-Coniacian because of most of the wells (except 6204/10-1) have extensive mass-flow deposits, with slide and slumping facies in cores. Short transport of sediment is also inferred by the petrographic and geochemical analysis. In addition discrete and point sourced sandstone units is reported by Sømme et al. (2013a;2013b) and Jackson et al. (2008). Slumping and debris flow are generally discontinuous and difficult to predict the sand distribution within the units. However, thick and highly amalgamated slump and debrite sands can form potential reservoir. Moreover, the sandstone injectites commonly increase the connectivity by bridging the isolated bodies. (Shanmugam et al., 1994).

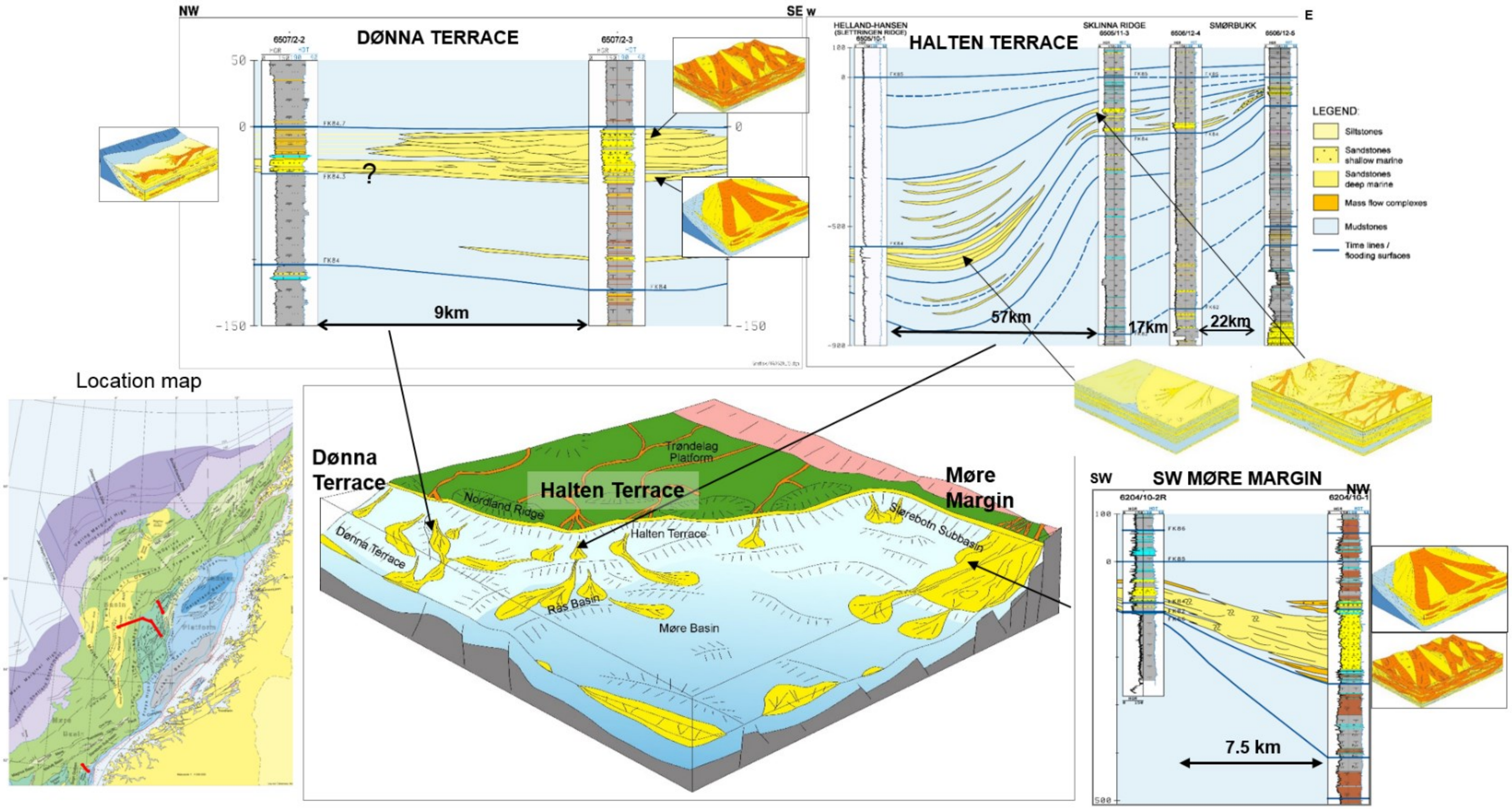

Fig.28. The depositional model and well correlations for the Turonian-Coniacian Lysing sandstone in the Dønna Terrace, Halten Terrace and Møre Terrace interpreted by core analysis and wire logs and combined with provenance direction. Well correlations are flattened on the flooding surface FS85 and show the reservoir sand distribution. (Shell in house)

,

Sand distribution in Halten-Dønna Terrace is controlled by the inherited complex slope topography (Lien, 2005; Fugelli and Olsen, 2005; 2007). Seismic interpretation from this area suggest that the nature of turbidite deposition on the terrace with a general eastern source and prograde towards the west and southwest (Quinto, 2017). This model is however, in contrast with earlier depositional models, which propose a north to south longitudal turbidite complex, parallel to Nordland Ridge (e.g. Fugelli and Olsen, 2007). An east to west or northeast to southwest direction proximal to distal trend is supported by a prominent lateral thinning, from proximal slope channel deposits to thin distal deposit, as showed in wells 6507/2-3 and 6507/2-2 on Halten-Dønna Terrace (Fig.28). Lateral thinning is also observed in well 6507/2-4. The petrographic and geochemical data is indicative of a larger drainage and transport delivery system, most likely within the fluvial-deltaic realm.

Depositional processes with implication for reservoir quality

The depositional processes and sediment-gravity flow types exert strong controls on reservoir quality in deep-marine systems. Across a deep-water channel to lobe system, the depositional reservoir quality decreases from the proximal to distal part and from the axis towards the margin. Generally, the facies textural and compositional implications reducing porosity is given in Fig.29. Channel fills, followed by braided mid-fan/channel to lobe transition are the facies association that show the best-developed reservoir quality. The channel sands (LB1) from the Møre Margin (6204/10-1) and the Halten-Dønna Terrace(6507/2-3) have similar facies but differs in composition, which give different texture and diagenetic characteristics, which in turn, impact the reservoir quality. Well 6204/10-1 have better reservoir properties, with channel sands comprised of medium-coarse sand, high proportions of detrital quartz and relatively low percentage of cements, matrix and authigenic clays. In contrast, wells with a predominance of lobe fringe and lobe margin facies associations have poorer reservoir quality due to lower net-to-gross sand content and higher mud proportions. Chalk and carbonate mass flow deposits are present in the Møre Margin, with low to none reservoir potential. In cases with bioturbated sandstone, the horizontal permeability are largely affected (Dutton and Hentz, 2002). The bioturbation is general low in Møre area. In contrast, Halten-Dønna Terrace, and typically in distal parts of Halten Terrace, have higher degree of bioturbation, but is facies controlled.

Slope- topography must also be concerned due to its control on depositional processes. Topographically complex slopes are inferred by core and seismic data from wells in Halten-Dønna Terrace (see also Quinito, 2017). Cores typically contain a high portion of hybrid beds, sand-rich debrites and backstopping turbidite sands. High-resolution seismic can reveal the slope

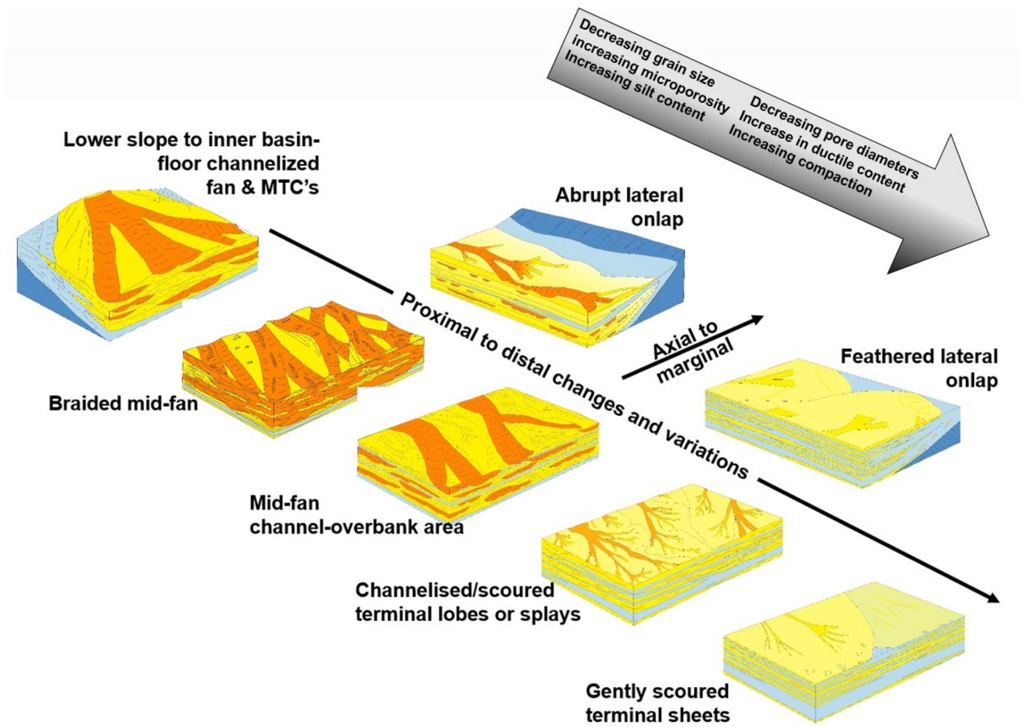

Fig. 29. Spatial variation from proximal to distal in submarine fans with relation to reservoir quality (Shell in house)

topography, and give accurate indication on sediment transportation routes as documented by Sømme et al. (2013a;2013b) and Quinito (2017) for the two study areas, Møre Margin and Dønna Terrace, respectively.

Provenance with implication for reservoir quality and impact on diagenesis

Reservoir quality of the Lange-Lysing sandstone is mainly controlled by burial history, composition, pore-fluid composition and depositional environment (Lien et al., 2006). The type of detrital components and framework grains, largely influence the physical-chemical composition and thus its behavior during burial.

The sandstone has been subjected to compaction as evidenced by the close packing of detrital framework grains during progressive burial, which has caused reduction in primary porosity. The sandstone in the Møre margin was mildly compacted so that the intergranular porosity was preserved and ductile grains were weakly compressed. The effect of mechanical compaction is more pronounced in sandstone from the Halten- Dønna Terrace, as demonstrated by bended micas, fractured quartz, ductile deformed mud intraclasts and brittle deformed grains. The samples from the Vøring Basin indicate a stronger control of mechanical compaction, supported by concave-convex and suture grain boundaries (cf. Engelhardt, 1960) and high degree of leaching of detrital grains and secondary porosity development, The only exception from these characteristics is the sample from 6605/8-2, 3909 m, which is dominated by floating grain-to-grain contact, surrounded by clay mircoporosity.

The chemical compaction are indicated by cementation, replacement of quartz, kaolinite and iron oxides and dissolution of detrital grains. Quartz cementation commonly results in a reduction in pore space and decrease reservoir quality (Imam, 1986; McBride, 1989; Worden and Morad, 2003). However, most of the samples in the study preserve low percentage of overgrowth because of the clay mineral pore-lining has limited the quartz overgrowth and thereby aided the preservation of primary pores. Authigenic quartz cement are lower in sandstone with high portion of illite cement and iron oxide cement, hence lowest in samples in the Møre Margin. The sandstone in the Vøring Basin is assumed to have moderate percentage of quartz overgrowth compared to the Møre Margin due to the finer grain fraction, discontinuous coating and deeper burial depth (cf. Walderhaug, 1996). Fractured quartz grains commonly are uncoated and has allowed increased precipitation of cement.

The iron oxide cement is more pronounced in samples from the Halten-Dønna Terrace and is most likely the product from hydration of detrital iron oxide (occur as opaque heavy minerals). Thin iron oxide rims cover detrital quartz grains and show the initial grain boundaries and inferred to represent recycled, original dry land to desert sandstone. Grain coating cement (clay minerals and quartz overgrowth) and poikilitopic carbonate cement tend to reduce the permeability of the sandstone by blocking pore throats. Calcite cementation is related to dissolution of abundant bioclasts or calcite saturated marine pore water.

The quartzofeldspathic petrofacies (Møre Margin) and the quartzarenitic petrofacies (Vøring Basin) contain more rigid minerals and are less affected by mechanical compaction than quartzolithic petrofacies (Halten-Dønna Terrace) with dominance of ductile lithic fragments and mud clasts. Secondary porosity development by leaching of detrital grains (commonly feldspar) and dissolution of carbonate cement are more prominent in quartzofeldspathic (Møre Margin) and quartzarenitic petrofacies (Vøring Basin), than in the quartzolithic petrofacies (Halten-Dønna Terrace). The intragranular porosity and moldic pores are more abundant in the sandstone samples from the Vøring Basin. The deeply buried sandstone samples (>3900 m) from the Vøring Basin have moderate to good porosity (>15%) but have lower permeability due to high content of authigenetic clay minerals and diagenetic dissolution byproducts of K-feldspar transformed into poor-filling clay minerals, occluding the porosity. In addition, the low permeability can be related to clay microporosity, particular marked in well 6605/8-2, 3909 m. Coating and pore-filling kaolinite and illite clay minerals is suggested to originate by alteration of feldspar and lithic fragments. Scarce to low content of kaolinite in the samples from the Møre Margin, and more abundant in samples from the Halten-Dønna Terrace and Vøring Basin are related to compositional variance, as well as shallower burial depth, which in turn has allowed preservation of the secondary porosity for the Møre Margin samples.

Texture and sorting are important constraints for the reservoir properties, also these parameters are partly controlled by the provenance and partly by the depositional environment. The Møre Margin (quartzofeldspathic petrofacies) have the largest grain sizes and better sorting which provide an important contributing to better reservoir properties. The point counted porosity from the modal analysis in samples from the Møre Margin show positive correlation with grain size, sorting, rounding and pore connectivity (Tab.5). In summary, the quartzofeldspathic petrofacies have the highest potential as hydrocarbon reservoir by preservation of primary porosity combined with the secondary pores not significantly occluded by cement. Lower values of intergranular porosities are related to higher abundance of clay, hence reflecting the higher degree of mechanical compaction.

Conclusion

An integrated analysis using zircon U-Pb age dating, whole-rock geochemical data and petrography of the Lange-Lysing sandstone in the Norwegian Sea has demonstrated the value of this approach to provenance assessment in terms of connecting the lithology, mineralogy and geochronological constraints. Three mineralogical distinct petrofacies are revealed, which is in agreement with a provenance shift in the mid-Norwegian Margin from southwest (Western

Gneiss Region) to northern and western (Lofoten Islands and Nordland) source domains. This is also consistent with proposed recycling effect, decreasing from the NE to SW.

The zircon U-Pb age distribution can reveal the lithological constituents of the provenance region. However, it is challenging to differentiate the source area(s) for the quartzolithic petrofacies (Halten-Dønna Terrace) as the Caledonian Nappe Domain, the tectonic basement windows and Lofoten Islands yield similar crust-forming events (Early Proterozoic). Likewise, a Svecofennian source cannot entirely be ruled out as they have resembling Early Proterozoic U-Pb ages. The deeply buried sandstone in the Vøring Basin probably reveals a mix of source areas, from East Greenland and the Norwegian Landmass, based on the complex U-Pb spectra and the scattered representation though the mid-Proterozoic, combined with Caledonian and Archean components.

The Archaean detrital zircon from Scandinavian landmass illustrates that such components are not typical for Greenland only. Therefore, future and earlier interpretation must be challenged if based on such dataset alone. An example of this is Morton et al. (2005), which excluded Lofoten Islands as potential source area because of the absence of Archean zircon grains. The New U-Pb data also suggest that the Kola Peninsula could have acted as potential source for the Late Archean zircon grains in the Halten-Dønna Terrace samples. However, derivation of the provenance for Late Archean zircon grains (>3000 Ma), in an otherwise obvious source area (WGR) for the sandstone in Møre Margin, is yet not ascertained.

The petrographic and geochemical data has demonstrated a link between provenance and reservoir properties. The quartzofeldspatic petrofacies has characteristics that are favorable over the quartzolithic petrofacies as a viable hydrocarbon reservoir. Predominance of the coarse-to medium-grained rigid sandstone framework minerals quartz and K-feldspar have allowed preservation of primary porosity although the intergranular volume (IGV) are reduced by compaction. The quartzarenitic petrofacies has comparable diagenetic features as the quatzofeldspathic petrofacies, with further reworking and diagenetic dissolution. The quartzarenitic and quartzofeldspathic petrofacies have both well-developed secondary porosity, in contrast to the quartzolithic petrofacies. The quartzolithic petrofacies displays heterogenic cementation and clay minerals, which give variable reservoir quality.

Appendix 1. Geochemical data

The calculated chondrite-normalized REE values for the Upper Lange -Lysing sandstone samples.

Sample	La	Ce	Nd	Sm	Eu	Gd	Tb	Dy	Ho	Er	Tm	Yb	ΣREE	Eu/Eu*	La/Yb
HD8-1.1	30.5	25.4	8.2	7.7	3.7	5.6	4.7	4.0	3.2	3.1	3.4	3.0	102.4	0.6	10.1
HD8-1.2	35.4	32.0	7.5	11.0	5.4	6.7	5.0	4.5	3.6	3.6	3.4	3.1	121.2	0.6	11.4
HD8-1.3	25.6	22.8	5.3	7.3	4.3	5.6	4.0	3.2	2.9	2.5	2.2	2.4	88.1	0.7	10.6
HD8-2.1	23.4	21.0	4.8	6.4	3.4	4.3	3.1	2.5	2.1	2.3	2.0	2.0	77.4	0.6	11.6
HD8-2.2	26.2	22.0	5.6	6.7	3.7	4.2	3.1	2.6	2.1	2.2	2.0	2.0	82.5	0.7	13.0
HD8-2.3	23.7	21.7	6.3	6.1	3.7	4.4	3.4	3.0	2.8	2.9	2.5	2.4	83.0	0.7	10.0
HD8-2.4	109.5	97.0	24.8	25.8	13.4	16.2	13.1	12.4	11.0	11.2	11.2	10.6	356.4	0.6	10.3
M10-1.1	34.3	28.9	7.9	7.9	5.4	5.7	4.1	3.3	2.7	2.7	2.5	2.2	107.8	0.8	15.5
M10-1.2	33.2	30.5	6.9	8.9	5.1	5.8	4.5	3.9	3.3	3.4	3.4	3.0	111.8	0.7	11.1
M10-1.3	38.4	34.5	4.1	9.6	5.7	6.0	4.5	4.1	3.4	3.1	3.4	3.2	119.9	0.7	11.9
M10-1.4	42.0	39.8	10.5	11.9	7.9	7.1	5.7	4.3	4.2	4.0	4.2	3.3	145.1	0.8	12.5
M10-2A.1	55.3	40.3	8.9	14.8	7.8	10.0	7.6	6.7	6.0	5.7	5.3	5.1	173.6	0.6	10.9
M10-2A.2	39.5	28.9	8.6	9.9	5.9	6.9	5.3	4.9	4.1	4.5	3.9	4.5	126.9	0.7	8.8
M10-2A.3	41.4	28.6	4.2	9.0	5.3	6.9	5.2	5.1	4.6	4.1	3.9	3.8	122.1	0.7	10.8
M10-2R.1	46.0	37.1	10.1	11.6	7.4	8.1	6.0	5.3	5.1	4.8	4.8	4.9	151.3	0.7	9.4
M10-2R.2	46.6	37.8	10.5	12.1	6.4	8.5	6.7	6.0	5.4	5.7	4.8	4.5	155.1	0.6	10.3
M10-2R.3	45.2	37.0	10.1	12.4	7.4	8.4	6.2	5.6	4.9	5.0	4.8	4.9	151.9	0.7	9.3
M11-1.1	28.9	23.6	9.8	7.7	4.5	5.3	3.8	3.3	2.9	3.0	2.5	2.7	98.2	0.7	10.5
M11-1.2	39.8	38.0	8.7	11.6	6.9	7.8	5.7	4.6	4.0	3.9	3.9	3.9	138.9	0.7	10.3
H 12-5. 11	18.5	16.8	5.5	4.4	3.0	3.0	2.2	2.0	1.5	1.6	1.4	1.5	61.4	0.8	12.8
H 12-5. 12	19.6	15.0	4.1	3.9	2.0	2.8	2.1	1.9	1.4	1.7	1.4	1.3	57.2	0.6	15.2
H 12-5. 13	15.0	12.9	2.4	4.1	2.4	3.3	2.2	2.3	1.8	1.7	1.4	1.7	51.1	0.7	8.8
H 12-5. 21	72.5	65.0	16.6	18.3	10.1	11.9	9.8	8.8	8.2	8.7	8.7	8.6	247.3	0.7	8.4
H 12-5. 22	40.9	35.2	11.3	9.6	4.9	6.4	4.7	4.4	3.6	4.0	3.4	3.6	132.0	0.6	11.3
H 12-5. 23	15.3	12.2	5.8	3.2	2.0	2.5	2.1	1.9	1.6	1.8	1.7	1.7	51.7	0.7	9.2
H12-4. 1	36.2	29.7	9.0	9.6	5.5	6.3	5.0	4.3	3.2	3.6	3.4	3.3	119.0	0.7	11.0
H12-4. 2	35.7	30.6	10.0	9.1	5.3	6.4	4.8	4.1	3.2	3.6	3.7	3.5	120.0	0.7	10.2
H12-4. 3	44.7	38.0	10.0	11.6	6.9	8.0	6.0	5.3	4.2	4.1	3.9	3.6	146.4	0.7	12.3
H10-1. 1	31.6	28.5	8.6	10.3	6.6	7.1	5.7	5.3	4.9	4.9	5.3	5.1	123.9	0.8	6.2
H10-1. 2	16.3	16.6	11.0	7.1	4.5	5.2	4.7	3.8	3.4	3.7	4.2	3.8	84.4	0.7	4.3
H10-1. 3	24.0	25.2	5.3	9.9	5.9	7.7	6.2	4.9	4.1	3.5	3.7	3.1	103.4	0.7	7.7
D3-9S. 11	27.8	21.4	8.6	6.3	2.6	4.2	3.1	2.8	2.5	2.9	2.8	2.8	87.8	0.5	10.0
D3-9S. 12	43.9	37.0	12.4	11.5	6.0	7.4	5.9	5.3	4.3	4.7	4.5	4.4	147.1	0.6	10.1
D3-9S. 13	43.3	35.0	15.2	10.0	5.4	6.6	5.2	4.1	4.1	4.4	4.5	4.8	142.6	0.7	9.1
D3-9S. 14	34.3	26.2	10.4	8.2	3.6	4.4	3.1	2.7	2.1	2.2	2.2	2.1	101.7	0.6	16.4
D3-9S. 15	29.7	23.9	10.8	7.3	3.9	5.1	4.0	3.3	3.2	3.2	3.1	3.0	100.5	0.6	10.0
D3-9S. 16	25.3	20.6	8.0	5.8	3.7	4.1	3.4	2.9	2.8	2.9	2.8	3.1	85.4	0.7	8.3
D3-9S. 17	37.1	27.8	9.1	8.2	5.1	5.2	4.5	4.0	3.2	2.8	3.1	2.9	113.0	0.8	12.8
D5-6S. 1	66.5	51.3	20.7	14.2	8.0	9.8	8.1	7.5	7.3	7.7	8.1	7.9	217.1	0.7	8.4
D5-6S. 2	44.7	39.3	12.9	12.3	6.2	7.7	6.0	5.0	4.5	4.2	4.2	4.2	151.2	0.6	10.6
D5-6S. 3	29.4	24.3	9.1	7.7	3.7	4.9	4.1	3.9	4.0	4.1	3.9	4.0	103.3	0.6	7.4
H11-3. 1	23.7	20.7	5.5	5.8	3.6	4.4	3.4	3.2	2.6	2.7	2.5	2.5	80.7	0.7	9.3

H11-3. 2	92.9	78.3	19.1	20.7	11.8	14.1	11.2	10.3	9.4	9.4	10.1	10.0	297.4	0.7	9.3
D5.3-1	23.4	18.8	5.1	4.9	2.8	3.5	2.4	2.3	2.0	2.0	2.0	2.1	71.2	0.7	11.4
D5.3-2	31.6	25.0	9.1	7.6	3.8	5.3	4.0	3.3	3.1	3.0	3.4	3.4	102.5	0.6	9.3
D5.3-3	43.9	37.4	9.7	10.9	6.1	7.1	5.3	4.4	3.9	3.8	3.9	3.6	139.9	0.7	12.2
D2-2.1	37.6	29.3	13.5	9.3	4.4	5.9	4.3	4.0	3.5	3.8	3.9	3.6	123.2	0.6	10.4
D2-2.2	48.5	39.0	14.8	13.4	6.8	8.5	6.6	5.5	4.9	4.4	4.5	4.2	160.9	0.6	11.7
D2-2.3	34.1	27.1	9.4	8.0	3.9	5.3	4.1	3.8	3.4	3.4	3.1	3.2	108.8	0.6	10.7
D2-3.1	41.1	34.0	10.8	9.6	6.0	6.7	4.7	4.1	3.5	3.8	3.4	3.2	131.0	0.7	12.8
D2-3.2	39.8	32.6	12.1	10.1	5.4	6.3	4.8	4.1	3.5	3.6	3.7	3.6	129.5	0.7	11.0
D2-3.3	43.3	34.4	14.3	10.4	5.6	6.7	5.3	4.6	4.5	4.4	4.5	4.7	142.7	0.7	9.3
D2-4.1	42.5	34.3	9.0	9.3	4.1	5.4	4.1	3.7	2.7	2.6	2.8	2.7	123.2	0.6	15.5
D2-4.2	39.5	32.9	11.0	9.7	5.7	6.4	4.8	4.4	3.4	3.6	3.7	3.7	128.9	0.7	10.8
D2-4.3	32.2	26.0	9.0	8.2	5.3	5.5	4.3	3.8	3.2	3.1	2.8	2.9	106.3	0.8	11.2

Major and trace elements for the Upper Lange-Lysing sandstone samples.

	SiO2	Al2O3	Fe2O3	MgO	CaO	Na2O	K2O	TiO2	P2O5	MnO	Cr2O3	Ba	Ni	Sc	LOI	Sum
Sample	%	%	%	%	%	%	%	%	%	%	%	PPM	PPM	PPM	%	%
HD8-1.1	90.56	3.50	1.06	0.36	0.69	0.50	0.44	0.22	0.04	<0.01	0.003	246	<20	3	2.6	99.96
HD8-1.2	87.49	4.56	1.78	0.47	0.73	0.46	0.86	0.22	0.05	0.01	0.004	150	<20	4	3.3	99.97
HD8-1.3	90.00	3.80	1.23	0.37	0.51	0.57	0.64	0.18	0.04	<0.01	0.003	132	<20	3	2.6	99.98
HD8-2.1	93.49	2.57	1.09	0.18	0.22	0.17	0.23	0.16	0.02	<0.01	0.002	56	<20	2	1.8	100.00
HD8-2.2	90.35	3.34	1.75	0.41	0.59	0.45	0.39	0.17	0.03	0.02	<0.002	389	<20	3	2.4	99.98
HD8-2.3	89.21	3.62	1.61	0.36	0.91	0.22	0.56	0.18	0.03	0.02	0.003	710	<20	3	3.2	99.98
HD8-2.4	59.31	17.05	5.51	1.63	1.31	1.39	2.64	0.89	0.07	0.03	0.014	537	53	15	9.9	99.84
M10-1.1	83.14	4.06	4.86	0.59	0.54	0.33	2.64	0.23	0.16	0.02	0.006	501	<20	3	3.3	99.97
M10-1.2	63.82	3.37	3.03	0.44	14.04	0.26	2.10	0.34	0.17	0.06	0.005	423	<20	3	12.3	99.94
M10-1.3	62.83	2.99	3.74	0.42	14.54	0.24	2.00	0.21	0.13	0.04	0.004	451	<20	3	12.8	99.97
M10-1.4	74.30	6.81	5.80	0.89	2.08	0.61	4.00	0.47	0.14	0.02	0.009	970	22	5	4.7	99.93
M10-2A. 1	60.47	6.08	2.92	0.79	13.38	0.51	1.68	0.40	0.16	0.03	0.006	389	23	6	13.4	99.90
M10-2A. 2	65.17	5.91	2.60	0.75	11.24	0.55	1.60	0.37	0.10	0.02	0.006	477	21	5	11.5	99.91
M10-2A. 3	47.96	3.57	1.50	0.51	24.06	0.32	0.72	0.18	0.09	0.05	0.004	312	27	4	20.9	99.90
M10-2R.1	59.52	4.68	3.36	0.67	14.62	0.48	2.08	0.48	0.17	0.05	0.005	506	<20	5	13.7	99.89
M10-2R.2	65.11	5.70	2.87	0.70	10.53	0.51	2.16	0.45	0.11	0.03	0.005	609	<20	5	11.7	99.89
M10-2R.3	59.90	5.30	3.40	0.63	13.93	0.46	3.09	0.49	0.14	0.04	0.007	759	<20	5	12.4	99.90
M10-2R.4	46.84	22.29	7.27	1.37	3.83	0.50	3.30	1.01	0.05	0.04	0.014	922	70	16	13.2	99.82
M11-1.1	69.63	4.90	3.59	0.59	8.93	0.46	2.31	0.46	0.11	0.03	0.006	529	<20	3	8.9	99.93
M11-1.2	74.27	4.18	3.93	0.54	7.02	0.32	2.11	0.43	0.22	0.02	0.005	490	<20	5	6.8	99.88
H 12-5. 11	94.01	2.00	0.58	0.12	0.10	0.37	0.59	0.09	0.03	<0.01	0.003	2936	<20	1	1.8	99.98
H 12-5. 12	94.75	2.43	0.58	0.11	0.07	0.34	0.53	0.08	0.03	<0.01	0.003	686	<20	1	1.0	100.00
H 12-5. 13	89.68	2.65	1.17	0.23	2.40	0.28	0.66	0.07	0.02	0.07	0.002	2649	<20	3	2.4	99.98
H 12-5. 21	63.04	16.21	6.32	1.59	0.43	1.35	2.17	0.77	0.09	0.02	0.014	631	51	14	7.8	99.87
H 12-5. 22	86.33	4.93	2.04	0.37	1.11	0.61	0.96	0.31	0.04	0.04	0.005	3037	<20	4	2.9	99.95
H 12-5. 23	91.63	3.44	1.32	0.25	0.14	0.46	0.71	0.20	0.03	<0.01	0.003	1993	<20	2	1.6	99.99

H12-4. 1	87.39	5.49	1.64	0.34	0.25	0.62	1.01	0.28	0.04	0.01	0.005	3162	<20	4	2.5	99.96
H12-4. 2	88.85	4.44	1.51	0.26	0.16	0.51	0.88	0.33	0.04	0.01	0.006	3499	<20	3	2.6	99.95
H12-4. 3	84.87	5.66	2.71	0.55	1.26	0.57	1.16	0.33	0.04	0.03	0.005	1222	<20	4	2.6	99.95
H10-1. 1	66.52	5.95	11.52	0.90	4.80	0.74	1.51	0.19	0.10	0.23	0.005	256	24	9	7.3	99.84
H10-1. 2	61.84	3.74	9.49	0.60	11.60	0.41	0.27	0.10	0.11	0.10	0.005	476	26	11	11.5	99.82
H10-1. 3	75.10	5.75	5.52	0.68	4.65	0.71	1.58	0.13	0.06	0.03	0.003	518	<20	7	5.6	99.87
D3-9S. 11	88.65	4.81	1.48	0.28	0.27	0.08	0.78	0.28	0.03	0.01	0.003	148	<20	4	3.2	99.91
D3-9S. 12	85.54	5.99	1.60	0.33	0.36	0.13	1.02	0.35	0.04	0.02	0.005	210	<20	5	4.5	99.91
D3-9S. 13	90.20	4.15	0.93	0.18	0.20	0.23	0.74	0.43	0.04	0.01	0.005	240	<20	2	2.7	99.89
D3-9S. 14	92.31	3.22	0.70	0.12	0.12	0.16	0.63	0.27	0.03	<0.01	<0.002	321	<20	1	2.3	99.92
D3-9S. 15	89.85	4.29	1.04	0.19	0.37	0.37	0.75	0.25	0.03	0.01	0.003	275	<20	2	2.7	99.91
D3-9S. 16	89.89	3.56	0.96	0.33	1.10	0.33	0.75	0.18	0.03	0.02	0.002	943	20	2	2.6	99.92
D3-9S. 17	90.24	4.32	0.76	0.17	0.56	0.37	0.78	0.23	0.02	0.01	0.003	252	<20	2	2.5	99.99
D5-6S. 1	75.80	10.11	2.55	0.64	0.63	0.24	1.49	0.61	0.06	0.03	0.010	276	34	8	7.7	99.87
D5-6S. 2	83.27	6.75	1.66	0.47	0.56	0.28	1.14	0.39	0.05	0.02	0.006	239	22	5	5.3	99.90
D5-6S. 3	88.27	4.25	1.19	0.24	0.15	0.18	0.83	0.28	0.04	<0.01	0.004	209	21	3	4.4	99.91
H11-3. 1	82.33	3.90	2.71	0.58	3.68	0.49	1.14	0.17	0.03	0.08	0.005	611	<20	4	4.7	99.90
H11-3. 2	64.73	15.75	5.13	1.41	0.37	1.83	2.49	0.81	0.09	0.02	0.012	657	57	14	7.1	99.85
D5.3-1	92.19	3.40	0.64	0.16	0.15	0.35	1.22	0.14	0.03	<0.01	<0.002	153	<20	1	1.6	99.93
D5.3-2	89.48	4.01	1.27	0.32	0.48	0.45	1.09	0.28	0.04	0.01	0.003	230	<20	4	2.5	99.91
D5.3-3	85.27	6.11	2.29	0.29	0.17	0.53	1.36	0.31	0.04	<0.01	0.005	832	<20	4	3.4	99.90
D2-2.1	81.36	4.65	1.24	1.05	2.45	0.22	1.30	0.33	0.05	0.02	0.006	8688	<20	3	6.2	99.86
D2-2.2	85.57	5.78	1.24	0.51	1.01	0.11	1.40	0.33	0.05	0.01	0.006	1352	<20	4	3.7	99.90
D2-2.3	69.83	3.48	3.00	3.12	7.68	0.07	0.70	0.25	0.04	0.05	0.004	360	<20	5	11.6	99.90
D2-3.1	87.52	4.69	1.78	0.22	0.13	0.12	1.12	0.30	0.05	0.04	0.005	7322	21	4	3.1	99.89
D2-3.2	88.88	4.89	1.21	0.22	0.20	0.44	1.31	0.33	0.04	0.01	0.004	830	<20	3	2.3	99.91
D2-3.3	81.93	6.77	2.10	0.42	2.08	0.66	1.54	0.32	0.05	0.04	0.007	291	<20	4	4.0	99.90
D2-4.1	88.84	4.12	0.84	0.28	0.71	0.16	0.90	0.29	0.04	0.02	0.004	4928	<20	2	3.1	99.89
D2-4.2	88.73	4.69	1.08	0.30	0.58	0.17	0.93	0.27	0.05	0.01	0.005	189	<20	3	3.1	99.91
D2-4.3	68.08	4.71	3.78	2.97	7.08	0.13	0.95	0.21	0.04	0.07	0.004	378	<20	5	11.9	99.92

	Be PPM	Co PPM	Cs PPM	Ga PPM	Hf PPM	Nb PPM	Rb PPM	Sn PPM	Sr PPM	Ta PPM	Th PPM	U PPM	V PPM	W PPM
HD8-1.1	2	2.3	0.5	5.5	5.9	5.8	10.4	<1	57.1	0.4	3.0	0.8	35	<0.5
HD8-1.2	<1	4.1	0.8	7.4	3.9	5.3	22.5	<1	57.9	0.3	3.0	0.9	46	<0.5
HD8-1.3	1	3.1	0.4	4.6	2.5	3.8	15.6	<1	49.4	0.3	2.3	0.7	38	<0.5
HD8-2.1	<1	2.5	0.3	2.7	2.8	3.4	7.6	<1	29.6	0.3	2.0	0.6	22	<0.5
HD8-2.2	<1	4.4	0.4	3.3	3.0	4.0	13.0	<1	49.6	0.3	2.4	0.7	41	<0.5
HD8-2.3	2	3.0	0.7	4.0	2.3	4.5	17.3	<1	63.2	0.4	2.2	0.7	31	<0.5
HD8-2.4	2	19.3	6.3	18.9	6.5	17.6	104.0	3	188.3	1.3	12.0	3.4	170	1.5
M10-1.1	<1	4.4	0.8	9.2	2.0	5.6	64.8	<1	112.9	0.3	2.4	0.2	40	0.7
M10-1.2	1	1.4	0.5	4.5	4.2	4.9	50.9	<1	266.6	0.4	1.9	0.4	32	<0.5
M10-1.3	2	1.8	0.4	3.0	1.4	2.9	44.2	<1	193.7	0.3	1.6	0.3	26	<0.5
M10-1.4	<1	4.0	1.4	7.8	4.4	7.5	87.0	<1	178.4	0.5	4.0	0.6	52	0.5
M10-2A. 1	2	6.3	1.8	7.1	4.6	6.3	48.3	<1	347.6	0.4	4.0	1.1	52	<0.5
M10-2A. 2	<1	6.1	1.7	5.2	4.0	6.1	42.7	<1	352.0	0.5	3.7	1.0	55	<0.5
M10-2A. 3	<1	4.7	0.9	2.5	1.6	3.0	21.0	<1	585.5	0.2	2.4	0.9	33	<0.5
M10-2R.1	2	2.2	1.1	5.3	8.2	7.2	54.7	<1	286.1	0.5	2.5	1.0	41	<0.5
M10-2R.2	2	4.4	1.5	6.9	6.4	7.5	56.0	<1	339.2	0.5	3.5	1.0	62	<0.5
M10-2R.3	<1	2.1	1.2	6.4	7.0	7.2	72.4	<1	245.2	0.5	3.0	0.9	47	<0.5
M10-2R.4	3	16.4	4.9	24.0	5.4	17.3	106.5	3	197.8	1.1	15.5	3.1	187	1.2
M11-1.1	2	2.5	1.0	6.7	5.0	7.0	58.3	<1	262.1	0.5	2.6	0.7	42	<0.5
M11-1.2	1	3.0	1.1	5.2	5.3	6.2	59.1	<1	222.8	0.4	2.6	0.8	46	<0.5
H 12-5. 11	2	1.0	0.2	1.9	1.8	3.9	16.9	2	107.0	0.3	1.6	0.4	33	<0.5
H 12-5. 12	1	1.0	0.2	2.2	1.3	2.9	14.6	<1	36.3	0.2	1.2	0.4	40	<0.5
H 12-5. 13	<1	0.6	0.4	3.2	1.1	1.7	20.4	<1	157.4	0.2	1.2	0.4	48	<0.5
H 12-5. 21	3	16.6	5.6	18.2	4.2	11.8	85.8	2	127.9	0.9	10.0	2.3	167	1.4
H 12-5. 22	1	4.0	0.9	5.4	4.4	8.0	28.6	1	138.6	0.5	3.2	0.9	54	4.4
H 12-5. 23	1	1.3	0.3	2.8	2.0	4.1	20.8	<1	75.2	0.5	1.7	0.4	42	<0.5
H12-4. 1	2	3.4	0.9	5.6	2.9	6.4	31.8	2	127.1	0.5	3.0	0.8	50	<0.5

H12-4. 2	1	3.4	0.7	4.6	4.0	7.1	27.9	3	128.9	0.5	3.1	0.8	42	0.9
H12-4. 3	2	3.8	1.1	6.3	3.1	7.1	38.7	<1	102.6	0.5	3.3	0.8	45	<0.5
H10-1. 1	2	10.5	1.7	13.2	2.1	6.1	64.7	<1	326.7	0.4	4.7	0.9	313	0.6
H10-1. 2	<1	21.0	0.1	9.3	2.4	7.8	5.5	<1	494.9	0.3	4.5	0.4	303	<0.5
H10-1. 3	4	2.9	0.9	10.6	2.0	3.8	58.2	<1	395.2	0.2	2.8	0.3	124	<0.5
D3-9S. 11	<1	3.7	0.6	6.4	3.4	6.1	25.4	1	21.8	0.4	3.2	0.8	43	<0.5
D3-9S. 12	<1	4.4	1.0	8.2	3.6	8.8	32.6	2	31.0	0.5	4.0	1.1	53	0.6
D3-9S. 13	<1	3.0	0.5	6.1	6.6	10.8	23.8	1	26.2	0.7	3.2	0.9	33	<0.5
D3-9S. 14	<1	1.8	0.5	4.2	4.1	7.4	18.5	1	27.1	0.4	2.8	0.8	24	0.6
D3-9S. 15	<1	2.9	0.7	5.4	3.6	7.7	23.0	1	37.4	0.4	2.9	0.7	32	0.7
D3-9S. 16	<1	2.9	0.5	5.0	1.9	5.7	22.4	1	59.9	0.3	1.9	0.6	26	<0.5
D3-9S. 17	<1	2.5	0.7	5.3	3.2	6.5	22.4	<1	35.2	0.5	3.0	0.7	26	<0.5
D5-6S. 1	<1	10.6	3.0	13.5	5.5	14.7	58.8	2	55.3	0.8	6.7	1.9	111	1.1
D5-6S. 2	1	5.7	1.1	8.2	3.5	9.2	36.3	1	47.1	0.6	4.0	1.1	62	0.6
D5-6S. 3	2	3.5	0.8	5.0	3.6	6.5	28.6	4	28.6	0.5	2.9	1.0	33	<0.5
H11-3. 1	3	3.9	1.2	6.4	2.0	3.9	46.1	<1	187.1	0.2	2.5	0.6	82	<0.5
H11-3. 2	2	17.8	4.8	17.7	5.2	13.6	97.2	2	151.2	0.9	10.2	2.7	136	1.7
D5.3-1	<1	1.1	0.4	4.7	2.2	3.6	26.6	1	28.2	0.3	1.8	0.5	35	<0.5
D5.3-2	<1	2.8	0.8	4.2	3.6	6.5	31.6	<1	42.9	0.4	2.8	0.8	36	<0.5
D5.3-3	2	4.8	1.1	5.8	4.0	6.9	39.1	<1	63.8	0.5	3.6	1.1	62	1.0
D2-2.1	<1	6.7	0.5	4.9	4.9	9.6	22.1	<1	338.2	0.7	3.4	1.1	41	<0.5
D2-2.2	2	3.5	0.6	6.9	3.6	10.5	28.3	<1	91.9	0.6	4.0	1.1	45	0.8
D2-2.3	<1	2.5	0.4	3.8	4.2	6.7	17.8	<1	152.8	0.4	2.6	0.8	40	<0.5
D2-3.1	<1	4.1	0.4	5.0	4.4	7.7	26.8	<1	201.6	0.6	3.3	0.8	50	0.9
D2-3.2	<1	3.4	0.9	5.0	4.2	8.6	33.3	<1	49.9	0.5	2.8	0.8	44	0.6
D2-3.3	<1	5.7	1.4	7.3	3.8	10.2	44.3	<1	80.4	0.6	4.1	1.0	55	<0.5
D2-4.1	<1	2.8	1.2	4.5	4.2	6.4	22.3	<1	200.8	0.5	3.4	0.8	42	0.6
D2-4.2	<1	3.2	0.9	5.3	3.3	7.8	24.6	<1	59.7	0.5	2.8	0.7	36	<0.5
D2-4.3	1	4.2	0.8	6.1	2.1	6.4	26.4	<1	177.9	0.4	2.6	0.6	37	<0.5

	Zr	Y	La	Ce	Pr	Nd	Sm	Eu	Gd	Tb	Dy	Ho	Er	Tm
Sample	PPM	PPM	PPM	PPM	PPM	PPM	PPM	PPM	PPM	PPM	PPM	PPM	PPM	PPM
HD8-1.1	220.4	7.4	11.2	24.3	2.66	9.9	1.77	0.32	1.72	0.27	1.52	0.27	0.78	0.12
HD8-1.2	147.6	7.7	13.0	30.6	3.15	11.7	2.55	0.47	2.06	0.29	1.72	0.31	0.89	0.12
HD8-1.3	95.1	5.5	9.4	21.8	2.33	8.5	1.68	0.37	1.71	0.23	1.21	0.25	0.62	0.08
HD8-2.1	98.9	4.6	8.6	20.1	2.08	7.8	1.47	0.30	1.31	0.18	0.97	0.18	0.58	0.07
HD8-2.2	108.8	5.0	9.6	21.1	2.21	7.8	1.55	0.32	1.29	0.18	0.99	0.18	0.56	0.07
HD8-2.3	77.9	5.6	8.7	20.8	2.19	8.4	1.41	0.32	1.35	0.20	1.14	0.24	0.72	0.09
HD8-2.4	241.8	23.3	40.2	92.8	9.24	33.7	5.97	1.17	4.96	0.76	4.73	0.94	2.78	0.40
M10-1.1	74.9	6.7	12.6	27.7	2.79	11.3	1.83	0.47	1.73	0.24	1.27	0.23	0.68	0.09
M10-1.2	163.6	8.3	12.2	29.2	2.92	10.8	2.05	0.44	1.76	0.26	1.50	0.28	0.85	0.12
M10-1.3	55.4	8.8	14.1	33.0	3.20	11.8	2.21	0.50	1.83	0.26	1.55	0.29	0.77	0.12
M10-1.4	175.6	9.9	15.4	38.1	3.97	15.1	2.76	0.69	2.18	0.33	1.63	0.36	0.99	0.15
M10-2A. 1	178.8	12.9	20.3	38.6	4.72	17.7	3.42	0.68	3.06	0.44	2.56	0.51	1.43	0.19
M10-2A. 2	147.8	9.6	14.5	27.7	3.44	12.7	2.29	0.51	2.10	0.31	1.86	0.35	1.11	0.14
M10-2A. 3	56.3	11.2	15.2	27.4	3.11	11.7	2.08	0.46	2.10	0.30	1.93	0.39	1.03	0.14
M10-2R.1	311.3	12.5	16.9	35.5	3.95	14.8	2.69	0.64	2.49	0.35	2.02	0.43	1.19	0.17
M10-2R.2	247.3	12.5	17.1	36.2	4.15	15.5	2.79	0.56	2.61	0.39	2.28	0.46	1.41	0.17
M10-2R.3	258.8	13.0	16.6	35.4	3.99	15.8	2.86	0.64	2.58	0.36	2.15	0.42	1.24	0.17
M10-2R.4	214.2	23.2	52.6	109.2	12.10	44.8	8.41	1.65	6.67	0.96	5.33	1.00	2.90	0.40
M11-1.1	194.1	7.4	10.6	22.6	2.53	9.7	1.79	0.39	1.62	0.22	1.25	0.25	0.75	0.09
M11-1.2	209.1	10.8	14.6	36.4	3.70	13.8	2.68	0.60	2.39	0.33	1.76	0.34	0.98	0.14
H 12-5. 11	63.7	3.0	6.8	16.1	1.64	6.0	1.02	0.26	0.91	0.13	0.77	0.13	0.39	0.05
H 12-5. 12	44.3	3.4	7.2	14.4	1.48	5.5	0.89	0.17	0.87	0.12	0.74	0.12	0.43	0.05
H 12-5. 13	45.3	3.7	5.5	12.3	1.32	5.3	0.95	0.21	1.00	0.13	0.87	0.15	0.43	0.05
H 12-5. 21	144.8	17.5	26.6	62.2	6.04	22.9	4.23	0.88	3.64	0.57	3.36	0.70	2.17	0.31
H 12-5. 22	161.1	7.3	15.0	33.7	3.43	12.5	2.21	0.43	1.96	0.27	1.69	0.31	1.00	0.12
H 12-5. 23	62.0	3.3	5.6	11.7	1.15	4.3	0.73	0.17	0.76	0.12	0.73	0.14	0.46	0.06

H12-4. 1	102.0	6.6	13.3	28.4	3.09	11.3	2.22	0.48	1.92	0.29	1.64	0.27	0.89	0.12	0.82	0.10
H12-4. 2	149.5	7.6	13.1	29.3	3.11	11.7	2.11	0.46	1.96	0.28	1.58	0.27	0.90	0.13	0.87	0.11
H12-4. 3	119.4	9.4	16.4	36.4	3.87	14.6	2.67	0.60	2.45	0.35	2.01	0.36	1.02	0.14	0.90	0.11
H10-1. 1	88.2	9.8	11.6	27.3	2.87	10.8	2.38	0.57	2.17	0.33	2.03	0.42	1.21	0.19	1.27	0.19
H10-1. 2	96.5	7.5	6.0	15.9	1.73	6.6	1.64	0.39	1.60	0.27	1.46	0.29	0.93	0.15	0.95	0.12
H10-1. 3	69.8	9.1	8.8	24.1	2.75	10.9	2.29	0.51	2.35	0.36	1.86	0.35	0.86	0.13	0.77	0.09
D3-9S. 11	132.7	5.5	10.2	20.5	2.24	8.6	1.46	0.23	1.28	0.18	1.07	0.21	0.72	0.10	0.69	0.09
D3-9S. 12	138.2	10.1	16.1	35.4	3.87	14.2	2.65	0.52	2.26	0.34	2.02	0.37	1.17	0.16	1.08	0.13
D3-9S. 13	251.0	9.4	15.9	33.5	3.82	13.6	2.30	0.47	2.02	0.30	1.58	0.35	1.10	0.16	1.18	0.14
D3-9S. 14	160.2	4.9	12.6	25.1	2.81	10.2	1.90	0.31	1.35	0.18	1.04	0.18	0.56	0.08	0.52	0.06
D3-9S. 15	148.1	6.6	10.9	22.9	2.52	9.4	1.69	0.34	1.55	0.23	1.27	0.27	0.79	0.11	0.74	0.09
D3-9S. 16	69.4	6.7	9.3	19.7	2.06	7.5	1.33	0.32	1.24	0.20	1.10	0.24	0.73	0.10	0.76	0.08
D3-9S. 17	111.3	6.4	13.6	26.6	3.01	10.3	1.90	0.44	1.60	0.26	1.52	0.27	0.70	0.11	0.72	0.11
D5-6S. 1	199.1	15.8	24.4	49.1	5.25	19.8	3.28	0.70	3.00	0.47	2.84	0.62	1.91	0.29	1.96	0.27
D5-6S. 2	125.0	9.4	16.4	37.6	3.95	14.2	2.83	0.54	2.35	0.35	1.90	0.38	1.04	0.15	1.05	0.14
D5-6S. 3	135.9	8.6	10.8	23.3	2.59	9.6	1.78	0.32	1.50	0.24	1.50	0.34	1.02	0.14	0.99	0.12
H11-3. 1	69.7	5.8	8.7	19.8	2.06	7.4	1.34	0.31	1.34	0.20	1.23	0.22	0.68	0.09	0.63	0.06
H11-3. 2	186.2	19.9	34.1	74.9	7.64	26.7	4.79	1.03	4.32	0.65	3.93	0.80	2.33	0.36	2.48	0.36
D5.3-1	78.0	4.6	8.6	18.0	1.98	7.1	1.13	0.24	1.06	0.14	0.88	0.17	0.50	0.07	0.51	0.04
D5.3-2	138.9	6.9	11.6	23.9	2.76	9.7	1.76	0.33	1.62	0.23	1.27	0.26	0.74	0.12	0.84	0.09
D5.3-3	159.0	7.9	16.1	35.8	3.72	13.8	2.51	0.53	2.16	0.31	1.68	0.33	0.94	0.14	0.89	0.11
D2-2.1	177.8	8.2	13.8	28.0	3.18	11.4	2.14	0.38	1.82	0.25	1.54	0.30	0.95	0.14	0.90	0.10
D2-2.2	139.2	10.2	17.8	37.3	4.21	16.1	3.10	0.59	2.59	0.38	2.10	0.42	1.09	0.16	1.03	0.12
D2-2.3	142.4	6.9	12.5	25.9	2.86	10.7	1.84	0.34	1.63	0.24	1.44	0.29	0.85	0.11	0.79	0.10
D2-3.1	149.1	7.7	15.1	32.5	3.47	12.3	2.22	0.52	2.06	0.27	1.57	0.30	0.95	0.12	0.80	0.10
D2-3.2	165.3	8.5	14.6	31.2	3.38	12.7	2.33	0.47	1.92	0.28	1.56	0.30	0.89	0.13	0.90	0.11
D2-3.3	127.6	9.5	15.9	32.9	3.61	13.1	2.40	0.49	2.05	0.31	1.76	0.38	1.09	0.16	1.16	0.13
D2-4.1	167.1	6.1	15.6	32.8	3.50	12.3	2.14	0.36	1.65	0.24	1.40	0.23	0.64	0.10	0.68	0.07
D2-4.2	123.8	8.0	14.5	31.5	3.41	13.5	2.25	0.50	1.97	0.28	1.67	0.29	0.90	0.13	0.91	0.09
D2-4.3	74.8	7.2	11.8	24.9	2.81	10.9	1.89	0.46	1.68	0.25	1.46	0.27	0.78	0.10	0.71	0.08

Sample	TOT/C %	TOT/S %	Mo PPM	Cu PPM	Pb PPM	Zn PPM	Ni PPM	As PPM	Cd PPM	Sb PPM	Bi PPM	Ag PPM	Au PPB	Hg PPM	Tl PPM	Se PPM
HD8-1.1	0.50	0.11	0.1	2.9	3.4	15	5.7	1.6	<0.1	<0.1	<0.1	<0.1	<0.5	0.04	<0.1	<0.5
HD8-1.2	0.75	0.30	0.2	4.4	7.8	22	12.3	4.2	<0.1	<0.1	<0.1	<0.1	1.7	0.08	<0.1	<0.5
HD8-1.3	0.56	0.10	0.2	2.4	6.0	18	6.0	2.1	<0.1	<0.1	<0.1	<0.1	<0.5	0.05	<0.1	<0.5
HD8-2.1	0.32	0.50	0.4	3.1	9.9	16	14.2	4.1	<0.1	0.2	<0.1	<0.1	<0.5	0.22	<0.1	<0.5
HD8-2.2	0.62	0.38	0.1	3.5	6.1	17	11.3	3.0	<0.1	<0.1	<0.1	<0.1	<0.5	0.11	<0.1	<0.5
HD8-2.3	0.81	0.78	1.2	4.7	8.3	16	11.9	5.1	<0.1	<0.1	<0.1	<0.1	1.8	0.25	<0.1	<0.5
HD8-2.4	2.38	1.09	0.4	27.5	19.9	95	40.1	16.5	<0.1	<0.1	0.3	<0.1	0.8	0.30	<0.1	0.7
M10-1.1	0.83	<0.02	<0.1	6.5	1.8	24	8.3	2.4	<0.1	0.1	<0.1	<0.1	<0.5	0.13	<0.1	<0.5
M10-1.2	3.38	0.04	<0.1	1.0	1.3	13	2.4	2.3	<0.1	<0.1	<0.1	<0.1	<0.5	0.01	<0.1	<0.5
M10-1.3	3.29	0.02	<0.1	1.9	2.0	11	4.4	2.7	<0.1	<0.1	<0.1	<0.1	<0.5	0.01	<0.1	<0.5
M10-1.4	0.64	0.03	<0.1	5.4	3.5	30	10.1	3.5	<0.1	0.1	<0.1	<0.1	<0.5	0.05	<0.1	<0.5
M10-2A. 1	3.52	0.21	0.1	16.4	6.3	35	16.2	2.3	<0.1	<0.1	<0.1	0.1	3.0	0.06	<0.1	<0.5
M10-2A. 2	2.94	0.38	0.1	12.7	6.4	36	17.2	2.9	<0.1	0.1	<0.1	<0.1	<0.5	0.05	<0.1	<0.5
M10-2A. 3	5.80	0.35	0.3	14.0	4.4	19	17.0	2.4	<0.1	<0.1	<0.1	<0.1	<0.5	0.04	<0.1	0.5
M10-2R.1	3.43	0.05	<0.1	5.9	3.2	30	5.5	0.7	<0.1	<0.1	<0.1	<0.1	<0.5	0.04	<0.1	<0.5
M10-2R.2	2.87	0.13	<0.1	9.2	5.5	24	10.3	2.1	<0.1	<0.1	<0.1	<0.1	<0.5	0.05	<0.1	<0.5
M10-2R.3	3.16	<0.02	<0.1	4.5	3.0	14	3.9	0.9	<0.1	<0.1	<0.1	<0.1	<0.5	0.02	<0.1	<0.5
M10-2R.4	2.36	0.30	0.3	49.4	19.0	88	49.0	18.7	<0.1	<0.1	0.2	<0.1	<0.5	0.06	<0.1	<0.5
M11-1.1	2.31	0.30	0.1	4.4	2.9	26	6.6	2.0	<0.1	<0.1	<0.1	<0.1	<0.5	0.02	<0.1	<0.5
M11-1.2	1.81	0.68	<0.1	3.5	3.0	24	6.0	3.0	<0.1	<0.1	<0.1	<0.1	<0.5	0.01	<0.1	<0.5
H 12-5. 11	0.48	0.13	0.5	12.6	15.5	15	4.5	1.6	<0.1	0.1	<0.1	<0.1	<0.5	0.08	<0.1	<0.5
H 12-5. 12	0.08	0.09	0.5	4.5	7.5	16	5.0	<0.5	<0.1	<0.1	<0.1	<0.1	<0.5	0.02	<0.1	<0.5
H 12-5. 13	0.66	0.10	<0.1	2.7	14.6	28	3.8	0.7	<0.1	0.1	<0.1	<0.1	<0.5	0.06	<0.1	<0.5
H 12-5. 21	1.28	1.18	0.3	26.4	19.0	109	45.9	10.0	<0.1	<0.1	0.3	<0.1	<0.5	0.06	<0.1	0.7
H 12-5. 22	0.51	0.53	0.5	11.1	14.3	30	12.3	5.5	<0.1	0.2	<0.1	<0.1	<0.5	0.08	<0.1	<0.5
H 12-5. 23	0.24	0.13	0.2	3.7	9.3	32	4.4	1.1	<0.1	0.1	<0.1	<0.1	<0.5	0.03	<0.1	<0.5

H12-4. 1	0.32	0.32	0.2	10.7	19.4	30	8.7	3.4	<0.1	0.3	<0.1	<0.1	<0.5	0.16	<0.1	<0.5
H12-4. 2	0.34	0.51	0.1	6.7	20.1	25	9.2	3.4	<0.1	0.3	<0.1	<0.1	<0.5	0.09	<0.1	<0.5
H12-4. 3	0.51	0.11	0.2	4.8	6.7	32	12.8	2.8	<0.1	0.1	<0.1	<0.1	<0.5	0.07	<0.1	<0.5
H10-1. 1	2.21	1.16	0.3	4.1	13.7	58	20.7	41.9	<0.1	0.2	0.1	<0.1	<0.5	0.02	<0.1	<0.5
H10-1. 2	3.00	0.03	<0.1	3.3	45.8	78	28.4	38.0	<0.1	<0.1	0.1	<0.1	<0.5	0.02	<0.1	<0.5
H10-1. 3	1.34	0.17	<0.1	2.2	9.9	50	6.6	5.0	<0.1	<0.1	<0.1	<0.1	<0.5	0.02	<0.1	<0.5
D3-9S. 11	0.74	0.38	0.1	5.1	3.4	31	8.9	4.4	<0.1	<0.1	<0.1	<0.1	<0.5	0.01	<0.1	<0.5
D3-9S. 12	1.48	0.34	0.2	8.6	5.0	20	9.1	4.7	<0.1	<0.1	<0.1	<0.1	<0.5	0.02	<0.1	<0.5
D3-9S. 13	0.56	0.15	<0.1	3.8	3.7	17	4.7	2.0	<0.1	<0.1	<0.1	<0.1	1.0	0.02	<0.1	<0.5
D3-9S. 14	0.63	0.15	<0.1	5.0	2.9	12	3.7	1.6	<0.1	<0.1	<0.1	<0.1	<0.5	0.02	<0.1	<0.5
D3-9S. 15	0.71	0.35	0.2	5.2	3.4	18	7.5	2.2	<0.1	<0.1	<0.1	<0.1	<0.5	0.01	<0.1	<0.5
D3-9S. 16	0.81	0.29	0.1	5.5	3.1	15	7.5	3.7	<0.1	<0.1	<0.1	<0.1	<0.5	<0.01	<0.1	<0.5
D3-9S. 17	0.62	0.17	<0.1	5.5	3.0	17	4.1	1.9	<0.1	<0.1	<0.1	<0.1	<0.5	0.01	<0.1	<0.5
D5-6S. 1	2.62	0.75	0.7	20.7	10.5	49	23.2	9.9	<0.1	<0.1	0.1	<0.1	<0.5	0.05	0.1	<0.5
D5-6S. 2	1.82	0.35	0.1	8.2	5.7	32	10.7	5.5	<0.1	<0.1	<0.1	<0.1	<0.5	0.01	<0.1	<0.5
D5-6S. 3	1.99	0.39	0.2	17.7	4.0	16	8.5	4.1	<0.1	<0.1	<0.1	<0.1	<0.5	0.01	<0.1	<0.5
H11-3. 1	1.38	0.63	<0.1	4.8	6.6	27	7.3	1.5	<0.1	<0.1	<0.1	<0.1	<0.5	0.04	<0.1	<0.5
H11-3. 2	1.23	1.08	0.9	19.8	16.3	83	49.0	13.1	<0.1	<0.1	0.2	<0.1	<0.5	0.07	0.1	1.0
D5.3-1	0.23	0.08	<0.1	2.9	1.8	8	1.7	0.6	<0.1	<0.1	<0.1	<0.1	<0.5	0.01	<0.1	<0.5
D5.3-2	0.56	0.22	<0.1	3.6	2.5	16	5.2	2.0	<0.1	<0.1	<0.1	<0.1	<0.5	0.03	<0.1	<0.5
D5.3-3	0.48	1.23	0.6	8.7	5.4	35	12.4	7.9	<0.1	0.1	<0.1	<0.1	<0.5	0.03	<0.1	<0.5
D2-2.1	1.36	0.36	0.7	8.2	41.5	29	5.6	2.2	<0.1	0.4	<0.1	0.2	<0.5	0.06	<0.1	<0.5
D2-2.2	0.63	0.27	0.2	3.9	11.3	26	6.8	2.5	<0.1	0.1	<0.1	<0.1	<0.5	0.02	<0.1	<0.5
D2-2.3	3.42	0.22	0.1	2.7	4.5	20	4.1	2.1	<0.1	<0.1	<0.1	<0.1	<0.5	0.01	<0.1	<0.5
D2-3.1	0.40	0.48	0.1	5.0	7.1	18	6.5	3.0	<0.1	0.2	<0.1	<0.1	<0.5	0.02	<0.1	<0.5
D2-3.2	0.22	0.30	0.1	2.7	3.9	19	6.1	2.1	<0.1	<0.1	<0.1	<0.1	<0.5	<0.01	<0.1	<0.5
D2-3.3	0.84	0.41	0.1	5.3	5.1	28	11.8	5.7	<0.1	<0.1	<0.1	<0.1	<0.5	0.02	<0.1	<0.5
D2-4.1	0.63	0.27	0.2	3.2	4.2	17	3.7	2.5	<0.1	<0.1	<0.1	<0.1	<0.5	0.03	<0.1	<0.5
D2-4.2	0.54	0.20	0.1	2.6	4.5	18	6.0	2.2	<0.1	<0.1	<0.1	<0.1	<0.5	0.04	<0.1	<0.5
D2-4.3	3.20	0.15	0.1	2.8	3.2	28	10.1	1.9	<0.1	<0.1	<0.1	<0.1	<0.5	0.04	<0.1	<0.5

Appendix 2. U-Pb data

Overview over the ICP-MS U-Pb dataset and U-Pb ages for all samples.

Summary for ICP-MS U-Pb zircon results for 6605/8-2, 3909.69m

	ppm				*Ratios*							*Discordance*		*Ages*					
Name	**U**	**^{206}Pb**	**$^{206}Pb_c$(%)**	**206/204**	**$^{207}Pb/^{206}Pb^{*}$**	**1σ**	**207Pb/235U***	**1σ**	**206Pb/238U***	**1σ**	**Rho**	**Central (%)**	**Minimum rim (%)**	**207/206**	**1σ**	**207/235**	**1σ**	**206/238**	**1σ**
6605-8-2_01	282	133.8	0.00E+00	13658	0.17011	0.00264	10.60935	0.22366	0.452322	0.00644	0.676	-7.2	-3.6	2559	26	2490	20	2406	29
6605-8-2_02	147	61.5	1.00E-01	23160	0.18442	0.00351	9.99449	0.24456	0.393048	0.00606	0.630	-24.2	-21	2693	31	2434	23	2137	28
6605-8-2_03	38	12	0.00E+00	3193	0.11513	0.00154	4.99883	0.09124	0.314917	0.00391	0.680	-7.1	-3.4	1882	23	1819	15	1765	19
6605-8-2_04	322	85.1	0.00E+00	20324	0.11571	0.00148	4.22807	0.06997	0.265006	0.00278	0.634	-22.3	-19.5	1891	22	1679	14	1515	14
6605-8-2_05B	103	57.2	0.00E+00	13723	0.19776	0.00446	13.48366	0.38625	0.494511	0.00872	0.616	-9.4	-5	2808	36	2714	27	2590	38
6605-8-2_06	40	14.7	0.00E+00	2520	0.12626	0.00258	5.86713	0.14869	0.337033	0.00506	0.592	-9.8	-5	2046	36	1956	22	1872	24
6605-8-2_07	335	88.1	0.00E+00	16780	0.11774	0.00122	4.62203	0.06955	0.284712	0.00311	0.726	-18	-15.5	1922	19	1753	13	1615	16
6605-8-2_08	113	8.3	0.00E+00	1785	0.05948	0.00078	0.6	0.01022	0.077675	0.00073	0.582	-18.2	-8.2	585	27	500	6	482	4
6605-8-2_09	176	23.6	0.00E+00	4531	0.06801	0.00073	1.24905	0.01926	0.133201	0.00148	0.722	-7.7	-2	869	22	823	9	806	8
6605-8-2_11	61	8	0.00E+00	7319	0.0927	0.00135	1.65465	0.03469	0.129459	0.00196	0.721	-49.9	-47.2	1482	28	991	13	785	11
6605-8-2_12	44	14.9	0.00E+00	162934	0.11762	0.00145	5.49539	0.09682	0.338843	0.00427	0.715	-2.4	.	1920	21	1900	15	1881	21
6605-8-2_13	252	28.5	0.00E+00	7639	0.13836	0.00202	2.42384	0.07034	0.127057	0.00319	0.864	-68.9	-67.4	2207	25	1250	21	771	18
6605-8-2_14	105	23.8	0.00E+00	8809	0.12048	0.00132	4.17935	0.08321	0.251587	0.00419	0.836	-29.3	-26.7	1963	20	1670	16	1447	22
6605-8-2_15	69	12.8	0.00E+00	4603	0.07793	0.00081	2.05903	0.0293	0.191639	0.00187	0.686	-1.4	.	1145	20	1135	10	1130	10
6605-8-2_10	156	26.7	0.00E+00	3785	0.12251	0.00181	2.98151	0.05972	0.176507	0.00238	0.673	-51.3	-49.3	1993	25	1403	15	1048	13
6605-8-2_16	40	4.5	0.00E+00	3816	0.06327	0.0008	1.0	0.01653	0.119259	0.00114	0.602	1.3	.	717	26	724	8	726	7
6605-8-2_18	53	13.7	0.00E+00	11622	0.10493	0.00128	3.80865	0.06223	0.263248	0.00285	0.664	-13.5	-10.3	1713	22	1595	13	1506	15
6605-8-2_19	201	25	0.00E+00	3099	0.09666	0.00106	1.75523	0.02527	0.131706	0.00123	0.648	-51.9	-50.2	1561	20	1029	9	798	7
6605-8-2 20	294	91.3	1.20E+00	7140	0.11487	0.00182	4.99988	0.0955	0.315686	0.00337	0.558	-6.6	-2.7	1878	28	1819	16	1769	16

6605-8-2 21	147	37.9	0.00E+00	11321	0.11499	0.0015	4.21238	0.07025	0.265691	0.00276	0.623	-21.5	-18.7	1880	22	1676	14	1519	14
6605-8-2 23	441	74.4	0.00E+00	21944	0.07661	0.00088	1.8984	0.02809	0.179727	0.00169	0.634	-4.4	.	1111	22	1081	10	1065	9
6605-8-2 22	170	32.7	0.00E+00	2264	0.11412	0.00148	3.54094	0.07538	0.225031	0.0038	0.793	-33	-30	1866	24	1536	17	1308	20
6605-8-2 24	32	17.3	0.00E+00	3790	0.19834	0.00524	13.64355	0.4391	0.498899	0.00917	0.571	-8.8	-3.9	2813	42	2725	30	2609	39
6605-8-2 27	69	19.4	0.00E+00	5058	0.11515	0.00164	4.59929	0.08377	0.289685	0.00329	0.623	-14.6	-11.2	1882	24	1749	15	1640	16
6605-8-2 26	284	71.7	0.00E+00	19469	0.10107	0.00124	3.70366	0.07587	0.265771	0.00435	0.799	-8.5	-4.3	1644	23	1572	16	1519	22
6605-8-2 28	122	28.7	0.00E+00	8254	0.09212	0.00099	3.10023	0.04585	0.244097	0.00248	0.687	-4.7	-1.1	1470	20	1433	11	1408	13
6605-8-2 29	100	34	0.00E+00	7363	0.12142	0.00145	5.76359	0.0972	0.344265	0.00411	0.708	-4.1	-0.7	1977	21	1941	15	1907	20
6605-8-2 30	71	22.9	0.00E+00	5249	0.12291	0.00151	5.55714	0.09473	0.327921	0.00388	0.694	-9.8	-6.6	1999	21	1909	15	1828	19
6605-8-2 31	124	29.5	4.60E-01	8462	0.10232	0.00138	3.25893	0.05807	0.230997	0.00268	0.651	-21.7	-18.4	1667	24	1471	14	1340	14
6605-8-2 32	76	5.7	0.00E+00	994	0.05861	0.00129	0.65197	0.01645	0.080675	0.00099	0.485	-9.9	.	553	46	510	10	500	6
6605-8-2 33	149	17.8	8.60E-01	6817	0.08654	0.00114	1.62354	0.02831	0.136065	0.00155	0.654	-41.6	-38.7	1350	25	979	11	822	9
6605-8-2 34	62	17.1	0.00E+00	13758	0.11363	0.00163	4.52247	0.08273	0.288646	0.00328	0.621	-13.6	-10.1	1858	24	1735	15	1635	16
6605-8-2 35	127	36.7	5.80E-02	11843	0.15643	0.00296	5.99408	0.13115	0.277909	0.00305	0.501	-38.9	-36.5	2417	33	1975	19	1581	15
6605-8-2 36	83	20.4	0.00E+00	3491	0.11498	0.00167	4.09813	0.07801	0.258498	0.00318	0.646	-23.6	-20.5	1880	25	1654	16	1482	16
6605-8-2 38	68	21.9	0.00E+00	8624	0.11304	0.00223	4.87661	0.13951	0.312882	0.00649	0.725	-5.8	.	1849	35	1798	24	1755	32
6605-8-2 39	95	23.1	0.00E+00	8783	0.09288	0.00122	3.2802	0.05672	0.256132	0.00288	0.650	-1.2	.	1485	24	1476	13	1470	15
6605-8-2 40	113	19.2	0.00E+00	6145	0.11534	0.00163	3.08754	0.05883	0.19414	0.00249	0.672	-42.9	-40.5	1885	25	1430	15	1144	13
6605-8-2 41	102	25.9	0.00E+00	5220	0.11185	0.00186	3.90664	0.08183	0.253314	0.00322	0.606	-22.8	-19.2	1830	29	1615	17	1456	17
6605-8-2 43	100	24.5	0.00E+00	4333	0.10444	0.00149	3.79672	0.07536	0.263645	0.00363	0.695	-12.9	-8.9	1705	25	1592	16	1508	19
6605-8-2 45	113	13.6	0.00E+00	1973	0.08843	0.00114	1.60409	0.02669	0.131567	0.00139	0.633	-45.4	-42.9	1392	23	972	10	797	8
6605-8-2 46	171	24.5	0.00E+00	6534	0.10516	0.0014	2.27313	0.04568	0.156771	0.00236	0.748	-48.6	-46.3	1717	24	1204	14	939	13
6605-8-2 47	24	4.9	0.00E+00	1609	0.08322	0.00133	2.49972	0.05095	0.217841	0.00277	0.623	-0.3	.	1274	30	1272	15	1270	15

Summary for ICP-MS U-Pb zircon results for 6605/8-1, 4198.65m

	ppm				*Ratios*							*Discordance*		*Ages*					
Name	**U**	**^{206}Pb**	**^{206}Pb$_c$ (%)**	**206/ 204**	**^{207}Pb/^{20} ^{6}Pb***	**1σ**	**207Pb/2 35U***	**1σ**	**206Pb/2 38U***	**1σ**	**Rh o**	**Centra l (%)**	**Minimu m rim (%)**	**207/2 06**	**1 σ**	**207/ 235**	**1 σ**	**206/2 38**	**1 σ**
6605-8-			0.00E		0.1140	0.000		0.122		0.007	0.9					183			
1_01	140	34.9	+00	7924	5	8	5.07583	52	0.322789	456	57	-3.8	-1.2	1865	12	2	20	1803	36
6605-8-			0.00E	1328	0.1010	0.000		0.091		0.006	0.9					164			
1_02	120	26.6	+00	4	7	66	4.03413	86	0.289478	313	58	-0.3	.	1644	12	1	19	1639	32
6605-8-			0.00E			0.000		0.097		0.006	0.9					168			
1_03	108	23.8	+00	4798	0.1074	71	4.27609	01	0.288763	264	56	-7.8	-5.3	1756	12	9	19	1635	31
6605-8-			0.00E	1963	0.1101	0.000		0.085		0.005	0.9					156			
1_04	307	56	+00	5	7	72	3.6614	24	0.241043	387	60	-25.3	-23.4	1802	12	3	19	1392	28
6605-8-			0.00E	4236	0.1158	0.000		0.101		0.006	0.9					172			
1_05	311	66.6	+00	5	5	73	4.48465	48	0.280761	099	60	-17.7	-15.8	1893	11	8	19	1595	31
6605-8-			0.00E		0.1068	0.000		0.100		0.006	0.9					169			
1_06	47	10.7	+00	2808	3	78	4.32083	94	0.293335	507	49	-5.7	-3	1746	13	7	19	1658	32
6605-8-			0.00E	1497	0.1140	0.000		0.118		0.007	0.9					182			
1_07	246	60.5	+00	9	2	73	5.01249	33	0.318833	242	62	-4.9	-2.6	1864	11	1	20	1784	35
6605-8-			0.00E		0.0670	0.000		0.026		0.002	0.9								
1_08	121	12.2	+00	3848	2	54	1.26331	72	0.136709	672	24	-1.6	.	838	15	829	12	826	15
6605-8-			0.00E		0.1083	0.001		0.131		0.008	0.9					165			
1_09	81	18.8	+00	5994	8	23	4.11233	11	0.275191	195	34	-13	-9.1	1772	20	7	26	1567	41
6605-8-			0.00E		0.1162	0.000		0.126		0.007	0.9					185			
1_10	108	27	+00	7469	9	79	5.2168	13	0.325345	55	60	-5.1	-2.7	1900	12	5	21	1816	37
6605-8-			0.00E	6043	0.1154	0.000		0.138		0.008	0.9					190			
1_12	161	43.1	+00	8	1	75	5.51765	66	0.346748	419	66	2	.	1886	11	3	22	1919	40
6605-8-			0.00E		0.0538	0.001		0.013		0.001	0.6								
1_13	37	1.6	+00	491	2	17	0.44209	21	0.059574	222	87	2.7	.	364	45	372	9	373	7
6605-8-			0.00E		0.1165	0.000		0.129		0.007	0.9					184			
1_14	89	22	+00	6994	2	76	5.13221	42	0.319447	778	66	-7	-4.7	1904	11	1	21	1787	38
6605-8-			0.00E		0.0761	0.003		0.042		0.003	0.8								
1_15	56	1.5	+00	4104	2	36	0.4977	72	0.047421	492	58	-74.5	-67.9	1098	89	410	29	299	21
6605-8-			0.00E		0.1157	0.001		0.226		0.013	0.9					197			
1_16	26	6.8	+00	4636	2	32	5.96071	05	0.373572	515	54	9.6	0.4	1891	20	0	33	2046	63
6605-8-			0.00E		0.1141	0.000		0.145		0.009	0.9					187			
1_17	77	20	+00	8806	9	74	5.33007	9	0.338544	001	71	0.8	.	1867	12	4	23	1880	43
6605-8-			0.00E		0.0785	0.000		0.051		0.004	0.9					119			
1_18	131	20.5	+00	9697	1	52	2.2547	47	0.208297	548	57	5.7	0.2	1160	13	8	16	1220	24

6605-8-1_19	38	7.8	0.00E+00	3415	0.11493	0.00119	4.22301	0.11274	0.266495	0.00656	0.922	-21.2	-18.2	1879	18	1679	22	1523	33
6605-8-1_20	107	5.7	0.00E+00	1639	0.05562	0.00051	0.57706	0.01185	0.075243	0.001386	0.897	7.2	.	437	21	463	8	468	8
6605-8-1_21	157	34.1	0.00E+00	7069	0.11355	0.00081	4.50248	0.10778	0.287581	0.006569	0.954	-13.9	-11.5	1857	12	1731	20	1629	33
6605-8-1_22	46	2.3	0.00E+00	1812	0.05659	0.00077	0.54106	0.01245	0.069348	0.001287	0.807	-9.4	.	475	29	439	8	432	8
6605-8-1_23	70	3.7	0.00E+00	970	0.05602	0.00072	0.56689	0.01442	0.073395	0.001615	0.865	0.8	.	453	28	456	9	457	10
6605-8-1_24	76	18.6	0.00E+00	4664	0.11388	0.00088	5.04034	0.12391	0.321001	0.007493	0.949	-4.2	-1.3	1862	13	1826	21	1795	37
6605-8-1_25	221	15.6	0.00E+00	3404	0.11132	0.00085	1.54294	0.04662	0.100521	0.002938	0.967	-69.2	-68.3	1821	13	948	19	617	17
6605-8-1_26	84	44.5	0.00E+00	13122	0.22568	0.00235	19.76617	0.80797	0.635223	0.02511	0.967	6.2	.	3022	16	3080	40	3170	99
6605-8-1_27	245	12.3	0.00E+00	8676	0.05537	0.00049	0.57461	0.01122	0.075267	0.001314	0.894	9.9	.	427	19	461	7	468	8
6605-8-1_28	172	39.2	0.00E+00	12964	0.11808	0.00084	4.88328	0.117	0.299952	0.006865	0.955	-13.9	-11.6	1927	12	1799	20	1691	34
6605-8-1_29	21	6.7	0.00E+00	2049	0.16707	0.00163	9.3021	0.27933	0.403803	0.011471	0.946	-15.9	-13.3	2529	16	2368	28	2187	53
6605-8-1_30	209	28.6	0.00E+00	9356	0.10463	0.00076	2.67191	0.05691	0.185211	0.003709	0.94	-38.9	-37.2	1708	13	1321	16	1095	20
6605-8-1_31	55	12.4	0.00E+00	4292	0.10743	0.00079	4.44328	0.10836	0.299966	0.006972	0.953	-4.2	-1.4	1756	12	1720	20	1691	35
6605-8-1_32	42	2	0.00E+00	6308	0.05502	0.00199	0.54957	0.03295	0.072447	0.003462	0.797	9.5	.	413	78	445	22	451	21
6605-8-1_33	45	11.3	0.00E+00	2474	0.11624	0.00147	4.78411	0.16359	0.298503	0.00948	0.929	-12.9	-8.7	1899	22	1782	29	1684	47
6605-8-1_34	33	8.9	0.00E+00	2597	0.12129	0.00096	5.88283	0.15266	0.351759	0.008695	0.953	-1.9	.	1975	13	1959	23	1943	41
6605-8-1_35	52	11.5	0.00E+00	9844	0.10699	0.00074	4.37542	0.10549	0.296611	0.006851	0.958	-4.8	-2.2	1749	12	1708	20	1674	34
6605-8-1_36	226	28.3	0.00E+00	119695	0.10506	0.00071	2.5049	0.05592	0.172929	0.003677	0.953	-43.3	-41.7	1715	12	1273	16	1028	20
6605-8-1_37	394	100	0.00E+00	32788	0.11577	0.00076	5.35009	0.13323	0.33516	0.008051	0.965	-1.7	.	1892	12	1877	21	1863	39
6605-8-1_39	106	24.2	0.00E+00	5959	0.1137	0.00086	4.75078	0.11565	0.303041	0.007013	0.951	-9.4	-6.8	1859	13	1776	20	1706	35
6605-8-1_40	397	89.2	0.00E+00	49045	0.1157	0.00079	4.7405	0.1137	0.297151	0.006828	0.958	-12.8	-10.6	1891	12	1774	20	1677	34

Summary for ICP-MS U-Pb zircon result 6204/10-1, 1970

	ppm		*Ratios*									*Discordance*		*Ages*					
Name	**U**	**^{206}Pb**	**$^{206}Pb_c$ (%)**	**206/204**	**^{207}Pb/^{206}Pb***	**1σ**	**207Pb/235U***	**1σ**	**206Pb/238U***	**1σ**	**Rho**	**Central (%)**	**Minimum rim (%)**	**207/206**	**1 σ**	**207/235**	**1 σ**	**206/238**	**1 σ**
6204-10-1 1970_67	357	29	0.00E+00	4283	0.05855	0.00034	0.7173	0.0122	0.088856	0.001422	0.941	-0.3	.	550	13	549	7	549	**8**
6204-10-1 1970_68	60	8.2	0.00E+00	2562	0.07205	0.00052	1.47609	0.02529	0.148596	0.002313	0.908	-10.2	-6.4	987	13	921	10	893	**13**
6204-10-1 1970_69	559	91.5	0.00E+00	16853	0.0722	0.00027	1.74996	0.02698	0.17578	0.002629	0.97	5.7	1.9	992	7	1027	10	1044	**14**
6204-10-1 1970_70	157	22.7	0.00E+00	4952	0.0704	0.00035	1.5	0.02313	0.155585	0.002251	0.945	-0.9	.	940	10	935	9	932	**13**
6204-10-1 1970_71	43	15.3	0.00E+00	2475	0.0992	0.00095	4.84022	0.13488	0.353882	0.009263	0.939	24.8	17.3	1609	17	1792	23	1953	**44**
6204-10-1 1970_72	78	13	0.00E+00	2731	0.07614	0.00056	1.89405	0.03441	0.180418	0.002993	0.913	-2.9	.	1099	15	1079	12	1069	**16**
6204-10-1 1970_73	265	41.7	0.00E+00	4859	0.07414	0.0006	1.60322	0.02256	0.156843	0.001808	0.819	-10.9	-7.2	1045	15	971	9	939	**10**
6204-10-1 1970_01	113	26.8	0.00E+00	5389	0.09784	0.00063	3.29026	0.06129	0.243905	0.004264	0.939	-12.4	-10	1583	11	1479	15	1407	**22**
6204-10-1 1970_02	209	31	0.00E+00	6320	0.07201	0.0004	1.5919	0.02548	0.160328	0.002409	0.939	-3	.	986	11	967	10	959	**13**
6204-10-1 1970_03	300	79.8	0.00E+00	175205	0.10502	0.00083	3.96047	0.07955	0.273505	0.005045	0.918	-10.2	-7.4	1715	14	1626	16	1559	**26**
6204-10-1 1970_04	334	52.6	0.00E+00	26371	0.07375	0.00041	1.72945	0.02784	0.170084	0.002571	0.939	-2.3	.	1035	11	1020	10	1013	**14**
6204-10-1 1970_06	143	33.9	0.00E+00	8212	0.09282	0.00051	3.22019	0.05751	0.251605	0.004276	0.952	-2.8	-0.5	1484	10	1462	14	1447	**22**
6204-10-1 1970_07A	150	23.1	0.00E+00	11885	0.07068	0.00039	1.60947	0.02586	0.165145	0.002489	0.938	4.2	0.1	948	11	974	10	985	**14**
6204-10-1 1970_07B	284	22.9	0.00E+00	4688	0.05579	0.00051	0.62839	0.0094	0.081695	0.00097	0.793	14.6	5.2	444	20	495	6	506	**6**
6204-10-1 1970_08	17	2.5	0.00E+00	492	0.07219	0.00165	1.48114	0.04088	0.148809	0.002293	0.558	-10.5	.	991	45	923	17	894	**13**
6204-10-1 1970_09	159	27.5	0.00E+00	4706	0.07529	0.00055	1.88228	0.03366	0.18131	0.00296	0.913	-0.2	.	1076	15	1075	12	1074	**16**
6204-10-1 1970_10	255	68.5	0.00E+00	13238	0.10034	0.00052	3.9364	0.07457	0.284516	0.005184	0.962	-1.1	.	1630	9	1621	15	1614	**26**

6204-10-1	89	14.8	0.00E	3514	0.0691	0.00	1.70467	0.02	0.17887	0.002	0.9	19.1	13.8	902	12	101	11	1061	**15**
1970_11			+00		2	045		894	7	8	22					0			
6204-10-1	92	20.1	0.00E	4760	0.0907	0.00	2.92531	0.05	0.23390	0.004	0.9	-6.6	-4	1440	11	138	14	1355	**21**
1970_12			+00			056		396	7	069	43					8			
6204-10-1	131	33.1	0.00E	1244	0.1007	0.00	3.71472	0.06	0.26754	0.004	0.9	-7.5	-5.5	1637	9	157	15	1528	**25**
1970_13			+00	6		05		972	5	84	64					5			
6204-10-1	6	1.7	0.00E	479	0.0980	0.00	3.91523	0.12	0.28953	0.008	0.9	3.7	.	1588	24	161	27	1639	**44**
1970_14			+00		7	131		967	4	775	15					7			
6204-10-1	122	20	0.00E	5856	0.0739	0.00	1.79842	0.03	0.17627	0.002	0.9	0.6	.	1041	15	104	11	1047	**15**
1970_15			+00		9	054		021	7	664	00					5			
6204-10-1	222	52.4	0.00E	1215	0.0985	0.00	3.42153	0.06	0.25193	0.004	0.9	-10.3	-8.6	1596	9	150	14	1448	**22**
1970_16			+00	3		046		142	1	369	66					9			
6204-10-1	165	26	0.00E	5426	0.0737	0.00	1.73181	0.02	0.17032	0.002	0.9	-2.2	.	1034	10	102	10	1014	**14**
1970_17			+00		4	039		757	2	558	44					0			
6204-10-1	72	20.8	0.00E	3874	0.1023	0.00	4.30825	0.08	0.30539	0.005	0.9	3.5	.	1667	9	169	16	1718	**29**
1970_18			+00		2	051		604	3	908	69					5			
6204-10-1	146	45.4	0.00E	1299	0.1014	0.00	4.56695	0.09	0.32656	0.006	0.9	11.9	6.8	1650	8	174	17	1822	**31**
1970_19			+00	8	3	045		111	4	354	75					3			
6204-10-1	86	13.8	0.00E	2064	0.0726	0.00	1.75746	0.03	0.17534	0.003	0.8	3.9	.	1005	18	103	13	1041	**17**
1970_20A			+00		9	067		55	5	149	89					0			
6204-10-1	43	5.9	0.00E	1310	0.0742	0.00	1.61206	0.03	0.15747	0.002	0.7	-10.8	-4.5	1048	26	975	14	943	**15**
1970_20B			+00		4	102		6	7	774	89								
6204-10-1	265	63.1	0.00E	1005	0.0984	0.00	3.4744	0.07	0.25592	0.005	0.9	-8.8	-7	1595	9	152	16	1469	**26**
1970_22			+00	5	6	047		055	3	051	72					1			
6204-10-1	201	31.3	0.00E	8574	0.0707	0.00	1.66579	0.02	0.17081	0.002	0.9	7.6	3.3	950	10	996	11	1017	**15**
1970_23			+00		3	038		827	7	752	49								
6204-10-1	239	59.9	0.00E	2083	0.0987	0.00	3.6835	0.07	0.27048	0.005	0.9	-4.1	-2	1601	9	156	15	1543	**26**
1970_24			+00	31	7	049		099	3	034	66					8			
6204-10-1	116	24.2	0.00E	5622	0.0952	0.00	2.98831	0.05	0.22746	0.003	0.9	-15.3	-13.2	1534	10	140	14	1321	**21**
1970_25			+00		8	055		486	4	963	49					5			
6204-10-1	30	4.1	0.00E	986	0.0699	0.00	1.44993	0.03	0.15025	0.002	0.7	-2.9	.	928	26	910	13	902	**14**
1970_26			+00		9	096		075	7	428	62								
6204-10-1	146	21.2	0.00E	4584	0.0716	0.00	1.5839	0.02	0.16037	0.002	0.9	-1.8	.	975	12	964	11	959	**14**
1970_27			+00		3	043		69	7	55	36								
6204-10-1	14	1.7	0.00E	433	0.0690	0.00	1.29964	0.03	0.13646	0.002	0.6	-9	.	901	45	846	17	825	**16**
1970_28			+00		7	155		917	2	753	69								
6204-10-1	399	45.2	0.00E	2678	0.0687	0.00	1.19102	0.01	0.12563	0.001	0.9	-15.3	-12.4	891	10	796	9	763	**11**
1970_29			+00	7	6	035		965	5	969	50								
6204-10-1	146	23.9	0.00E	1314	0.0711	0.00	1.75329	0.02	0.17882	0.002	0.9	11.3	6.9	961	11	102	11	1061	**16**
1970_30			+00	5	1	038		938	9	839	47					8			
6204-10-1	59	10.1	0.00E	2835	0.0751	0.00	1.92543	0.03	0.18580	0.003	0.9	2.6	.	1073	12	109	11	1099	**16**
1970_32A			+00		6	044		311	6	003	40					0			
6204-10-1	23	3.8	0.00E	714	0.0780	0.00	1.88676	0.05	0.17534	0.003	0.7	-10	-2.4	1148	34	107	18	1042	**19**
1970_32B			+00		4	143		128	7	525	40					6			

6204-10-1	88	13.3	0.00E	2790	0.0723	0.00	1.64497	0.02	0.16483	0.002	0.8	-1.4	.	997	15	988	11	984	**14**
1970_31			+00		8	056		843		551	95								
6204-10-1	238	60.9	0.00E	2359	0.0978	0.00	3.70251	0.06	0.27444	0.004	0.9	-1.4	.	1583	9	157	15	1563	**25**
1970_33			+00	3	5	048		922	1	95	65					2			
6204-10-1	24	3.7	0.00E	851	0.0816	0.00	1.89171	0.04	0.16814	0.002	0.7	-20.4	-15.6	1236	26	107	14	1002	**15**
1970_34			+00			115		082	5	754	59					8			
6204-10-1	236	34.9	0.00E	6423	0.0712	0.00	1.59422	0.02	0.16221	0.002	0.9	0.4	.	965	11	968	10	969	**14**
1970_35			+00		8	04		628	5	511	39								
6204-10-1	22	5.2	0.00E	837	0.0694	0.00	2.42773	0.05	0.25340	0.004	0.8	66.5	56.6	913	19	125	16	1456	**26**
1970_35B			+00		8	067		324	5	987	97					1			
6204-10-1	196	54.6	0.00E	2350	0.1013	0.00	4.16376	0.08	0.29801	0.005	0.9	2.3	.	1649	9	166	16	1681	**28**
1970_36			+00	2	3	052		08	1	575	64					7			
6204-10-1	91	16.3	0.00E	5928	0.0702	0.00	1.90852	0.03	0.19691	0.003	0.9	25.9	20.1	937	13	108	12	1159	**18**
1970_37			+00		9	046		549	4	429	36					4			
6204-10-1	160	43.1	0.00E	1249	0.1021	0.00	4.0612	0.07	0.28836	0.005	0.9	-2	.	1663	10	164	16	1633	**27**
1970_38			+00	6	4	053		896	6	402	63					7			
6204-10-1	88	12.5	2.20E	3770	0.0692	0.00	1.481	0.02	0.15521	0.002	0.9	3	.	905	13	923	10	930	**14**
1970_39			-01			046		531	1	448	23								
6204-10-1	55	6.8	0.00E	1455	0.0684	0.00	1.29294	0.02	0.13692	0.002	0.9	-6.8	-2.4	883	15	843	10	827	**12**
1970_40			+00		9	049		257	3	176	11								
6204-10-1	314	72.7	0.00E	1678	0.0950	0.00	3.28764	0.06	0.25081	0.004	0.9	-6.3	-4.4	1529	9	147	14	1443	**23**
1970_41			+00	6	7	045		035	3	45	66					8			
6204-10-1	132	23.2	0.00E	6548	0.0809	0.00	2.14723	0.03	0.19232	0.003	0.9	-7.8	-5.1	1221	11	116	12	1134	**17**
1970_42			+00		7	047		709	2	133	43					4			
6204-10-1	38	5.4	0.00E	2154	0.0704	0.00	1.50095	0.02	0.15458	0.002	0.8	-1.6	.	941	23	931	12	927	**14**
1970_43			+00		2	079		974	8	526	25								
6204-10-1	240	45.6	0.00E	4135	0.0849	0.00	2.43721	0.04	0.20806	0.003	0.9	-8	-5.9	1315	9	125	13	1218	**19**
1970_44			+00	0	6	041		297		53	62					4			
6204-10-1	202	37.9	0.00E	6195	0.0824	0.00	2.32799	0.03	0.20488	0.003	0.9	-4.7	-2.5	1255	9	122	12	1201	**18**
1970_44B			+00		1	039		978	3	366	62					1			
6204-10-1	146	33.7	0.00E	9841	0.0946	0.00	3.2535	0.05	0.24933	0.004	0.9	-6.3	-4.3	1521	9	147	14	1435	**23**
1970_45A			+00		4	045		969	7	416	65					0			
6204-10-1	125	18.8	0.00E	4044	0.0677	0.00	1.54678	0.02	0.16566	0.002	0.9	16.1	10.3	860	15	949	12	988	**16**
1970_45B			+00		2	048		893	9	863	24								
6204-10-1	111	15.9	0.00E	5721	0.0701	0.00	1.52899	0.02	0.15800	0.002	0.9	1.4	.	934	14	942	11	946	**14**
1970_47			+00		8	049		658	3	517	16								
6204-10-1	593	91.3	0.00E	1829	0.0790	0.00	1.8489	0.03	0.16963	0.002	0.9	-15	-13.1	1173	9	106	11	1010	**15**
1970_48			+00	5	5	035		145	5	786	66					3			
6204-10-1	22	2.3	0.00E	4626	0.0702	0.00	1.15753	0.02	0.11950	0.002	0.7	-23.5	-16.7	936	31	781	13	728	**12**
1970_49			+00		5	112		776	7	143	48								
6204-10-1	913	58.1	0.00E	1422	0.0570	0.00	0.57059	0.01	0.07255	0.001	0.8	-8.7	.	493	23	458	8	452	**8**
1970_50B			+00	0	4	062		273	2	414	74								
6204-10-1	179	17.2	0.00E	4295	0.0647	0.00	0.87963	0.01	0.09859	0.001	0.7	-21.7	-14.4	765	28	641	10	606	**9**
1970_51			+00		1	089		826	3	535	5								

6204-10-1	696	68.3	0.00E	1380	0.0686	0.00	1.0921	0.02	0.11538	0.002	0.9	-21.9	-17.6	888	17	750	11	704	**13**
1970_52			+00	0	4	057		261	9	187	16								
6204-10-1	104	27.8	0.00E	6509	0.1005	0.00	3.98867	0.07	0.28761	0.005	0.9	-0.4	.	1635	10	163	16	1630	**27**
1970_53			+00		8	057		885	1	445	58					2			
6204-10-1	211	49.7	0.00E	2868	0.0960	0.00	3.40501	0.06	0.25704	0.004	0.9	-5.4	-3.2	1549	10	150	15	1475	**25**
1970_54			+00	7	8	053		717		87	6					6			
6204-10-1	45	6.2	0.00E	1728	0.0694	0.00	1.45278	0.02	0.15165	0.002	0.8	-0.3	.	913	19	911	11	910	**14**
1970_55			+00		8	063		729	6	49	74								
6204-10-1	158	22.6	0.00E	4837	0.0706	0.00	1.54297	0.02	0.15832	0.002	0.9	-0.1	.	948	11	948	11	947	**14**
1970_56			+00		8	037		633	5	573	52								
6204-10-1	382	49.3	0.00E	1123	0.0681	0.00	1.34513	0.02	0.14320	0.002	0.9	-1.2	.	872	9	865	10	863	**13**
1970_57			+00	38	2	029		248	9	311	66								
6204-10-1	206	42.6	0.00E	1263	0.0906	0.00	2.91255	0.08	0.23300	0.006	0.9	-6.9	-2.6	1439	19	138	22	1350	**33**
1970_58			+00	1	6	092		494	1	374	38					5			
6204-10-1	96	16.3	0.00E	2993	0.0735	0.00	1.88844	0.03	0.18632	0.003	0.9	7.8	3.2	1028	12	107	12	1101	**17**
1970_59			+00		1	043		438	7	208	46					7			
6204-10-1	12	2.4	0.00E	1186	0.0711	0.00	2.12164	0.07	0.21625	0.005	0.7	34.4	20.7	962	42	115	24	1262	**31**
1970_60			+00		6	149		284	1	893	94					6			
6204-10-1	115	28.2	0.00E	9569	0.0960	0.00	3.53716	0.06	0.26716	0.005	0.9	-1.6	.	1548	10	153	15	1526	**26**
1970_61B			+00		2	051		916	9	026	62					6			
6204-10-1	435	99.6	0.00E	3555	0.1032	0.00	3.564	0.07	0.25043	0.004	0.9	-16	-14.4	1683	9	154	16	1441	**25**
1970_62			+00	3	2	051		007	4	768	68					2			
6204-10-1	72	16.1	0.00E	3894	0.0947	0.00	3.17278	0.06	0.24284	0.004	0.9	-8.9	-6	1523	14	145	15	1401	**23**
1970_63			+00		6	069		303	3	49	31					1			
6204-10-1	57	18.9	0.00E	5700	0.0985	0.00	3.53693	0.11	0.26032	0.008	0.9	-7.4	-3.9	1597	16	153	26	1491	**42**
1970_64			+00		4	089		62	1	226	62					6			
6204-10-1	74	21.5	0.00E	4872	0.0887	0.00	2.75225	0.07	0.22504	0.006	0.9	-7	-4.4	1398	11	134	21	1308	**33**
1970_65			+00			055		921	4	322	76					3			
6204-10-1	269	60	0.00E	1014	0.075	0.00	1.84435	0.04	0.17834	0.004	0.9	-1.1	.	1069	10	106	16	1058	**24**
1970_66			+00	2		037		618	9	378	80					1			
6204-10-1	251	78.2	1.20E	9590	0.0845	0.00	2.79378	0.07	0.23979	0.005	0.8	7	0.1	1304	24	135	21	1386	**31**
1970_74			-01	1		109		789	7	934	88					4			
6204-10-1	314	113	8.70E	4418	0.0994	0.00	3.78122	0.11	0.27567	0.008	0.9	-3.1	-0.9	1614	11	158	24	1570	**41**
1970_79			-03	2	8	056		42	6	179	82					9			
6204-10-1	404	97.9	0.00E	1197	0.0814	0.00	2.19253	0.06	0.19523	0.005	0.9	-7.3	-4.9	1232	10	117	19	1150	**29**
1970_80			+00	7	5	043		108	7	34	82					9			
6204-10-1	315	63.8	0.00E	1221	0.0709	0.00	1.5944	0.03	0.16295	0.003	0.9	1.9	.	956	12	968	15	973	**22**
1970_81			+00	3	6	04		918	8	895	73								
6204-10-1	316	98.3	2.90E	2326	0.0919	0.00	3.1124	0.08	0.24546	0.006	0.9	-3.9	-1.7	1467	10	143	22	1415	**35**
1970_82			-02	8	6	048		811	4	83	83					6			
6204-10-1	197	69.4	0.00E	2885	0.1004	0.00	3.81987	0.11	0.27575	0.008	0.9	-4.3	-2.2	1633	10	159	24	1570	**41**
1970_83			+00	5	7	055		376	7	07	83					7			
6204-10-1	142	50.4	0.00E	8125	0.1010	0.00	3.9	0.11	0.27678	0.008	0.9	-4.7	-2.6	1644	10	160	24	1575	**41**
1970_84			+00		9	056		481	1	095	83					5			

6204-10-1 1970_85	73	13.7	0.00E+00	2118	0.06964	0.0005	1.46889	0.03627	0.152977	0.003617	0.958	.	.	918	15	918	15	918	**20**
6204-10-1 1970_86	178	16.9	0.00E+00	3762	0.05746	0.00045	0.63102	0.01551	0.079649	0.001854	0.947	-3.1	.	509	17	497	10	494	**11**
6204-10-1 1970_87	110	35.8	0.00E+00	5033	0.10112	0.00079	3.70911	0.1489	0.26602	0.010476	0.981	-8.5	-5.6	1645	14	1573	32	1521	**53**
6204-10-1 1970_88	215	39.7	0.00E+00	7464	0.07068	0.00038	1.48577	0.03929	0.152451	0.003945	0.979	-3.8	-0.6	948	10	925	16	915	**22**
6204-10-1 1970_89	650	205.4	0.00E+00	23169	0.09033	0.00043	3.10888	0.08662	0.24962	0.006854	0.985	0.3	.	1432	8	1435	21	1437	**35**
6204-10-1 1970_90	288	58.3	0.00E+00	13823	0.07099	0.00039	1.60586	0.03962	0.164073	0.003947	0.975	2.5	.	957	10	972	15	979	**22**
6204-10-1 1970_91	147	35.6	0.00E+00	28415	0.08903	0.00131	2.36723	0.08113	0.19284	0.005968	0.903	-20.8	-15.5	1405	27	1233	24	1137	**32**
6204-10-1 1970_92	342	67	0.00E+00	25216	0.07073	0.00037	1.6	0.03825	0.159633	0.003833	0.977	0.6	.	950	10	953	15	955	**21**
6204-10-1 1970_93	49	16.6	0.00E+00	8645	0.09936	0.00074	3.68791	0.11037	0.269198	0.007803	0.969	-5.3	-2.3	1612	13	1569	24	1537	**40**
6204-10-1 1970_94	45	18.9	0.00E+00	4718	0.10231	0.00069	4.62577	0.15279	0.327903	0.010601	0.979	11.1	2.7	1667	12	1754	28	1828	**51**
6204-10-1 1970_95	230	71.8	0.00E+00	63268	0.092	0.00046	3.15471	0.08922	0.248702	0.00692	0.984	-2.7	-0.6	1467	9	1446	22	1432	**36**
6204-10-1 1970_96	114	22.1	0.00E+00	8368	0.07095	0.00047	1.54306	0.03849	0.157725	0.003791	0.964	-1.3	.	956	13	948	15	944	**21**

Summary for ICP-MS U-Pb zircon results for 6204/10-1, 1993.82 M

	ppm				*Ratios*							*Discordance*		*Ages*					
Name	**U**	**^{206}Pb**	**$^{206}Pb_c$ (%)**	**206/204**	**$^{207}Pb/^{206}Pb^*$**	**1σ**	**207Pb/235U***	**1σ**	**206Pb/238U***	**1σ**	**Rho**	**Central (%)**	**Minimum rim (%)**	**207/206**	**1 σ**	**207/235**	**1 σ**	**206/238**	**1 σ**
6201-10-1 1993_01	172	37.1	0.00E+00	4297	0.07658	0.00073	1.80052	0.02591	0.170525	0.001829	0.745	-9.3	-5.2	1110	19	1046	9	1015	10
6201-10-1 1993_02	165	28.5	6.90E-02	5792	0.06815	0.00067	1.27246	0.0283	0.135414	0.002704	0.898	-6.6	-0.7	873	20	833	13	819	15
6201-10-1 1993_03	69	16.3	1.60E-01	5561	0.07491	0.00069	1.85962	0.03834	0.180047	0.003322	0.895	0.1	.	1066	18	1067	14	1067	18
6201-10-1 1993_04	647	182.2	0.00E+00	19001	0.09743	0.00089	3.02896	0.04339	0.225479	0.002491	0.771	-18.6	-15.8	1575	16	1415	11	1311	13
6201-10-1 1993_05	464	150.1	0.00E+00	29595	0.09919	0.00088	3.49584	0.05133	0.25562	0.002984	0.795	-9.8	-6.9	1609	16	1526	12	1467	15
6201-10-1 1993_06	190	63.1	7.70E-02	10290	0.0959	0.00078	3.40851	0.05342	0.257786	0.003446	0.853	-4.9	-1.7	1546	15	1506	12	1479	18
6201-10-1 1993_07	123	45.4	0.00E+00	4996	0.1013	0.00076	3.91568	0.09098	0.28035	0.006163	0.946	-3.8	-0.8	1648	14	1617	19	1593	31

6201-10-1 1993_08B	223	60.2	0.00E+00	7571	0.09452	0.00102	2.67417	0.0907	0.205198	0.006595	0.948	-22.7	-19.1	1518	19	1321	25	1203	35
6204-10-1 1993_10	67	17.5	0.00E+00	4262	0.09166	0.00103	2.57859	0.0771	0.204025	0.005657	0.927	-19.8	-15.7	1460	21	1295	22	1197	30
6204-10-1 1993_09	78	24.3	0.00E+00	4230	0.09634	0.00085	3.3	0.07116	0.247491	0.004893	0.913	-9.2	-5.9	1554	16	1478	17	1426	25
6204-10-1 1993_12	115	36.7	0.00E+00	4029	0.09707	0.00115	3.53651	0.06231	0.264246	0.003445	0.74	-4.1	.	1568	21	1535	14	1512	18
6204-10-1 1993_13	493	86.4	0.00E+00	11988	0.07127	0.00066	1.4456	0.02717	0.147113	0.002409	0.871	-8.9	-4	965	18	908	11	885	14
6204-10-1 1993_14	10	3.2	0.00E+00	685	0.09855	0.00125	3.6041	0.10649	0.265237	0.007073	0.902	-5.6	-0.7	1597	23	1550	23	1517	36
6204-10-1 1993_15	205	43.9	0.00E+00	12469	0.07702	0.00054	1.84206	0.03948	0.173466	0.003514	0.945	-8.7	-5.2	1122	14	1061	14	1031	19
6204-10-1 1993_16	48	9.3	0.00E+00	2457	0.07153	0.00069	1.57353	0.03437	0.159549	0.003128	0.898	-2	.	973	19	960	14	954	17
6204-10-1 1993_17	464	68.9	0.00E+00	26826	0.0659	0.00041	1.11216	0.02211	0.122394	0.002311	0.949	-7.8	-3.6	803	13	759	11	744	13
6204-10-1 1993_18	30	10.6	0.00E+00	27558	0.10126	0.00091	3.9	0.0971	0.280277	0.006479	0.932	-3.7	-0.2	1647	17	1616	20	1593	33
6204-10-1 1993_19B	273	98.2	0.00E+00	31298	0.10109	0.00072	4.02036	0.09699	0.28845	0.006645	0.955	-0.7	.	1644	13	1638	20	1634	33
6204-10-1 1993_20	53	8.8	0.00E+00	1245	0.069	0.00091	1.31785	0.02929	0.138514	0.002476	0.804	-7.4	-0.2	899	27	854	13	836	14
6204-10-1 1993_21	55	17.3	0.00E+00	2192	0.09443	0.00094	3.32045	0.06362	0.255039	0.004175	0.854	-3.8	.	1517	18	1486	15	1464	21
6204-10-1 1993_22	45	13.8	0.00E+00	2838	0.09314	0.00086	3.19182	0.07161	0.248543	0.005079	0.911	-4.5	-0.6	1491	17	1455	17	1431	26
6204-10-1 1993_22B	398	133.6	0.00E+00	12874	0.0975	0.00105	3.60381	0.11162	0.268088	0.007782	0.937	-3.3	.	1577	20	1550	25	1531	40
6204-10-1 1993_11	361	126.8	0.00E+00	39573	0.10028	0.00067	3.84478	0.08117	0.27807	0.005564	0.948	-3.3	-0.6	1629	12	1602	17	1582	28
6204-10-1 1993_23	153	52.3	0.00E+00	19009	0.09522	0.0011	3.93951	0.05945	0.300068	0.002899	0.640	11.8	8	1532	22	1622	12	1692	14
6204-10-1 1993_24	348	72.6	0.00E+00	9912	0.07056	0.00101	1.789	0.03467	0.183896	0.002412	0.677	16.5	9.5	945	28	1041	13	1088	13
6204-10-1 1993_25	139	25.8	0.00E+00	10530	0.07287	0.00068	1.6612	0.01975	0.165335	0.001219	0.620	-2.6	.	1010	17	994	8	986	7
6204-10-1 1993_26	49	8.3	0.00E+00	1704	0.07028	0.0007	1.46292	0.01823	0.150963	0.001121	0.596	-3.5	.	937	21	915	8	906	6
6204-10-1 1993_27	59	15.4	0.00E+00	3288	0.09093	0.00093	2.88965	0.03714	0.230495	0.001799	0.607	-8.3	-5.1	1445	20	1379	10	1337	9
6204-10-1 1993_28	24	2.3	0.00E+00	501	0.06658	0.00144	0.77273	0.01814	0.084174	0.000755	0.382	-38.3	-28.6	825	43	581	10	521	4
6204-10-1 1993_29	165	52.7	0.00E+00	8830	0.10268	0.00104	4.01117	0.05587	0.283331	0.0027	0.684	-4.4	-1.3	1673	18	1636	11	1608	14
6204-10-1 1993_30	97	17.6	0.00E+00	3349	0.07136	0.00078	1.5955	0.0199	0.162149	0.000992	0.491	0.1	.	968	22	968	8	969	6
6204-10-1 1993_31	255	84.2	0.00E+00	20225	0.10022	0.0009	4.00191	0.04869	0.28962	0.002378	0.675	0.8	.	1628	17	1635	10	1640	12

6204-10-1 1993_32	80	18	0.00E+00	1977	0.09023	0.00118	2.5	0.0407	0.203248	0.001905	0.582	-18.2	-14.5	1430	25	1280	12	1193	10
6204-10-1 1993_33	51	15.6	0.00E+00	2222	0.07789	0.00254	2.88417	0.10215	0.268542	0.003676	0.386	38.3	29.2	1144	63	1378	27	1533	19
6204-10-1 1993_33B	156	24.1	2.50E-01	3591	0.07019	0.00078	1.3596	0.02113	0.140491	0.001526	0.699	-9.9	-4.5	934	22	872	9	847	9
6204-10-1 1993_34	157	47.5	0.00E+00	5606	0.09592	0.00221	3.5773	0.08662	0.270487	0.002041	0.312	-0.2	.	1546	42	1545	19	1543	10
6204-10-1 1993_35	67	11.4	0.00E+00	1797	0.06936	0.00073	1.46476	0.01916	0.153161	0.001195	0.597	1.1	.	910	20	916	8	919	7
6204-10-1 1993_36	28	8.4	0.00E+00	3464	0.09572	0.00109	3.51297	0.05057	0.266189	0.002344	0.612	-1.5	.	1542	20	1530	11	1521	12
6204-10-1 1993_37	108	20.6	0.00E+00	5690	0.07343	0.00073	1.72616	0.02035	0.170498	0.001081	0.538	-1.2	.	1026	20	1018	8	1015	6
6204-10-1 1993_38	32	10.3	0.00E+00	4561	0.10103	0.00113	4.0311	0.0563	0.289395	0.002421	0.599	-0.3	.	1643	20	1640	11	1639	12
6204-10-1 1993_39	29	6.3	0.00E+00	2031	0.07599	0.00135	2.1	0.04869	0.201263	0.002973	0.64	8.7	1.8	1095	35	1152	16	1182	16
6204-10-1 1993_40	9	1.5	0.00E+00	815	0.07247	0.00256	1.59865	0.06855	0.159993	0.003882	0.566	-4.6	.	999	69	970	27	957	22
6204-10-1 1993_41	52	4.8	0.00E+00	26699	0.06174	0.00082	0.71485	0.01201	0.08398	0.00086	0.610	-22.7	-14.7	665	28	548	7	520	5
6204-10-1 1993_42	22	6.5	0.00E+00	1363	0.09719	0.00126	3.5296	0.06757	0.2634	0.003717	0.737	-4.5	-0.2	1571	24	1534	15	1507	19
6204-10-1 1993_43	229	84.9	0.00E+00	4586	0.11722	0.0029	5.30852	0.15402	0.328461	0.004984	0.523	-5	.	1914	43	1870	25	1831	24
6204-10-1 1993_44	354	101.1	0.00E+00	23845	0.10081	0.0012	3.58902	0.06029	0.258219	0.003068	0.707	-10.8	-7.3	1639	20	1547	13	1481	16
6204-10-1 1993_45	260	68.3	0.00E+00	19537	0.10174	0.00104	3.30252	0.04325	0.235432	0.001926	0.625	-19.6	-17.1	1656	18	1482	10	1363	10
6204-10-1 1993_46	11	2.2	0.00E+00	432	0.07157	0.00121	1.71879	0.03994	0.17417	0.002765	0.683	6.8	.	974	34	1016	15	1035	15
6204-10-1 1993_47	450	44.4	0.00E+00	5179	0.07486	0.00069	0.92699	0.01183	0.089806	0.000793	0.692	-50	-47.8	1065	18	666	6	554	5
6204-10-1 1993_48	53	7.8	0.00E+00	1593	0.06964	0.00109	1.30441	0.03536	0.135843	0.003009	0.817	-11.2	-3	918	31	848	16	821	17
6204-10-1 1993_49B	20	1.4	0.00E+00	828	0.05185	0.00224	0.46998	0.0216	0.065741	0.001021	0.338	48.8	18.9	279	96	391	15	410	6
6204-10-1 1993_50	28	5.4	0.00E+00	1795	0.07608	0.00094	1.81744	0.02893	0.173264	0.001734	0.629	-6.6	-1.4	1097	24	1052	10	1030	10
6204-10-1 1993_51	18	5.4	0.00E+00	1133	0.09863	0.00132	3.75821	0.07044	0.276371	0.003615	0.698	-1.8	.	1598	24	1584	15	1573	18
6204-10-1 1993_52	90	15.7	0.00E+00	2400	0.08038	0.00094	1.73347	0.02424	0.156408	0.001198	0.548	-24	-20.5	1206	22	1021	9	937	7
6204-10-1 1993_54	23	2.9	0.00E+00	818	0.07206	0.00088	1.56833	0.0267	0.157838	0.001867	0.695	-4.7	.	988	24	958	11	945	10
6204-10-1 1993_55	23	2.5	0.00E+00	1177	0.06631	0.00108	1.11984	0.02286	0.122484	0.001501	0.600	-9.3	.	816	33	763	11	745	9
6204-10-1 1993_55B	106	21.1	0.00E+00	11164	0.09372	0.00063	3.16323	0.04522	0.244787	0.003085	0.882	-6.7	-4.1	1503	12	1448	11	1412	16

6204-10-1 1993_56B	39	6	0.00E+00	3512	0.06984	0.00121	1.62847	0.03564	0.169107	0.002255	0.609	9.8	2.5	924	35	981	14	1007	12
6204-10-1 1993_57	140	25.8	0.00E+00	7280	0.0913	0.00058	2.84888	0.03951	0.226317	0.002795	0.891	-10.5	-8	1453	12	1369	10	1315	15
6204-10-1 1993_58	4	0.5	0.00E+00	120	0.06782	0.00291	1.4373	0.07532	0.15371	0.004634	0.575	7.3	.	863	84	905	31	922	26
6204-10-1 1993_59	20	2.1	0.00E+00	657	0.07017	0.00091	1.34348	0.02563	0.138856	0.001942	0.733	-10.9	-4.5	933	25	865	11	838	11
6204-10-1 1993_60	27	6.1	0.00E+00	1296	0.09841	0.00083	3.7	0.06132	0.276017	0.003871	0.857	-1.6	.	1594	16	1581	13	1571	20
6204-10-1 1993_61	214	27.1	0.00E+00	9155	0.0706	0.0004	1.5498	0.01719	0.159202	0.001514	0.857	0.7	.	946	11	950	7	952	8
6204-10-1 1993_62	61	7.5	0.00E+00	16594	0.06993	0.00058	1.49381	0.01957	0.154933	0.001579	0.778	0.3	.	926	16	928	8	929	9
6204-10-1 1993_63	9	1	0.00E+00	637	0.06893	0.00102	1.37222	0.02914	0.144375	0.002204	0.719	-3.3	.	897	30	877	12	869	12
6204-10-1 1993_64	111	13.1	0.00E+00	3004	0.0709	0.00045	1.4503	0.01688	0.148354	0.001444	0.836	-7.1	-3.7	955	13	910	7	892	8
6204-10-1 1993_65	33	6.7	0.00E+00	2730	0.09849	0.001	3.48663	0.06609	0.256759	0.004111	0.845	-8.6	-4.9	1596	19	1524	15	1473	21
6204-10-1 1993_66	25	3	0.00E+00	1030	0.07222	0.00089	1.52154	0.02489	0.152804	0.00165	0.66	-8.2	-2.5	992	24	939	10	917	9
6204-10-1 1993_67	10	1.2	0.00E+00	1415	0.07076	0.00154	1.7	0.05343	0.170447	0.004027	0.735	7.3	.	950	43	994	20	1015	22
6204-10-1 1993_68	147	17.8	0.00E+00	5301	0.07003	0.00044	1.48316	0.01767	0.153613	0.001553	0.848	-0.9	.	929	12	924	7	921	9
6204-10-1 1993_69	18	1.9	0.00E+00	1116	0.07651	0.00157	1.68231	0.04596	0.159482	0.00287	0.659	-15	-6.8	1108	40	1002	17	954	16
6204-10-1 1993_70	21	1.9	0.00E+00	523	0.06399	0.00088	0.9916	0.01746	0.112383	0.001234	0.624	-7.8	.	741	28	700	9	687	7
6204-10-1 1993_71	179	37.6	0.00E+00	11028	0.09753	0.00063	3.46381	0.04594	0.25758	0.002979	0.872	-7.1	-4.7	1577	12	1519	10	1477	15
6204-10-1 1993_72	51	11.6	0.00E+00	3134	0.10079	0.00071	3.88824	0.05333	0.279792	0.003296	0.859	-3.3	-0.7	1639	13	1611	11	1590	17
6204-10-1 1993_73	68	8.2	0.00E+00	3129	0.07112	0.00054	1.50276	0.01876	0.153254	0.001522	0.796	-4.6	-0.7	961	15	932	8	919	9
6204-10-1 1993_74	95	21.5	0.00E+00	8188	0.10009	0.00064	3.81529	0.05059	0.276469	0.003213	0.876	-3.6	-1.2	1626	12	1596	11	1574	16
6204-10-1 1993_75	16	1.9	0.00E+00	448	0.07205	0.00095	1.54803	0.02818	0.155832	0.001954	0.689	-5.8	.	987	26	950	11	934	11
6204-10-1 1993_76	116	24	0.00E+00	6526	0.09824	0.0006	3.45859	0.04348	0.255327	0.002808	0.875	-8.8	-6.6	1591	11	1518	10	1466	14
6204-10-1 1993_77	299	43.1	0.00E+00	20140	0.08687	0.00048	2.17633	0.02542	0.181699	0.001866	0.879	-22.5	-20.5	1358	11	1174	8	1076	10
6204-10-1 1993_78	6	1.3	0.00E+00	324	0.10004	0.00166	3.94361	0.1239	0.28591	0.00763	0.849	-0.3	.	1625	31	1623	25	1621	38
6204-10-1 1993_79	11	1.4	0.00E+00	376	0.07907	0.00122	1.96183	0.04247	0.179957	0.002729	0.700	-9.9	-3.8	1174	30	1103	15	1067	15
6204-10-1 1993_80	104	17.9	0.00E+00	7375	0.0799	0.00061	2.36988	0.03741	0.21511	0.00297	0.875	5.7	1.6	1195	15	1234	11	1256	16

6402-10-1 1993_81B	20	2.4	0.00E+00	678	0.07106	0.00087	1.54016	0.02837	0.157193	0.002164	0.747	-2	.	959	24	947	11	941	12
6402-10-1 1993_82	35	8.9	0.00E+00	2821	0.09909	0.00076	4.27555	0.06646	0.312927	0.004222	0.868	10.5	6.8	1607	14	1689	13	1755	21
6402-10-1 1993_83	32	7	0.00E+00	1119	0.09426	0.00135	3.09161	0.05786	0.237877	0.002866	0.644	-10.1	-5.7	1513	26	1431	14	1376	15
6402-10-1 1993_84	31	3.9	0.00E+00	1512	0.07043	0.0008	1.56568	0.02669	0.16124	0.00205	0.746	2.6	.	941	23	957	11	964	11
6402-10-1 1993_85	158	22.4	0.00E+00	14336	0.0718	0.00049	1.79699	0.02437	0.181511	0.002127	0.864	10.5	6.3	980	14	1044	9	1075	12
6402-10-1 1993_86	89	18.2	0.00E+00	5191	0.1005	0.00073	3.51888	0.04846	0.253952	0.002978	0.851	-11.9	-9.5	1633	13	1531	11	1459	15
6402-10-1 1993_87	44	5.8	0.00E+00	2882	0.07105	0.00069	1.63185	0.02589	0.16658	0.002098	0.794	3.9	.	959	19	983	10	993	12
6402-10-1 1993_88	23	5.1	0.00E+00	1168	0.09853	0.00105	3.47553	0.07604	0.255839	0.004893	0.874	-9	-5	1596	19	1522	17	1469	25
6402-10-1 1993_89	9	1.6	0.00E+00	1351	0.09359	0.00122	2.9995	0.06604	0.232448	0.004128	0.807	-11.3	-6.7	1500	23	1407	17	1347	22
6402-10-1 1993_90	38	5.3	0.00E+00	6668	0.07319	0.00077	1.89677	0.03164	0.187964	0.002441	0.779	9.7	4.3	1019	20	1080	11	1110	13
6402-10-1 1993_91	209	33	0.00E+00	32425	0.07008	0.00056	1.68316	0.0202	0.174183	0.001553	0.743	12.1	7.8	931	15	1002	8	1035	9
6402-10-1 1993_92	96	24.8	0.00E+00	5551	0.10085	0.00066	4.42246	0.06744	0.318035	0.004384	0.904	9.8	6.3	1640	11	1717	13	1780	21
6402-10-1 1993_93	197	26.2	0.00E+00	8312	0.07448	0.00045	1.74921	0.0214	0.170324	0.001814	0.871	-4.2	-1.1	1055	11	1027	8	1014	10
6402-10-1 1993_94	176	34.5	0.00E+00	20427	0.0866	0.00054	2.95344	0.04448	0.247341	0.003385	0.909	6	2.5	1352	11	1396	11	1425	17
6402-10-1 1993_95	38	8.7	0.00E+00	6062	0.09878	0.0009	3.48613	0.05591	0.255964	0.003378	0.823	-9.2	-6.1	1601	16	1524	13	1469	17
6402-10-1 1993_96	109	18.3	0.00E+00	2986	0.07454	0.00057	1.9668	0.02589	0.191359	0.002051	0.814	7.5	3.5	1056	15	1104	9	1129	11
6402-10-1 1993_97	134	16.3	0.00E+00	8002	0.07033	0.00051	1.47002	0.01824	0.151599	0.001532	0.815	-3.2	.	938	14	918	7	910	9
6402-10-1 1993_98	107	24.4	0.00E+00	6250	0.10189	0.00066	3.86406	0.05344	0.275043	0.003356	0.882	-6.3	-3.9	1659	11	1606	11	1566	17
6402-10-1 1993_99	225	51.1	0.00E+00	9521	0.10028	0.00061	3.78619	0.05158	0.273843	0.00334	0.895	-4.8	-2.4	1629	11	1590	11	1560	17
6402-10-1 1993_100	148	19.4	0.00E+00	42608	0.07205	0.00047	1.62998	0.0211	0.164074	0.00184	0.867	-0.9	.	987	12	982	8	979	10
6402-10-1 1993_101	454	36.7	0.00E+00	2328	0.08953	0.00078	1.26125	0.01933	0.102176	0.001292	0.825	-58.4	-56.9	1415	16	828	9	627	8
6402-10-1 1993_102	116	17.4	0.00E+00	6520	0.09434	0.00084	2.85445	0.0513	0.219442	0.003424	0.868	-17.2	-14.1	1515	16	1370	14	1279	18
6204-10-1 1993_103	15	3.3	0.00E+00	723	0.09926	0.0011	3.73695	0.0736	0.273055	0.004437	0.825	-3.8	.	1610	19	1579	16	1556	22
6204-10-1 1993_104	1	0.3	0.00E+00	102	0.07974	0.00427	3.08238	0.35753	0.280365	0.028849	0.887	38.2	1.8	1190	100	1428	89	1593	145
6204-10-1 1993_105	170	21.7	0.00E+00	8495	0.07663	0.00066	1.80596	0.03062	0.170933	0.002491	0.859	-9.2	-5.1	1111	17	1048	11	1017	14

6204-10-1993_106	217	16.1	0.00E+00	6287	0.06098	0.00046	0.77583	0.01032	0.092275	0.001011	0.824	-11.4	-6	639	16	583	6	569	6
6204-10-1993_107	16	2	0.00E+00	552	0.074	0.00145	1.71005	0.04255	0.167606	0.00257	0.616	-4.4	.	1041	39	1012	16	999	14
6204-10-1993_108	222	44	0.00E+00	10591	0.09676	0.00072	3.41408	0.05443	0.25591	0.003602	0.883	-6.7	-3.8	1563	14	1508	13	1469	18
6204-10-1993_109	111	12	0.00E+00	3453	0.06716	0.00051	1.25722	0.01777	0.135774	0.001622	0.846	-2.8	.	843	15	827	8	821	9
6204-10-1993_110	88	10.2	0.00E+00	2306	0.06979	0.00057	1.40534	0.01896	0.146056	0.00156	0.792	-5	-0.6	922	17	891	8	879	9
6204-10-1993_111	135	15.6	0.00E+00	32001	0.06739	0.00048	1.34972	0.019	0.145261	0.001763	0.862	3.1	.	850	15	867	8	874	10
6204-10-1993_112	35	5.5	0.00E+00	2704	0.07047	0.00078	1.84961	0.03134	0.19036	0.002442	0.757	21	14.5	942	22	1063	11	1123	13
6204-10-1993_113	243	31	0.00E+00	16168	0.07142	0.00044	1.57915	0.02039	0.160356	0.001819	0.878	-1.2	.	970	12	962	8	959	10

Summary for ICP-MS U-Pb zircon results for 6507/2-3, 2887.53m

	ppm			*Ratios*								*Discordance*		*Ages*					
Name	**U**	**^{206}Pb**	**^{206}Pb$_c$ (%)**	**206/204**	**^{207}Pb/^{206}Pb***	**1σ**	**207Pb/235U***	**1σ**	**206Pb/238U***	**1σ**	**Rho**	**Central (%)**	**Minimum rim (%)**	**207/206**	**1s**	**207/235**	**1s**	**206/238**	**1s**
6507-2-3 2887_01	47	12.7	0.00E+00	9339	0.11806	0.00092	5.29234	0.12356	0.32513	0.007156	0.943	-6.7	-4	1927	14	1868	20	1815	35
6507-2-3 2887_02	77	0.8	0.00E+00	287	0.05008	0.00138	0.09902	0.0031	0.014342	0.000212	0.472	-54.1	.	198	64	96	3	92	1
6507-2-3 2887_03	206	50.7	0.00E+00	12149	0.11398	0.00066	4.7405	0.10262	0.301633	0.006295	0.964	-10	-8.1	1864	10	1774	18	1699	31
6507-2-3 2887_05	79	3.4	0.00E+00	1489	0.05405	0.00058	0.41501	0.00749	0.055692	0.00081	0.806	-6.5	.	373	22	352	5	349	5
6507-2-3 2887_04	101	26.9	0.00E+00	3314	0.11622	0.00165	4.853	0.1463	0.302843	0.008053	0.882	-11.6	-7	1899	25	1794	25	1705	40
6507-2-3 2887_06	486	20.8	0.00E+00	7750	0.05388	0.00032	0.4135	0.00648	0.055661	0.000807	0.926	-4.7	.	366	13	351	5	349	5
6507-2-3 2887_07	86	1	0.00E+00	431	0.04943	0.00105	0.10172	0.00262	0.014925	0.000218	0.566	-43.6	.	168	47	98	2	95	1
6507-2-3 2887_08	200	46.8	0.00E+00	21063	0.10472	0.00063	4.14689	0.08858	0.287209	0.005889	0.96	-5.4	-3.1	1709	10	1664	17	1628	29
6507-2-3 2887_09	686	176.4	0.00E+00	37939	0.11557	0.00071	5.0	0.1132	0.313972	0.006838	0.963	-7.8	-5.6	1889	11	1820	19	1760	34
6507-2-3 2887_11	169	37.4	0.00E+00	80630	0.10629	0.00062	4.04349	0.07792	0.275898	0.005067	0.953	-10.8	-8.7	1737	10	1643	16	1571	26
6507-2-3 2887_12	173	37.5	0.00E+00	98289	0.10535	0.00075	3.86399	0.08449	0.26602	0.005504	0.946	-13	-10.6	1720	12	1606	18	1521	28
6507-2-3 2887_13	66	14.9	0.00E+00	6763	0.10759	0.00079	4.18121	0.09256	0.281845	0.005882	0.943	-10.2	-7.5	1759	13	1670	18	1601	30
6507-2-3 2887_14	206	2.5	0.00E+00	649	0.05262	0.00174	0.11556	0.00419	0.015927	0.000237	0.41	-67.9	-22.1	312	74	111	4	102	2
6507-2-3 2887_15	50	0.6	0.00E+00	234	0.05538	0.00202	0.12896	0.0051	0.016888	0.000258	0.387	-75.4	-53.6	428	79	123	5	108	2
6507-2-3 2887_16	1008	54.4	0.00E+00	15353	0.05673	0.00028	0.55523	0.00857	0.070988	0.00104	0.949	-8.4	-3.3	481	10	448	6	442	6
6507-2-3 2887_17	51	0.6	0.00E+00	206	0.05925	0.00283	0.1189	0.00597	0.014555	0.000225	0.308	-84.4	-71.3	576	99	114	5	93	1
6507-2-3 2887_18	95	1	0.00E+00	201	0.04807	0.00193	0.1	0.00412	0.014643	0.000207	0.332	-8.9	.	103	86	94	4	94	1
6507-2-3 2887_19	249	54.1	0.00E+00	19504	0.10623	0.00058	4.03171	0.08114	0.275252	0.005333	0.963	-10.9	-9	1736	10	1641	16	1567	27
6507-2-3 2887_20	63	1	0.00E+00	270	0.06311	0.00273	0.17896	0.00837	0.020566	0.000363	0.378	-82.4	-73.8	712	88	167	7	131	2
6507-2-3 2887_21	286	81.1	0.00E+00	15988	0.11496	0.00069	5.52497	0.12889	0.348556	0.007861	0.967	3	.	1879	10	1904	20	1928	38

6507-2-3 2887_22	372	41.6	0.00E+00	11519	0.07002	0.00036	1.40779	0.026	0.145824	0.002586	0.96	-5.9	-2.8	929	10	892	11	878	15
6507-2-3 2887_24	48	0.6	3.10E+00	250	0.05018	0.00386	0.11186	0.00882	0.016169	0.000275	0.216	-49.5	.	203	159	108	8	103	2
6507-2-3 2887_25	286	11.6	0.00E+00	5049	0.05406	0.00042	0.4037	0.0068	0.054162	0.000807	0.885	-9.2	.	373	17	344	5	340	5
6507-2-3 2887_26	328	79.9	0.00E+00	29911	0.11314	0.00069	4.78288	0.10455	0.306593	0.006439	0.961	-7.8	-5.7	1850	11	1782	18	1724	32
6507-2-3 2887_27	617	151.3	0.00E+00	107706	0.11457	0.00066	4.86774	0.10599	0.308142	0.006467	0.964	-8.6	-6.6	1873	10	1797	18	1732	32
6507-2-3 2887_28	80	0.8	0.00E+00	395	0.0481	0.00119	0.09811	0.00286	0.014792	0.000228	0.53	-9.4	.	104	56	95	3	95	1
6507-2-3 2887_29	129	6	0.00E+00	1297	0.05551	0.00054	0.47874	0.00873	0.062546	0.000968	0.848	-10	.	433	21	397	6	391	6
6507-2-3 2887_30	43	0.5	0.00E+00	176	0.04801	0.00235	0.09966	0.00517	0.015054	0.000263	0.337	-3.6	.	100	107	96	5	96	2
6507-2-3 2887_31	466	119.2	0.00E+00	38395	0.11563	0.00069	5.1216	0.11463	0.321234	0.006932	0.964	-5.7	-3.6	1890	10	1840	19	1796	34
6507-2-3 2887_32	286	14.9	0.00E+00	4446	0.05548	0.00043	0.53394	0.00935	0.069798	0.001097	0.897	0.8	.	432	16	434	6	435	7
6507-2-3 2887_33	99	12.5	0.00E+00	4652	0.07201	0.00042	1.63919	0.02951	0.165087	0.002815	0.947	-0.1	.	986	11	985	11	985	16
6507-2-3 2887_34	344	72.3	0.00E+00	22489	0.11211	0.00066	4.14938	0.08736	0.268441	0.005423	0.959	-18.4	-16.6	1834	10	1664	17	1533	28
6507-2-3 2887_35	114	25.7	0.00E+00	18855	0.10648	0.00063	4.23089	0.08998	0.28818	0.005884	0.96	-7	-4.8	1740	11	1680	17	1632	29
6507-2-3 2887_36	10	1.7	2.70E+00	299	0.08307	0.00226	2.4179	0.13838	0.2111	0.010632	0.88	-3.1	.	1271	51	1248	41	1235	57
6507-2-3 2887_37	11	0.2	0.00E+00	216	0.14108	0.00628	0.50415	0.02951	0.025917	0.000984	0.649	-93.8	-93	2241	75	415	20	165	6
6507-2-3 2887_38	170	41.2	0.00E+00	44530	0.11768	0.00073	4.98358	0.11109	0.307144	0.006576	0.960	-11.5	-9.5	1921	11	1817	19	1727	32
6507-2-3 2887_39	258	6.6	0.00E+00	3007	0.05078	0.00045	0.2425	0.00436	0.034635	0.000542	0.870	-5	.	231	20	220	4	219	3
6507-2-3 2887_40	298	70.6	0.00E+00	18094	0.11811	0.00072	4.92503	0.11111	0.302434	0.006571	0.963	-13.2	-11.3	1928	10	1807	19	1703	33
6507-2-3 2887_41	490	83.6	0.00E+00	25342	0.08337	0.00044	2.56414	0.05063	0.22307	0.004245	0.964	1.7	.	1278	10	1290	14	1298	22
6507-2-3 2887_42	90	21.1	0.00E+00	47468	0.10691	0.00072	4.41302	0.09949	0.29937	0.006437	0.954	-3.9	-1.3	1747	12	1715	19	1688	32
6507-2-3 2887_43	75	34.4	0.00E+00	59847	0.24369	0.00249	18.3398	0.63889	0.545817	0.018181	0.956	-13.2	-10.6	3144	16	3008	34	2808	76
6507-2-3 2887_44	38	10.4	0.00E+00	1602	0.12421	0.00124	6.00766	0.15864	0.350796	0.008581	0.926	-4.5	-1.1	2018	17	1977	23	1938	41
6507-2-3 2887_45	85	36.6	8.20E-02	11805	0.20231	0.00179	14.49035	0.47867	0.519462	0.01653	0.963	-6.4	-3.9	2845	14	2782	31	2697	70
6507-2-3 2887_46	77	5.2	0.00E+00	1368	0.05789	0.00058	0.7348	0.0143	0.092056	0.001535	0.856	8.3	.	526	22	559	8	568	9

Summary for ICP-MS U-Pb zircon results for 6507/2-3, 2869.69

	ppm				***Ratios***							***Discordance***		***Ages***					
Name	**U**	**^{206}Pb**	**^{206}Pb$_c$ (%)**	**206/204**	**^{207}Pb/^{206}Pb***	**1σ**	**207Pb/235U***	**1σ**	**206Pb/238U***	**1σ**	**Rho**	**Central (%)**	**Minimum rim (%)**	**207/206**	**1 σ**	**207/235**	**1 σ**	**206/238**	**1 σ**
6507-2-3_2869_01	146	2.4	0.00E+00	1260	0.04901	0.00102	0.09801	0.00252	0.014503	0.00022	0.590	-37.7	.	148	46	95	2	93	1
6507-2-3_2869_02	49	1.2	0.00E+00	621	0.05717	0.00184	0.1752	0.00576	0.022226	0.000154	0.211	-72.3	-57.5	498	66	164	5	142	1
6507-2-3_2869_03	125	7.2	0.00E+00	1538	0.05259	0.00064	0.38672	0.00543	0.05333	0.000378	0.505	7.8	.	311	26	332	4	335	2
6507-2-3_2869_04	118	5.4	0.00E+00	8252	0.0518	0.00086	0.29573	0.00525	0.04141	0.000266	0.362	-5.5	.	276	35	263	4	262	2
6507-2-3_2869_05	863	69.5	0.00E+00	13817	0.05508	0.00029	0.54893	0.00406	0.072281	0.000375	0.700	8.6	3.7	415	11	444	3	450	2
6507-2-3_2869_06	1203	324	0.00E+00	64708	0.15969	0.00125	5.22189	0.05388	0.237168	0.001594	0.651	-48.8	-47.8	2452	13	1856	9	1372	8
6507-2-3_2869_07	592	188.7	0.00E+00	114655	0.11037	0.0008	4.38178	0.05673	0.287933	0.003097	0.831	-10.9	-8.6	1806	13	1709	11	1631	16
6507-2-3_2869_08	408	153.5	0.00E+00	14985	0.11962	0.0008	5.43568	0.05467	0.329576	0.002485	0.750	-6.7	-4.8	1951	11	1890	9	1836	12
6507-2-3_2869_09	417	33.4	0.00E+00	16121	0.05505	0.00054	0.55116	0.00657	0.072615	0.000487	0.562	9.4	2.3	414	22	446	4	452	3
6507-2-3_2869_10B	65	3.2	0.00E+00	2920	0.05226	0.00085	0.31607	0.00565	0.043864	0.000328	0.418	-6.9	.	297	35	279	4	277	2
6507-2-3_2869_11B	139	29.3	0.00E+00	6579	0.07545	0.00047	1.95188	0.01685	0.187638	0.001113	0.687	2.8	0.3	1080	12	1099	6	1109	6
6507-2-3_2869_12	73	1.1	0.00E+00	228	0.04827	0.00128	0.09273	0.00257	0.013933	0.000106	0.274	-20.9	.	113	59	90	2	89	1
6507-2-3_2869_14	527	24.8	0.00E+00	10518	0.05191	0.00037	0.30513	0.00321	0.042633	0.000329	0.732	-4.5	.	281	16	270	3	269	2
6507-2-3_2869_15	65	18.1	0.00E+00	20155	0.09019	0.00061	3.0841	0.03093	0.248019	0.001839	0.739	-0.1	.	1429	13	1429	8	1428	10
6507-2-3_2869_16	105	8.2	0.00E+00	2163	0.0557	0.00061	0.54483	0.00675	0.070937	0.000416	0.473	0.3	.	441	23	442	4	442	3

6507/5-3, 2846.18 m +2854.33 m

	ppm				*Ratios*							*Discordance*		*Ages*					
Name	**U**	**^{206}Pb**	**$^{206}Pb_c$ (%)**	**206/204**	**^{207}Pb/^{206}Pb***	**1σ**	**207Pb/235U***	**1σ**	**206Pb/238U***	**1σ**	**Rho**	**Central (%)**	**Minimum rim (%)**	**207/206**	**1 σ**	**207/235**	**1 σ**	**206/238**	**1 σ**
6507-5-3_01	150	32	0.00E+00	6744	0.07962	0.00067	1.93316	0.03645	0.176087	0.002975	0.896	-13	-9.3	1188	16	1093	13	1046	16
6507-5-3_02	44	13.7	0.00E+00	644	0.13944	0.0015	5.17014	0.07166	0.268918	0.002356	0.632	-34.6	-32.8	2220	17	1848	12	1535	12
6507-5-3_03	70	23.2	0.00E+00	4362	0.10314	0.0007	4.06311	0.0465	0.285719	0.002638	0.807	-4.1	-1.8	1681	13	1647	9	1620	13
6507-5-3_04	273	21.7	0.00E+00	5700	0.05479	0.00042	0.53267	0.00513	0.070508	0.000415	0.611	9.1	2.9	404	16	434	3	439	2
6507-5-3_05	39	13.7	0.00E+00	2316	0.10409	0.00098	4.3082	0.0693	0.300185	0.003912	0.81	-0.4	.	1698	17	1695	13	1692	19
6507-5-3_07	861	192.2	0.00E+00	37582	0.07872	0.00042	2.11443	0.01601	0.19482	0.001049	0.711	-1.6	.	1165	10	1154	5	1147	6
6507-5-3_08	40	22.2	0.00E+00	7204	0.17685	0.00158	11.26378	0.14824	0.461938	0.004472	0.736	-8	-5.9	2624	14	2545	12	2448	20
6507-5-3_09	180	13.7	0.00E+00	4064	0.056	0.00046	0.51864	0.00537	0.067165	0.000431	0.619	-7.6	.	453	18	424	4	419	3
6507-5-3_10	157	87.6	0.00E+00	21892	0.18211	0.00215	11.48616	0.23813	0.457436	0.007799	0.822	-10.9	-8	2672	19	2563	19	2428	34
6507-5-3_11	97	22.8	0.00E+00	13732	0.08051	0.00049	2.27012	0.01948	0.204497	0.001225	0.698	-0.9	.	1210	12	1203	6	1199	7
6507-5-3_13	180	58.1	0.00E+00	11202	0.11968	0.00121	4.61137	0.084	0.279446	0.004234	0.832	-21	-18.2	1951	17	1751	15	1589	21
6507-5-3_14	116	45.6	0.00E+00	9911	0.11173	0.00073	5.22585	0.0539	0.339225	0.002711	0.775	3.5	1.2	1828	11	1857	9	1883	13
6507-5-3_16	1155	655.9	0.00E+00	103334	0.18811	0.00162	12.51143	0.14062	0.482386	0.003497	0.645	-8.3	-6.6	2726	14	2644	11	2538	15
6507-5-3_15	143	38.8	0.00E+00	9085	0.10715	0.00071	3.49505	0.03546	0.236579	0.00181	0.754	-24.2	-22.5	1751	12	1526	8	1369	9
6507-5-3_17	230	80.9	0.00E+00	22882	0.10777	0.0007	4.5435	0.04121	0.305768	0.001945	0.701	-2.7	-0.8	1762	11	1739	8	1720	10
6507-5-3_18	22	9.5	0.00E+00	2487	0.10884	0.00123	5.49981	0.12974	0.366487	0.007585	0.877	15.2	9.6	1780	20	1901	20	2013	36

References

Alexander, J., Mulder, T., 2002. Experimental quasi-steady density currents. Marine Geology 168, 195-210.

Al-Harbi, O.A. and Khan, M.M., 2008. Provenance, diagenesis, tectonic setting and geochemistry of Tawil Sandstone (Lower Devonian) in central Saudi Arabia. Journal of Asian Earth Sciences, 33(3), 278-287.

Andresen, A. and Tull, J.F., 1983. The age of the Lødingen granite and its possible regional significance. Norsk geologisk tidsskrift, 63, 269-276.

Andersen, T.B., 1998. Extensional tectonics in the Caledonides of southern Norway, an overview. Tectonophysics, 285(3), 333-351.

Andersen, A., Corfu, F., Agyei-Dwarko N.Y., and Lanrionov, L.N. 2014. The Bratten-Landegode gneiss complex: a fragment of Laurentian continental crust in the Uppermost Allochthon of the Scandinavian Caledonides. In: Corfu, F., Gasser, D., and Chew, D.M. (Eds.) New perspectives on the Caledonides of Scandinavia and Related Areas. Geological Society, London, Special Publications, 390, 633-654.

Amireh, B.S., 1991. Mineral composition of the Cambrian-Cretaceous Nubian series of Jordan: provenance, tectonic setting and climatological implications. Sedimentary Geology, 71(2), 99-119Augland, L.E.,

Augland, L.E., Andresen, A., Gasser, D. and Steltenpohl, M.G., 2013. Early Ordovician to Silurian evolution of exotic terranes in the Scandinavian Caledonides. Tectonophysics, 231 (1-3), 59-70.

Austrheim, H., Corfu, F., Bryhni, I. and Andersen, T.B., 2003. The Proterozoic Hustad igneous complex: a low strain enclave with a key to the history of the Western Gneiss Region of Norway. Precambrian Research, 120, 149-175.

Baas, J.H., Best, J.L., Peakall, J. and Wang, M., 2009. A phase diagram for turbulent, transitional, and laminar clay suspension flows. Journal of Sedimentary Research, 79(4), 162-183.

Barnes, C.G., Frost, C.D., Yoshinobu, A.S., McArthur, K., Barnes, M.A., Allen, C.M., Nordgulen, Ø. and Prestvik, T., 2007. Timing of sedimentation, metamorphism, and plutonism in the Helgeland Nappe Complex, north-central Norwegian Caledonides. Geosphere, 3(6), 683-703.

Bhatia, M.R., 1983. Plate tectonics and geochemical composition of sandstones. The Journal of Geology, 91(6), 611-627.

Bhatia, M. R., & Crook, K. A.,1986. Trace element characteristics of graywackes and tectonic setting discrimination of sedimentary basins-Contributions to mineralogy and petrology, 92(2), 181-193.

Basu, A., Young, S., Suttner, L.J., James, W.C., Mack, C.H., 1975. Re-evaluation of the use of Undulatory extinction and polycrystallinity in detrital quartz for provenance interpretation. Journal of Sedimentary Petrology, 45, 873-882.

Bergh, S.G., Kullerud, K., Armitage, P.E., Bouke Zwaan, K., Corfu, F., Ravna, E.J. and Inge Myhre, P., 2010. Neoarchaean to Svecofennian tectono-magmatic evolution of the West Troms Basement Complex, North Norway. Norwegian Journal of Geology/Norsk Geologisk Forening, 90.

Bergh, S.G., Corfu, F., Myhre, P.I., Kullerud, K., Armitage, P.E., Zwaan, K.B., Ravna, E.K., Holdsworth, R.E. and Chattopadhya, A., 2012. Was the Precambrian basement of Western Troms and Lofoten-Vesterålen in northern Norway linked to the Lewisian of Scotland? A comparison of crustal components, tectonic evolution and amalgamation history. Tectonics, In Tech, 283-330.

Bergh, S.G., Kullerud, K., Myhre, P.I., Corfu, F., Armitage, P.E.B., Zwaan, K.B. and Ravna, E.J.K., 2014. Archaean elements of the basement outliers west of the Scandinavian Caledonides in Northern Norway: architecture, evolution and possible correlation with Fennoscandia. *In*: Dilek, Y., Furnes, H.(Eds.) *Evolution of Archean Crust and Early Life*, Modern Approches in Solid Earth Science, 7ed. Springer Science Netherlands, 103-126..

Bergh, S.G., Corfu. F., Nadezhda Priyatkina, Kullerud, K., Myhre, P.I., 2015. Multiple post-Svecofennian 1750-1560 Ma pegmatite dykes in Archean-Palaeoproterozoic rocks of the West Troms Basement Complex, North Norway: Geological significance and regional implications. Precambrian Reseach. 266, 425-439.

Bingen, B., Andersson, J., Soderlund, U. and Moller, C., 2008. The Mesoproterozoic in the Nordic countries. Episodes, 31, 29-34.

Brekke, H., 2000. The tectonic evolution of the Norwegian Sea continental margin, with emphasis on the Voring and More basins. Special Publication-Geological Society of London, 167, 327-378.

Brekke, H., Dahlgren, S., Nyland, B., & Magnus, C. (1999). The prospectivity of the Vøring and Møre basins on the Norwegian Sea continental margin. Geological Society, London, Petroleum Geology. In:A.J. Fleet and S.A.R Boldy (Editors), Petroleum Geology of Northwest Europe. Conference series (5), 261-274.

Brekke, H., Sjulstad, H.I., Magnus, C. and Williams, R.W., 2001. Sedimentary environments offshore Norway—an overview. Norwegian Petroleum Society Special Publications, 10, pp.7-37.

Briggs, R. M., Middleton, M. P., & Nelson, C. S. (2004). Provenance history of a Late Triassic-Jurassic Gondwana margin forearc basin, Murihiku Terrane, North Island, New Zealand: Petrographic and geochemical constraints. New Zealand Journal of geology and geophysics, 47(4), 589-602.

Blystad, P., Brekke, H., & Faerseth, R. B., 1995. Structural Elements of the Norwegian Continental Shelf. Pt. 2. The Norwegian Sea Region. NDP (8),1-45

Boggs, S.Jr., 2009. Petrology of Sedimentary Rocks, 2.ed. Cambridge University Press, New York, p. 607.

Bouma, A.H.,1962. Sedimentology of some Flysch Deposits: A Graphic Approach to Facies Interpretation. Elsevier, Amsterdam, 168pp.

Bryhni, I., Strut, B., 1985. Caledonides of southwestern Norway. In: Gee, D.G., Sturt, B.A. (Eds.), The Caledonides Orogen- Scandinavia and related areas: Part 1. Wiley, Chichester, 89-107.

Carter, A., & Moss, S. J.,1999. Combined detrital-zircon fission-track and U-Pb dating: A new approach to understanding hinterland evolution. Geology, 27(3), 235-238.

Cawood, P.A., Nemchin, A.A., 2001. Paleogeogaphic development of the east Laurentian margin: constraints from U-Pb dating of detrital zircons in the Newfoundland Appalachians. Geological Society of America Bulletin,113 (9), 1234-1246.

Corfu, F., 2004. U–Pb age, setting and tectonic significance of the anorthosite–mangerite–charnockite–granite suite, Lofoten–Vesterålen, Norway. Journal of Petrology, 45(9), 1799-1819.

Corfu, F. and Andersen, T.B., 2002. U-Pb ages of the Dalsfjord Complex, SW Norway, and their bearing on the correlation of allochthonous crystalline segments of the Scandinavian Caledonides. International Journal of Earth Sciences, 91(6), 955-963.

Corfu, F., Hanchar, J.M., Hoskin, P.W. and Kinny, P., 2003. Atlas of zircon textures. Reviews in mineralogy and geochemistry, 53, 469-500.

Corfu,F., Hanchar, J. M., Hoskin, P.W.O., and Kinny, P., 2003, Atlas of zircon textures. In: Hanchar, J.M., and Hoskin, P.W.O.(Eds)., Zircon: Reviews in Mineralogy and Geochemistry, 53, 469-500.

Corfu, F., Austrheim, H. and Ganzhorn, A.C., 2014. Localized granulite and eclogite facies metamorphism at Flatraket and Kråkeneset, Western Gneiss Region: U–Pb data and tectonic implications. Geological Society, London, Special Publications, 390, 425-442.

Compton, R.R., 1962. Manual of field geology. Willey, London. *In:* Tucker, M.E., (ed.) 1991 Sedimentary Petrology 2.ed. Blackwell Scientific, Oxford, 260pp.

Condie, K.C., 1993. Chemical composition and evolution of the upper continental crust: contrasting results from surface samples and shales. Chemical geology, 104(1-4), 1-37.

Cullers, R.L., 2000. The geochemistry of shales, siltstones and sandstones of Pennsylvanian–Permian age, Colorado, USA: implications for provenance and metamorphic studies. Lithos, 51(3), 181-203.

Cullers, R.L., Basu, A. and Suttner, L.J., 1988. Geochemical signature of provenance in sand-size material in soils and stream sediments near the Tobacco Root batholith, Montana, USA. Chemical Geology, 70(4), 335-348.

Cullers, R.L. and Podkovyrov, V.N., 2000. Geochemistry of the Mesoproterozoic Lakhanda shales in southeastern Yakutia, Russia: implications for mineralogical and provenance control, and recycling. Precambrian Research, 104, 77-93.

Dabbagh, M.E. and Rogers, J.J., 1983. Depositional environments and tectonic significance of the Wajid Sandstone of southern Saudi Arabia. Journal of African Earth Sciences (1983), 1(1), 47-57.

Dalland, A., Worsley, D., & Ofstad, K. (1988). A lithostratigraphic scheme for the Mesozoic and Cenozoic and succession offshore mid-and Northern Norway. NPD Bull, 4, 1-65.

Daly, J.S., Balagansky, V.V., Timmerman, M.J. and Whitehouse, M.J., 2006. The Lapland-Kola orogen: Palaeoproterozoic collision and accretion of the northern Fennoscandian lithosphere. Geological Society, London, Memoirs, 32, 579-598.

Dickinson, W.R., 1970. Interpreting detrital modes of graywacke and arkose. Journal of Sedimentary Research, 40(2). 696-707.

Dickinson, W. R. Bread, L.S: Brakenrigde, G.R., Erjavec, J.L., Ferguson, R.C., Inman, K.F., Knepp, R.A., Lindberg, F.A. and Ryberg, P.T., 1983. Provenance of North American Phanerozoic sandstones in relation to tectonic setting. Geological Society of America Bulletin, 94(2), 222-235.

Doré, A. G., and Lundin, E. R. 1996. Cenozoic compressional structures on the NE Atlantic margin; nature, origin and potential significance for hydrocarbon exploration. Petroleum Geoscience, 2(4), 299-311.

Doré, A. G., Lundin, E. R., Fichler, C., & Olesen, O., 1997. Patterns of basement structure and reactivation along the NE Atlantic margin. Journal of the Geological Society, 154, 85-92.

Doré, A.G., Lundin, E.R., Jensen, L.N., Birkeland, Ø., Eliassen, P.E. and Fichler, C., 1999. Principal tectonic events in the evolution of the northwest European Atlantic margin: In Geological society, London, Petroleum Geology Conference Series 5, 41-61.

Dutton, S.P. and Hentz, T.F., 2002. Reservoir quality of lower Miocene sandstones in lowstand prograding wedge successions, Vermilion Block 31, offshore Louisiana. Gul Coast Association of Geological Societies Transactions, 52

Eide, E.A., Torsvik, T.H. and Andersen, T.B., 1997. Absolute dating of brittle fault movements: Late Permian and late Jurassic extensional fault breccias in western Norway. Terra Nova, 9(3), 135-139.

Ehrenberg, S.N., 1989. Assessing the relative importance of compaction processes and cementation to reduction of porosity in sandstones: discussion; compaction and porosity evolution of Pliocene sandstones, Ventura Basin, California: discussion. AAPG Bulletin, 73(10), 1274-1276.

Elvevold, S. and Gilotti, J.A., 2000. Pressure–temperature evolution of retrogressed kyanite eclogites, Weinschenk Island, north–east Greenland Caledonides. Lithos, 53(2), 127-147.

Engekhardt, W.V., 1960, Der Porenraum der Sedimente: Berlin, Springer Verlag, 201p.

Escher, J.C. and Pulvertaft, T.C.R., 1995. Geological Map of Greeland, 1:2,500,000. Geological Survey of Greenland, Copenhagen

Fedo, C.M., Nesbitt, H.W. and Young, G.M., 1995. Unraveling the effects of potassium metasomatism in sedimentary rocks and paleosols, with implications for paleoweathering conditions and provenance. Geology, 23(10), 921-924.

Fisher, R.V., 1971. Features of coarse-grained, high-concentration fluids and their deposits. Journal of Sedimentary Research, 41(4).

Fjellanger, E., Surlyk, F., Wamsteeker, L. C., & Midtun, T., 2005. Upper Cretaceous basin-floor fans in the Vøring Basin, Mid Norway shelf. Norwegian Petroleum Society Special Publications, 12, 135-164.

Folk, R.L., 1980. Petrology of sedimentary rocks. Hemphill Publishing Company, Austin, 182 pp.

Fonneland, H. C., Lien, T., Martinsen, O. J., Pedersen, R. B., & Košler, J. 2004. Detrital zircon ages: a key to understanding the deposition of deep marine sandstones in the Norwegian Sea. Sedimentary Geology, 164, 147-159.

Fossen, H., 2010. Extensional tectonics in the North Atlantic Caledonides: a regional view. Geological Society, London, Special Publications, *335*, 767-793.

Fossen, H. and Dunlap, W.J., 1998. Timing and kinematics of Caledonian thrusting and extensional collapse, southern Norway: evidence from 40 Ar/39 Ar thermochronology. Journal of structural geology, 20(6), 765-781.

Fossen, H. and Dallmeyer, R.D., 1998. 40 Ar/39 Ar muscovite dates from the nappe region of southwestern Norway: dating extensional deformation in the Scandinavian Caledonides. Tectonophysics, 285, 119-133.

Fugelli, E.M.G., and Olsen, T.R., 2005. Screening for deep-marine reservoirs in frontier basins: Part 1—Examples from offshore mid-Norway. AAPG bulletin, 89(7), 853-882.

Fugelli, E. M.G., & Olsen, T. R.,2007. Delineating confined slope turbidite systems offshore mid-Norway: The Cretaceous deep-marine Lysing Formation. AAPG bulletin, 91(11), 1577-1601.

Furnes, H., Mitchell, J.G., Ryan,P. and Skjerlie, F.J., 1982. Petrography and geochemistry of peralkaline, ultrapotassic syneite dykes of Middel Permian ages, Sunnfjord, West Norway. Norsk Geologisk Tidsskrift, 62, 147-159.

Færseth, R. B., & Lien, T., 2002. Cretaceous evolution in the Norwegian Sea—a period characterized by tectonic quiescence. Marine and Petroleum Geology, 19(8), 1005-1027.

Færseth, R.B., Macintyre, R.M. and Naterstad, J., 1976. Mesozoic alkaline dykes in the Sunnhordland region, western Norway: ages, geochemistry and regional significance. Lithos, 9(4), 331-345.

Garver, J.I., Royce, P.R. and Smick, T.A., 1996. Chromium and nickel in shale of the Taconic foreland: a case study for the provenance of fine-grained sediments with an ultramafic source. Journal of Sedimentary Research, 66(1).

Gaál, G., & Gorbatschev, R., 1987. An outline of the Precambrian evolution of the Baltic Shield. Precambrian Research, 35, 15-52.

Gee, D. G. (1975). A tectonic model for the central part of the Scandinavian Caledonides. American Journal of Science, 275, 468-515.

Gower, C.F., Heaman, L.M., Loveridge, W.D., Schärer, U. and Tucker, R.D., 1991. Grenvillian magmatism in the eastern Grenville Province, Canada. Precambrian Research, 51(1-4), pp.315-336.

Gu, X.X., Liu, J.M., Zheng, M.H., Tang, J.X. and Qi, L., 2002. Provenance and tectonic setting of the Proterozoic turbidites in Hunan, South China: geochemical evidence. Journal of sedimentary Research, 72(3), 393-407.

Griffin, W.L., Taylor, P.N., Hakkinen, P.W., Heier, K.S., Iden, I.K., Krogh, E.J., Malm, O.,Olsen, K.I., Ormaasen, D.E., Tveten,E., 1978. Archean and Proterozoic crustal evolution in Lofoten- Vesterålen, N Norway. Journal of the Geological Society, London, 13, 629-647.

Hacker, B.R., Andersen, T.B., Root, D.B., Mehl, L., Mattinson, J.M. and Wooden, J.L., 2003. Exhumation of high-pressure rocks beneath the Solund Basin, western gneiss region of Norway. Journal of Metamorphic Geology, 21(6), 613-629.

Halland, E.K., Mujezinovic, J., Riis, F., Bjørnestad, A., Meling, I., Gjeldsvik, I., Tappel, I., Bjørheim, M., Rød, R. and Pham, V., 2013. CO2 Storage Atlas: Norwegian Continental Shelf. Norwegian Petroleum Directorate, Stavanger, Norway.

Hart, M.B., 2007. Late Cretaceous climates and formaminiferid distributions. In: Williams, M., A.M. Gregory, F.J. and Schmidt D.N. (Eds.) Deep-Time Perspective on Climate Change: Marrying the signal from Computer Models and Biological proxies. The Micropalaeontological Society, Special Publications. The Geological Society, London, 235-250.

Hastings, D. S., 1987. Sand-prone facies in the Cretaceous of mid-Norway, In: Brooks, J. and Glennie (eds.) Petroleum geology of North West Europe: London, Graham and Trotman, 1065-1078.

Haughton, P.D.W., Barker, S.P., and McCafferey, 2003. "Linked" debrites in sand-rich turbidite systems- Origin and Significance: Sedimentology, 50. 459-482.

Henstra, G.A., Rotevatn, A., Gawthorpe, R.L., Ravnås, R., 2015. Evolution of a major segmented normal fault during multiphase rifting: The origin of plan-view zigzag geometry. (Part 2), PhD. Thesis, Department of Earth Science, University of Bergen.

Henriksen, N., 1985, The Caledoides of central East Greenland 70-76N, In: Gee, D.G. and Strut, B.A., (Eds.) The Caledonide orogen, Scandinavia and related areas, 2, 182-246.

Herron, M.M., 1988. Geochemical classification of terrigenous sand and shales from core and log data. Journal of Sedimentary Petrology 58, 820-829.

Imam, M.B., 1986. Scanning electron microscopy study of the quartz overgrowths within Neogene sandstones of Bengal Basin, Bangladesh. Geological Society of India, 28(5), 407-413.

Imam, M.B. and Shaw, H.F., 1987. Diagenetic controls on the reservoir properties of gas bearing Neogene Surma Group sandstones in the Bengal Basin, Bangladesh. Marine and petroleum geology 4(2), 103-111.

Ingersoll, R.V., Bullard, T.F., Ford, R.L., Grimm, J.P., Pickle, J.D. and Sares, S.W., 1984. The effect of grain size on detrital modes: a test of the Gazzi-Dickinson point-counting method. Journal of Sedimentary Research, 54, 103-116.

Jackson, S.E., Pearson, N.J., Griffin, W.L. and Belousova, E.A., 2004. The application of laser ablation-inductively coupled plasma-mass spectrometry to in situ U–Pb zircon geochronology. Chemical Geology, 211, 47-69.

Jacobsen, S. B. and Wasserburg, G. J., 1978. Interpretation of Nd, Sr and Pb isotope data from Archean migmatites in Lofoten-Vesterålen, Norway. Earth and Planetary Science Letters, 41, 245-253.

Kalsbeek, F., Nutman, A.P. and Taylor, P.N., 1993. Palaeoproterozoic basement province in the Caledonian fold belt of North-East Greenland. Precambrian Research, 63(1-2), 163-178.

Kalsbeek, F., Jepsen, H.F. and Jones, K.A., 2001. Geochemistry and petrogenesis of S-type granites in East Greenland Caledonides. Lithos 57, 91-109.

Kneller, B.C. and Branney, M.J., 1995. Sustained high-density turbidity currents and the deposition of thick massive sands. Sedimentology, 42(4), 607-616.

Kneller, B.C. and McCaffrey, W.D., 2003. The interpretation of vertical sequences in turbidite beds: the influence of longitudinal flow structure. Journal of Sedimentary Research, 73(5), 706-713.

Koistinen, T., Stephens, M.B., Bogatchev, V., Nordgulen, Ø., Wennerström, M. and Korhonen, J., 2001. Geological map of the Fennoscandian Shield, scale 1: 2,000,000: Geol. Surv. Finland, Norway and Sweden and the North-West Dept. of Nat. Res. of Russia.

Korja, A., Lahtinen, R. and Nironen, M., 2006. The Svecofennian orogen: A collage of microcontinents and island arcs. Geological Society, London, Memoirs, 32, 561-578.

Kullerud, K., Corfu, F., Bergh, S.G., Davidsen, B. and Ravna, E.K., 2006. U-Pb constraints on the Archaean and Early Proterozoic evolution of the West Troms Basement Complex, North Norway. Bulletin of the Geological Society of Finland Special Issue I, 79.

Lahtinen, R., Garde, A.A. and Melezhik, V.A., 2008. Paleoproterozoic evolution of Fennoscandia and Greenland. Episodes, 31, 20-28.

Leslie, A.G., Higgins, A.K., 1999. On the Caledonian (and Grenvillian) geology of Bartolin Land, Ole Rømer Land and adjacent nunataks, East Greenland. Danmark og Grønlands Geologiske Undersøgelse 19, 11-26.

Leslie, A.G. and Nutman, A.P., 2000. Episodic tectono-thermal activity in the southern part of the East Greenland Caledonides. Geology of Greenland Survey Bulletin, 186, 42-49.

Leslie, A.G. and Nutman, A.P., 2003. Evidence for Neoproterozoic orogenesis and early high temperature Scandian deformation events in the southern East Greenland Caledonides. Geological Magazine, 140(03), 309-333.

Lien, T., Midtho, R. E., & Martinsen, O. J., 2006. Depositional facies and reservoir quality of deep-marine sandstones in the Norwegian Sea. Norsk Geologisk Tidsskrift, 86(2), 71.

Lowe, D.R., 1982. Sedimentary gravity flows II, Depositional models with special reference of high- density turbidite currents. Journal of Sedimentary Petrology. 52. 279-297.

Lowe, D.R., 2004. Deepwater Sandstones: Submarine Canyon to Basin Plain Western California. America Association of Petroleum Geologists and the Pacific Section AAPG 2004, Special Publications CB, 79pp.

Ludwig, K.R., 2003. User manual for Isoplot 3.0. Berkeley Geochronology Center Special Publication, 4.

Martinsen, O. J., Lien, T., & Jackson, C. (2005). Cretaceous and Palaeogene turbidite systems in the North Sea and Norwegian Sea Basins: source, staging area and basin physiography controls on reservoir development. In: Doré, A.G., and Vining, B.A., (Eds.) Petroleum Geology: North-West Europe and Global Perspectives –Proceedings of the 6th Petroleum Geology Conference: London, Geological Society of London, Petroleum, 1147-1164.

McBride, E.F., 1989. Quartz cement in sandstones: a review. Earth-Science Reviews, 26(1-3), 69-112.

McLennan, S.M., Taylor, S.R. and Eriksson, K.A., 1983. Geochemistry of Archean shales from the Pilbara Supergroup, western Australia. Geochimica et Cosmochimica Acta, 47(7), 1211-1222.

McLennan, S.M., Taylor, S.R., McCulloch, M.T. and Maynard, J.B., 1990. Geochemical and Nd-Sr isotopic composition of deep-sea turbidites: Crustal evolution and plate tectonic associations. Geochimica et Cosmochimica Acta, 54(7), 2015-2050.

McLennan, S. M., Hemming, S., McDaniel, D. K., & Hanson, G. N. (1993). Geochemical approaches to sedimentation, provenance, and tectonics. Geological Society of America Special Papers, 284, 21-40.

Milnes, A.G., and Koestler, A.G., 1985. Geological structure of Jotunheimen, southern Norway (Sognefjell-Valdres cross-section). In: Gee, D.G., Sturt, B.A. (Eds.), The Caledonides Orogen- Scandinavia and related areas: Part 1. Wiley, New York, 123-124.

Morton, A. C., & Grant, S.,1998. Cretaceous depositional systems in the Norwegian Sea: Heavy mineral constraints. AAPG Bulletin, 82(2), 274-290.

Morton, A. C., Whitham, A. G., & Fanning, C. M., 2005. Provenance of Late Cretaceous to Paleocene submarine fan sandstones in the Norwegian Sea: integration of heavy mineral, mineral chemical and zircon age data. Sedimentary Geology, 182, 3-28.

Morton, A., Fanning, M. and Milner, P., 2008. Provenance characteristics of Scandinavian basement terrains: constraints from detrital zircon ages in modern river sediments. Sedimentary Geology, 210, 61-85.

Morton, A. and Chenery, S., 2009. Detrital rutile geochemistry and thermometry as guides to provenance of Jurassic–Paleocene sandstones of the Norwegian Sea. Journal of Sedimentary Research, 79(7), 540-553.

Mosar, J., Eide, E. A., Osmundsen, P. T., Sommaruga, A., & Torsvik, T. H. (2002). Greenland–Norway separation: a geodynamic model for the North Atlantic. Norwegian Journal of Geology, 82, 282.

Mulder, T., Alexander, J., 2001. The physical character of subaqueous sedimentary density flows and their deposits. Sedimentology 48, 269-299.

Mørk, M.B.E., and Johansen, S.O., 2005, Jurassic sandstone provenance and basement erosion in the Møre margin –Froan Basin area: Norges Geologiske Undersøkelse Bulletin, 443, 5-18

Nesbitt, H.W. and Young, G.M., 1982. Early Proterozoic climates and plate motions inferred from major element chemistry of lutites. Nature, 299(5885), 715-717

Nesbitt, H.W. and Young, G.M., 1984. Prediction of some weathering trends of plutonic and volcanic rocks based on thermodynamic and kinetic considerations. Geochimica et Cosmochimica Acta, 48(7), 1523-1534.

Nutman, A.P., Kalsbeek, F., 1994. Search for Archaean basement in the Caledonian fold belt of North-East Greenland. Grønlands Geologiske Undersøgelse Raport, 162, 129-134.

Osae, S., Asiedu, D.K., Banoeng-Yakubo, B., Koeberl, C. and Dampare, S.B., 2006. Provenance and tectonic setting of Late Proterozoic Buem sandstones of southeastern Ghana: Evidence from geochemistry and detrital modes. Journal of African Earth Sciences, 44, 85-96.

Osmundsen, P.T. and Ebbing, J., 2008. Styles of extension offshore mid-Norway and implications for mechanisms of crustal thinning at passive margins. Tectonics, 27(6).

Pedersen, R.B. and Furnes, H., 1991. Geology, magmatic affinity and geotectonic environment of some Caledonian ophiolites in Norway. Journal of Geodynamics, 13(2), 183-203.

Pettijohn, F.J., 1975. Sedimentary Rocks, 3. Ed. Haper and Row New York,.628 pp.

Powers, M.C., 1982. Comparison chart for estimating roundness and sphericity. AGI Datasheet 18. American Geological Institute. In Tucker, M.E. (Ed.) 1991 Sedimentary Petrology 2.ed. Blackwell Scientific, Oxford, 260 pp.

Quinto, J.C., 2017. Seismic characterization of the Lange and lysing sandstones MSc Thesis, University of Stavanger, Norway.

Qvale, H. and Stigh, J., 1985. Ultramafic rocks in the Scandinavian Caledonides. In: Gee. D.G., Sturt, B.A. (Eds.), The Caledonides Orogen- Scandinavia and related areas: Part 1. Wiley, Chichester,. 693-715.

Rainbird, R.H., Hamilton, M.A. and Young, G.M., 2001. Detrital zircon geochronology and provenance of the Torridonian, NW Scotland. Journal of the Geological Society, 158(1), 15-27

Ramberg, I. B., Bryhni, I., and Nøttvedt, A., 2008. Landet blir til: Norges geologi. 2. Edition, Norsk Geologisk Forening, 608 pp.

Ravnås, R., Nøttvedt, A., Steel, R. J., & Windelstad, J. (2000). Syn-rift sedimentary architectures in the Northern North Sea. Geological Society, London, Special Publications, 167(1), 133-177.

Rehnström, E.F. and Corfu, F., 2004. Palaeoproterozoic U–Pb ages of autochthonous and allochthonous granites from the northern Swedish Caledonides—regional and palaeogeographic implications. Precambrian Research, 132(4), 363-378.

Roberts, D., Gee., D.G., 1985. An Introduction to the structure of the Scandinavian Caledonides. In: Gee. D.G., Sturt, B.A. (Eds.), The Caledonides Orogen- Scandinavia and related areas: Part 1. Wiley, New York, 55-68.

Rosa, D.R.N., Finch, A.A., Andersen, T. and Inverno, C.M.C., 2009. U–Pb geochronology and Hf isotope ratios of magmatic zircons from the Iberian Pyrite Belt. Mineralogy and Petrology, 95(2), 47.

Roser, B. P., & Korsch, R. J., 1986. Determination of tectonic setting of sandstone-mudstone suites using content and ratio. The Journal of Geology, 94(5), 635-650.

Schärer, U., 1980. U-Pb and Rb-Sr dating of a polymetamorphic nappe terrain: the Caledonian Jotun Nappe, southern Norway. Earth and Planetary Science Letters, 49(2), 205-218.

Scott, R.A., 2000. Mesozoic- Cenozoic evolution of East Greenland: implication of a reinterpreted continent-ocean boundary location. Polarforschung 68, 83.91.

Shanmugam, G., 1996. High-density turbidity currents: are they sandy debris flows? Journal of Sedimentary Research 66. 2-10.

Shanmugam, G., Lehtonen, L.R., Straume, T., Syvertsen, S.E., Hodgkinson, R.J. and Skibeli, M., 1994. Slump and debris-flow dominated upper slope facies in the Cretaceous of the Norwegian and northern North Seas (61-67 N): Implications for sand distribution. AAPG bulletin, *78*(6), 910-937.

Shell prop.data

Sigmond, E.M.O., 1992 Bedrock map of Norway and adjacent ocean area, 1:3,000,000: Oslo, Geological Survey of Norway.

Sigmond, E.M.O., Gustavson, M. and Roberts, D., 1984. Bedrock map of Norway, 1:1 million. Trondheim: Norges Geologiske Undersøkelse.

Skogseid, J., Planke, S., Faleide, J.I., Pedersen, T., Eldholm, O., Neverdal, F., 2000. NE Atlantic Continental rifting and volcanic margin formation. In: Nøttvedt, A. (Eds), Dynamics of the Norwegian Margin. Geological Society Special Publications, 167, 295-326.

Skår, Ø., 1998. Field relations and geochemical evolution of the pre-Sveconorwegian rocks in the Kvamsøy area, southern Western Gneiss Complex. Norway. PhD Thesis, University of Bergen, Norway.

Skår, O., 2000. Field relations and geochemical evolution of the Gothian rocks in the Kvamsoy area, southern Western Gneiss Complex, Norway. NGU (Norsk geologisk undersøkelse), 437,.5-24.

Skår, Ø., 2002. U–Pb geochronology and geochemistry of early Proterozoic rocks of the tectonic basement windows in central Nordland, Caledonides of north-central Norway. Precambrian Research, 116(3), 265-283.

Skår,Ø., Furnes, H., Claesson, S., 1994. Proterozoic orogenic magmatism within the Western Gneiss Region, Sunnfjord, Norway. Norsk Geologisk Tidsskrift 74. 114-126

Slabunov, A.I., Azimov, P.Y., Glebovitskii, V.A., Zhang, L. and Kevlich, V.I., 2016, March. Archaean and palaeoproterozoic migmatizations in the Belomorian Province, Fennoscandian Shield: Petrology, geochronology, and geodynamic settings. In Doklady Earth Sciences, Pleiades Publishing. 467, 259-263.

Smith, M.P., Robertson, S., 1999. The nathorst land group (Late Proterozoic) of East Greenland-lithostratigraphy, basin geometry and tectonic history. Danmarks og Grønlands Geologiske Undersøgelse Rapport 19, 127-143.

Stephens, M.B., Gustavson, M. M., Ramberg, I.B., Zachrisson, E., 1985. The Caledonides of central- north Scandinavia- a tectonostratgraphic overview. In: Gee, D.G., Sturt, B.A. (Eds.), The Caledonides Orogen-Scandinavia and related areas: Part 1. Wiley, Chichester, 135-162.

Stephens, M.G., Hames, W. E. and Andersen, A., 2004. The Silurian to Permian history of a metamorphic core complex in Lofoten, Norteren Scandinavian Caledonides. Tectonics, 23.

Steel, R.J., 1993, Triassic–Jurassic megasequence stratigraphy in the Northern North Sea: rift to post-rift evolution. In Geological Society, London, Petroleum Geology Conference series, 4, 299-315.

Strachan, R.A., Nutman, A.P. and Friderichsen, J.D., 1995. SHRIMP U-Pb geochronology and metamorphic history of the Smallefjord sequence, NE Greenland Caledonides. Journal of the Geological Society, 152(5), 779-784.

Slabunov, A.I., Lobach-Zhuchenko, S.B., Bibikova, E.V., Sorjonen-Ward, P., Balangansky, V.V., Volodichev, O.I., Shchipansky, A.A., Svetov, S.A., Chekulaev, V.P., Arestova, N.A. and Stepanov, V.S., 2006. The Archaean nucleus of the Fennoscandian (Baltic) Shield. *Geological Society,* London, Memoirs, 32, 627-644.

Surlyk, F., 1978. Submarine fan sedimentation along fault scarps on tilted fault blocks (Jurassic –Cretaceous boundary, East Greenland) Bulletin-GrÓnlands Geologiske UndersÓgelse 128, 109.

Suttner, L.J., Basu, A. and Mack, G.H., 1981. Climate and the origin of quartz arenites. Journal of Sedimentary Research, 51, 1235-1246.

Swiecicki, T., Gibbs, P. B., Farrow, G. E., and Coward, M. P. ,1998. A tectonostratigraphic framework for the Mid-Norway region. Marine and Petroleum Geology, 15(3), 245-276.

Sømme, T. O., Jackson, C. A. L., and Vaksdal, M. 2013a. Source-to-sink analysis of ancient sedimentary systems using a subsurface case study from the Møre-Trøndelag area of southern Norway: Part 1. Basin Research, 25(5), 489-511.

Sømme, T. O., & Jackson, C. A. L. 2013b. Source-to-sink analysis of ancient sedimentary systems using a subsurface case study from the Møre-Trøndelag area of southern Norway: Part 2. Basin Research, 25(5), 512-531.

Taylor, S. R. and McLennan, S.M. 1985. The Continental Crust: Its Composition and Evolution. Oxford: Blackwell, pp. 312

Terry, M.P. and Robinson, P., 2003. Evolution of amphibolite-facies structural features and boundary conditions for deformation during exhumation of high-and ultrahigh-pressure rocks, Nordøyane, Western Gneiss Region, Norway. Tectonics, 22(4).

Thrane, K., 2002. Relationships between Archaean and Palaeoproterozoic crystalline basement complexes in the southern part of the East Greenland Caledonides: an ion microprobe study, Precambrian Research, 113, 19-42.

Thon, A, 1985. Late Ordovician and early Silurian cover sequences to the west Norwegian ophiolite fragments: stratigraphy and structural evolution. In: Gee, D.G., Sturt, B.A.(Eds.), The Caledonide Orogen - Scandinavia and Related Areas, Wiley, Chichester, 407-415.

Tortosa, A., Palomares, M. and Arribas, J., 1991. Quartz grain types in Holocene deposits from the Spanish Central System: some problems in provenance analysis. Geological Society, London, Special Publications, 57, 47-54.

Tucker, R.D., 1986. Geology of the Hemnefjord-Orkanger area, south-central Norway. Norges geologiske undersøkelse, 404, 1-24.

Tucker, M.E., 1998. Techniques in Sedimentology. Blackwell Scientific Publications, Oxford, 394 pp.

Tucker, R. D., Boyd, R., and Barnes, S. J.,1990. A U-Pb zircon age for the Råna intrusion, N. Norway: new evidence of basic magmatism in the Scandinavian Caledonides in Early Silurian time. Norsk geologisk tidsskrift, 70, 229-239.

Tucker, R.D., Krogh, T.E., and Råheim, A., 1990. Proterozoic evolution and age-province boundaries in the central part of the Western Gneiss Region, Norway: results of U-Pb dating of accessory minerals from Trondheimsfjord to Geiranger. In: Gower, C.F., Rivers, T. and Ryan, B. (Eds.) Mid-Proterozoic Geology of the Southern Margin of Proto-Laurentia-Baltica. Geological Association of Canada, Special Paper 241, 33-50.

Tveten, E., 1978. Geological map of Norway, bed rock map Svolvær 1:250 000, Geological Survey of Norway

Vander Auwera, J., Bolle, O., Bingen, B., Liégeois, J.P., Bogaerts, M., Duchesne, J.C., De Waele, B. and Longhi, J., 2011. Sveconorwegian massif-type anorthosites and related granitoids result from post-collisional melting of a continental arc root. Earth-Science Reviews, 107(3), 375-397.

Vergara, L., Wreglesworth, I., Trayfoot, M. and Richardsen, G., 2001. The distribution of Cretaceous and Paleocene deep-water reservoirs in the Norwegian Sea basins. Petroleum Geoscience, 7(4), 395-408.

Walderhaug, O., 1996. Kinetic modeling of quartz cementation and porosity loss in deeply buried sandstone reservoirs. AAPG bulletin, 80(5), 731-745.

Watt and Thrane, 2001. Early Neoproterozoic events in East Greenland. Precambrian Research 110, 165-184.

Watt, G.R., Kinny, P.D. and Friderichsen, J.D., 2000. U–Pb geochronology of Neoproterozoic and Caledonian tectonothermal events in the East Greenland Caledonides. Journal of the Geological Society, 157(5), pp.1031-1048.

Weltje, G.J., Meijer, X.D. and de Boer, P.L., 1998. Stratigraphic inversion of siliciclastic basin fills: a note on the distinction between supply signals resulting from tectonic and climatic forcing. Basin Research, 10, 129-153.

Whitehouse, M.J., Claesson, S., Sunde, T. and Vestin, J., 1997. Ion microprobe U- Pb zircon geochronology and correlation of Archaean gneisses from the Lewisian Complex of Gruinard Bay, northwestern Scotland. Geochimica et Cosmochimica Acta, 61(20), 4429-4438.

Whitham, A.G., Price, S.P., Koraini, A.M., Kelly, S.R.A., 1999. Cretaceous (post-Valanginian) sedimentation and rift events in NE Greeland (71°-77°N). In: Fleet, A.J., Boldy, S.A.R. (Eds.), Petroleum Geology of Northwest Europe: Proceedings of the 5th Conference. Geological Society of London, London, UK, 325-336.

Wiedenbeck, M. Alle, P., Corfu, F., Griffin W.L., Meier, M., Oberli, F., Von Quadt, A., Roddick, J.C., Spiegel, W., 1995. Three natural zircon standards for U-Th-Pb, Lu-Hf trace element and REE analyses. Geostand Newsl. 19, 1-23

Williams, I.S. and Claesson, S., 1987. Isotopic evidence for the Precambrian provenance and Caledonian metamorphism of high grade paragneisses from the Seve Nappes, Scandinavian Caledonides. Contributions to mineralogy and petrology, 97(2), 205-217.

Winchester, J.A. and Floyd, P.A., 1977. Geochemical discrimination of different magma series and their differentiation products using immobile elements. Chemical geology, 20, .325-343.

Worden, R.H. and Morad, S., 2003. Clay minerals in sandstones: controls on formation, distribution and evolution Blackwell Publishing Ltd, 1-41.

Young, S.W., 1976. Petrographic textures of detrital polycrystalline quartz as an aid to interpreting crystalline source rocks. Journal of Sedimentary Petrology. 46(3)

Ziegler, P.A., 1988. Evolution of the Arctic-north Atlantic and the western tethys--a visual presentation of a series of paleogeographic-paleotectonic maps. *AAPG memoir*, *43*, 164-196.

Åhall, K.I and Connelly, J., 1998. Intermittent 1.53-1.13 Ga magmatism in western Baltica; age constrainst and correlations within a postulated supercontinent. Precambrian Research, 92, 1-20.